IONIZATION, BONDING, AND SOLVATION ENERGETICS OF ORGANOMETALLIC COMPLEXES

By

MATTHEW F. RYAN

A DISSERTATION PRESENTED TO THE GRADUATE SCHOOL
OF THE UNIVERSITY OF FLORIDA IN PARTIAL FULFILLMENT
OF THE REQUIREMENTS FOR THE DEGREE OF
DOCTOR OF PHILOSOPHY

UNIVERSITY OF FLORIDA
1993

To my Grandparents

ACKNOWLEDGEMENTS

The sacrifices I have made over the past several years cannot be counted; perhaps they should not even be considered. But sacrifice was a major factor towards completion of this final work--a lot of time and a lot of energy and a lot of sacrifice all concentrated for a sole purpose. Unusual things happen to a person who focuses so long and hard on a single goal. The memories in between the battles become clouded and unfocused. So many memories have amassed, most are happy, but some are sad and lonely. However, the indecision and the doubt and the pure rage are paled by the handful of triumphs. Perchance it is these triumphs that make the journey fulfilling.

I recall the time when I felt that I needed to understand more about science and more importantly, the world around me. Although graduate school was not the sole source of my salvation it was a beginning: the fresh start that I needed. When I spoke with Professor Russell Drago in the spring of 1987 (I remember the conversation well), I told him that if I was accepted to the University of Florida I would succeed. With the support of Professor Drago and Professor Jack Kotz of S.U.N.Y. Oneonta, I was admitted to U.F. in the fall of 1987. I am very grateful for their support and the trust they had in me. I believe I was given an important break.

I would like to thank Professors David E. Richardson and John R. Eyler for all their guidance. Dr. Eyler has helped me in many capacities and I am grateful to him

for all the discussions we have had. His confidence in me and my work has been very important to me. David Richardson, my research advisor, has helped me develop many skills necessary to be a scientist. Although it was sometimes a struggle, for both him and me, I learned a great deal from him. His door was always open and he always had time for discussions with me. I will always admire his work as an educator and a mentor.

Several people assisted in various capacities with this work. I would like to thank Dr. Allen Siedle, Dr. Mark Burk, Professor Charles Winter, Professor Russell Hughes, Professor Dennis Lichtenberger, Dr. San Li, Professor William Weltner, and my friends, Dr. Md. Nazrul I. Khan and Dr. Paul Sharpe for their help.

Throughout my graduate work, I have drawn strength from several vital sources: my family, my friends, and Debbie Simpson. My family shared with me the most exciting and frustrating moments. My parents understood and appreciated my efforts to "catchup" and adjust to my new surroundings. When I spoke with them, any discouragement I had was made insignificant; I spoke with them often because their confidence and love are inspirational. My brothers and sisters, Mark, Joe, Cassandra, and Andrea, were there to fill in the gaps. Their love for me was manifested in many ways. I am grateful for all the things they have done for me for they have given me so much and asked for nothing in return. I am blessed to have such a close family.

My friends Steve and Mike Messick helped me to persevere. Through Steve and Mike, I learned how to focus my thoughts and emotions. The jaunts to Cape

Vincent (and points north) and California were extremely therapeutic. Although the briar patch at the Tesla concert was not efficacious, Vegas was completely necessary.

When I came to U.F., I left behind several close friends, and I have remained close with only a few people during my time in Florida. Jack Santos (soon to be a father) and I have known each other forever. Although I may have neglected our friendship occasionally, Jack always understood. He is a great friend.

I am very grateful to my friend John Moore for his help in the beginning and his encouragement until the final moment. Before I moved to Florida, John found me an apartment and, more importantly, introduced me to the U.F. Rugby Team soon after my arrival. Rugby, in addition to supplying me with dozens of wonderful friendships, was a vent for frustrations like no other I can imagine.

Steve Glatter and Steve Rubin have supplied me with everlasting laughter. In addition to their advice and refreshing perspective on things in general, I would like to thank them for their companionship throughout the years.

Mike Naugton and I were roommates for nearly five years. I enjoyed his company, and I am glad we have remained friends.

Before I met Debbie Simpson, I often felt that I was isolated and alone. My family and friends are all far away and the rugby team has a specific purpose. Debbie is a wonderful friend, her smile is contagious, and her warmth and love never fade. Debbie has always listened to me and has helped me to find the answers. We have been through a great deal together, and our friendship, love, and respect for each other is constantly growing with each passing challenge.

TABLE OF CONTENTS

LIST OF TABLES

LIST OF FIGURES

Abstract of Dissertation Presented to the Graduate School
of the University of Florida in Partial Fulfillment of the
Requirements for the Degree of Doctor of Philosophy

IONIZATION, BONDING, AND SOLVATION ENERGETICS OF ORGANOMETALLIC COMPLEXES

By

Matthew F. Ryan

May, 1993

Chairperson: David E. Richardson
Major Department: Chemistry

Free energies of ionization ($\Delta G_i°$) for Cp_2M complexes (Cp = η^5-cyclopentadienyl; M = V, Cr, Mn, Fe, Co, Ni, Ru, Os) and Cp^*_2M complexes (Cp* = η^5-pentamethylcyclopentadienyl; M = Mn, Fe, Ni, Ru, Os) have been determined from electron-transfer equilibrium methods by using Fourier transform ion cyclotron resonance mass spectrometry. The $\Delta G_i°$ values for ferrocene derivatives, alkylnickelocene derivatives and various ruthenocene complexes have also been investigated through ETE studies.

Temperature dependence studies involving ETE of ferrocene with N,N'-diethyltoluidine lead to values for the ionization enthalpy and entropy for ferrocene. Experimental results of $\Delta S_i°(Cp_2Fe)$ are compared to results from statistical mechanical analyses. Thermochemical cycles are used to derive estimates of heterolytic and homolytic bond M-Cp enthalpies for the first transition row

metallocenes and to derive estimates for the differential solvation free energies, $\Delta\Delta G_{solv}°$, for the $Cp_2M^{+/0}$ couples. With the exception of $Cp_2V^{+/0}$, first transition row $Cp_2M^{+/0}$ couples are estimated to have $\Delta\Delta G_{solv}°$ values of -38 ± 3 kcal mol^{-1}. The average $\Delta\Delta G_{solv}°$ for the $Cp^*_2M^{+/0}$ couples is -26 ± 3 kcal mol^{-1}.

The $\Delta G_i°$ values and electron attachment free energies ($\Delta G_a°$) for a series of alkylnickelocene complexes (RCp)(R'Cp)Ni have been determined. The ionization energies follow the expected trends (increased alkylation yields a decrease in $\Delta G_i°$) but the $\Delta G_a°$ values become more negative for R = Et and t-Bu and more positive for R = Me. Several parameter schemes are used to interpret the $\Delta G_i°$ and $\Delta G_a°$ data. Values of $\Delta\Delta G_{solv}°$ for the $Cp_2Ni^{+/0/-}$ and $(t\text{-butylCp})_2Ni^{+/0/-}$ couples are discussed. From the $Cp_2Ni^{+/0/-}$ data, an average $\Delta\Delta G_{solv}°$ value is estimated.

The $\Delta G_i°$ values and $E_{1/2}$ estimates for series of ruthenocene derivatives have been determined. A parameter scale that correlates electronic effects for Cp ligands, rather than individual substituents, has been developed based on $\Delta G_i°$ values of the ruthenocene complexes. The utility of the parameters for predicting reactivity of metal complexes bearing Cp ligands is considered.

CHAPTER 1
INTRODUCTION

Thermochemical information is of primary importance to the understanding of chemical reactivity. Reaction pathways and mechanisms can be better understood if salient thermochemical data pertaining to reactant species or products exist. Thermodynamics can inform us if a chemical reaction will proceed and can tell us the efficiency of the reaction. Although information concerning the velocity of a reaction can not be readily assessed from a thermodynamic analysis, theories of chemical kinetics are based on the laws of thermodynamics.[1] Thus, the utility of thermochemistry as a tool to both predict and comprehend chemical transformations is essential to chemistry.

Organic chemistry has benefitted enormously from the depth and breadth of available thermochemical data for simple and complex organic systems.[2,3] Furthermore, the thermochemical foundation of organic chemistry allows complex reaction mechanisms to be understood and reaction efficiencies to be maximized. The utility of thermochemistry to predict reactivity based on known quantities is well documented in organic chemistry.[2,3] For instance, the derivation of parameterization schemes by Hammett[4] and Taft[5] based on various equilibrium dissociation and ionization constants elegantly demonstrates how thermochemistry can be used to predict additional thermochemical information and interpret existing systems. The

quantification of field and resonance effects, wrought from extensive experimentation,[4,5] enables the direct application of thermochemistry to interpret the energetics of chemical systems.

The application of thermochemistry to estimate additional thermochemical information is undoubtedly dependent on accurate data. Although compilations of thermochemical data are available for organic and simple inorganic molecules,[6,7] the situation for organometallic complexes is different. Because of the distinct differences of organometallic complexes relative to organic systems, application of existing organic thermochemistry to organometallics is limited. Inorganic thermochemical data are primarily available for simple binary and tertiary molecules[7] or main group molecules,[8] and parallels to large metal-centered complexes are inappropriate.

The thermochemistry of organometallic systems has gained increased attention recently, driven by their increased importance in specialized areas of chemistry.[9-11] The increased application of organometallic systems in the areas of catalysis and material sciences has led to increased investigations into the thermodynamic contributions to the reactivity of these systems. For example, knowledge of metal-carbon and metal-hydrogen bond enthalpies is essential for the understanding of catalytic reaction mechanisms that often involve metal-ligand bond cleavage.[9] Bonding energetics of metal complex ions are important for heterogenous catalysis if a complex ion is the active catalytic species.[10] Additionally, knowledge concerning the oxidation/reduction energetics of organometallic systems can be used to determine solid-state lattice or binding energies for organometallic materials and ceramics.

Most thermochemical studies of organometallic complexes have focused on the use of combustion or reaction calorimetry to determine bond energetics and heats of formation in the condensed phase.[12] Combustion calorimetry has been used to estimate condensed-phase metal-ligand bond enthalpies for model organometallic complexes (i.e. metal carbonyl and metal-arene complexes),[13] and reaction calorimetry has been used to derive metal-ligand bond enthalpies for metal complexes which are useful as homogeneous catalysts.[9] In spite of the accuracy of these techniques, there are some disadvantages. If a reaction involves more than one metal-ligand bond cleavage, the calorimetric study can yield ambiguous results. Further, the large quantities of sample needed for calorimetry, along with the thermal instability of metal complexes, renders traditional calorimeters ineffective for many organometallic systems.[9,12]

Gas-phase investigations of metal complexes can lead to intrinsic properties of a molecular species in the absence of solvent effects.[9,14-17] For example, gas-phase studies of isolated metal complexes or metal-complex ions can yield ionization energetics data[15,18-20] and bond dissociation enthalpies.[15,16] Further, direct comparison of the gas-phase energetics of metal species to their solution analogues reveals solvent effects for the metal complex system.[15-20]

Gas-phase bond enthalpy studies have frequently involved coordinatively unsaturated ionic metal species such as M^+-R, where R = H, CH_2, CH_3 and so forth.[21-23] Although these studies are useful for estimating bare metal-substituent bond enthalpies, direct solution analogues for the bare-metal ion species do not exist.

Bond enthalpies of the coordinatively unsaturated M^+-R species may deviate significantly from a related metal complex.[9] Additionally, because the bare-metal species lack supporting ligation, their stability and reactivity will not parallel that of a comparable metal complex ion. The electronic properties of supporting ligands will alter the bonding and solvation energetics for Cp_2MR^+ complexes (Cp = η^5-cyclopentadienyl) relative to M^+-R, for example.[9-11]

Numerous investigations on the stepwise bond energetics for organometallic ions such as $M(CO)_n^{\pm}$ have been determined from mass spectrometric and spectroscopic methods. For example, Norwood and coworkers have estimated the sequential Fe^+-CO bond strengths for ironpentacarbonyl by using a combination of spectroscopic and mass spectrometric techniques.[24] Recently, Schultz et al. have measured the sequential Fe^+-CO bond strengths for $Fe(CO)_5$ by mass spectrometry.[25] Further, Sunderlin et al. have recently reported the metal-ligand bond enthalpies for various transition metal carbonyl anions in the gas-phase by using mass spectrometric flow tube techniques.[26]

Another approach used to determine organometallic bond energetics has been the application of thermochemical cycles which incorporate ionization and/or reduction potentials.[15,16] A limiting factor of this technique is the accuracy of the organometallic oxidation/reduction data; auxiliary data needed for the cycles, such as ligand heats of formation and metal atom ionization energies are typically accurately known.[8,27] Thermochemical cycles can also be used to determine solvation energetics associated with metal complexes from direct comparisons of gas-phase and solution

oxidation/reduction energetics.[15-20] Understanding solvation energetics is essential for maximizing reaction efficiencies and understanding reaction pathways.[28] Moreover, analysis of the redox properties of metal-centered systems in the gas-phase and solution can be utilized to interpret condensed-phase electrostatic interactions such as ionic solvation effects,[29] acid/base reactions,[30] and electron-transfer phenomena.[31]

Ionization and reduction energetics are also useful for understanding and developing periodic and group trends for an ensemble of metal complexes.[16] For example, the electronic effects of alkylation or ligand substitution can be readily assessed by comparing relative redox potentials of a series of related metal complexes.[32] Then from an understanding of substituent electronic effects, complexes can be modified to alter reactivity.[5] Steric effects of substituents are easily rationalized as they are primarily conceptional[33] whereas electronic effects are less obvious.[2,3,5] Comparisons of ionization/reduction energies in the gas-phase enable accurate assessment of substituent electronic effects. In the condensed phase, solvent effects are predominant and often electronic effects in solution do not parallel trends observed in the gas phase.[5]

The majority of data concerning ionization energetics for organometallic complexes are either electrochemical potentials, $E_{1/2}$,[34] or vertical ionization energies, vIP, measured by photoelectron spectroscopy.[35] These data are not always appropriate for deriving thermodynamic properties of ions near or at room temperature. For example, a vertical ionization will not be a true assessment of a thermal ionization process (free energy of ionization) if the equilibrium geometries of the ion and the

neutral are significantly different.[27] Vertical ionization energies refer to an ionization process in which the geometry of the parent ion is essentially the same as the ground state neutral. Specifically, the most probable ionization transition will be that in which the positions and momenta of the nuclei remain unchanged.[36] The ion is formed with excess internal rotational and vibrational energy and is therefore not in its ground state.[27] A thermal ionization process, $\Delta G_{i,T}°$, which is similar to an adiabatic ionization energy, or $\Delta H_{i,0}$, is a process in which both the neutral and the ion are in their equilibrium geometries at temperature T.[16] At temperatures greater than $T = 0$ K, there are entropy and heat capacity contributions to the ionization process.[16,27] If the structures of a neutral and an ion are significantly different, a vertical ionization will not be an accurate assessment of the thermal ionization. Potential well diagrams which represent both vertical and thermal ionization processes are shown in Figure 1-1. Although the vertical ionization process is the most probable transition,[27,36] ion relaxation (from ion-molecule collisions,[14] for example), which removes excess rotational and vibrational internal energy, results in a thermal ionization process. The difference in vertical ionization energy and $\Delta G_i°$ is the ion relaxation energy given by E_r = vIP - $\Delta G_i°$.[16]

Electrochemistry is a useful method for evaluating redox potentials. However, electrochemical potentials for many organometallics are irreversible, making determination of a true $E_{½}$ value difficult.[34] Organometallic complexes that form unstable solvated ions will produce electrochemical responses inconsistent with gas-phase data. Although the vertical ionization energy for manganocene has been

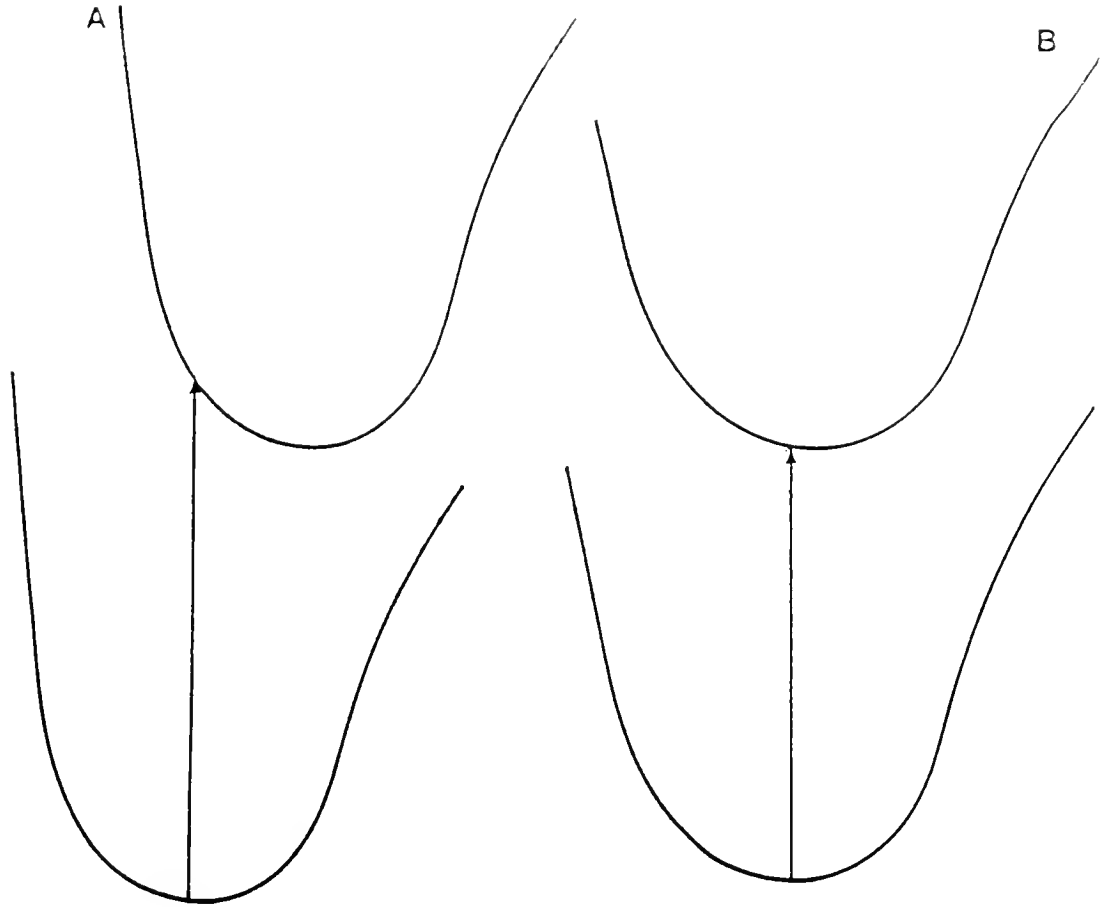

Figure 1-1 Potential well diagrams demonstrating vertical and adiabatic ionization processes. Arrows represent vertical ionization transitions. Figure A is an example in which the equilibrium geometries of the ion and the neutral are significantly different. Figure B represents a process in which the geometries of the ion and neutral are similar. For this example shown, vIP ~ aIP.

measured by photoelectron spectroscopy,[35,37,38] the $E_{½}$ value for Cp_2Mn has not been reported due to the instability of Cp_2Mn^+ in solution.[34]

The study of gas-phase electron-transfer equilibrium is a well-established means for determining thermal ionization energies for organic[39-42] and inorganic[14-20] complexes at or near room temperature. The ability to trap ions and monitor an electron-transfer equilibrium reaction is a powerful application of mass spectrometry. Previous electron-transfer equilibrium studies have been reported by several groups using various mass spectral techniques.[15,39,42] An earlier study on the electron-transfer equilibrium of the gas-phase ionization thermochemistry of ferrocene by using pulsed high pressure mass spectrometry has been reported by Mautner.[43]

In this work thermal free energies of ionization for metallocenes and metallocene derivatives have been determined from electron-transfer equilibrium studies by using Fourier transform ion cyclotron mass spectrometry, FTMS.[44-47] From the measured equilibrium constants for the electron transfer reaction, ΔG_{et}° values are determined, and the free energies of ionization are estimated for the metallocenes for the process shown below, where L represents a Cp ligand or a Cp derivative,

$$L_2M \rightarrow L_2M^+ + e^- \qquad (1\text{-}1)$$

where Cp = η^5-cyclopentadienyl. Ionization free energies for the first transition row metallocenes, ruthenocene, and osmocene are presented.[16] Metallocenes were chosen because they represent the foundation of organometallic chemistry and have numerous

applications in the areas of homogeneous catalysis,[9] material science,[48] and nonlinear optics.[49]

Following established methods,[15,16] the ionization energetics data are incorporated into thermochemical cycles to provide estimates of bond disruption enthalpies for the first transition row metallocenes and metallocenium ions.[16] Although bond enthalpies for the neutrals have been reported,[13] accurate bond enthalpy values for the metallocenium ions have only recently been established.[16]

Cyclopentadienyl ring substituent effects for metallocene complexes have been studied by electrochemistry[34] and occasionally by photoelectron spectroscopy.[35] Relatively few gas-phase studies on the substituent effects for metal complexes have been reported for comparison to the electrochemical potentials.[50,51] In this work the electron-transfer equilibrium method has been applied to a series of alkyl ferrocene[16] and nickelocene[19] derivatives to investigate the effects that substitution has on the gas-phase redox energetics of metallocene complexes. Nickelocene is a useful complex because it forms stable cations and anions in the gas-phase;[19] therefore, effects of alkylation on the positive and negative nickelocene complexes were studied. The ΔG_i° and ΔG_a° values for the metallocene derivatives are correlated with alkyl substituent parameters. Various parameterization schemes[5,52,53] are considered to interpret and understand the gas-phase investigations and electron-transfer energies. These data are potentially useful in understanding and predicting ionization energies[51] and optical transition energies for metallocene derivatives.[49] Optical transition energies are important in the selection of chromophores for potentially useful nonlinear optical

devices. Since ligand substituents affect molecular orbital energies,[5] metal complexes can be designed with specific optical transitions based on knowledge derived from gas-phase redox potentials.

The $\Delta G_i°$ values for a series of ruthenocene derivatives have been determined from electron-transfer equilibrium reactions.[20] The $\Delta G_i°$ values span over 2 eV within the series. Because of the widespread variations of the Cp ligands, bulk ligand effects were considered rather than individual ring substituent effects. A parameterization scale for correlating electronic effects for Cp type ligands was developed.[20] The application of ligand substituent effects to understanding and predicting reactivity for organometallics complexes is discussed.

Relatively little is known concerning the solvation energetics for organometallic complexes.[16] In order to better understand solvation effects of metal complex redox couples, an understanding of the intrinsic (solvent free) electron-transfer chemistry is important. Electrochemical potentials for several metallocene derivatives have been measured in order to fully characterize the effects ligation and solvation has on the redox chemistry of metal centered molecules. Thermochemical cycles, which incorporate gas-phase and solution metallocene redox potentials,[16,19,20] have been used to derive estimates of solvation energetics. Electrostatic models for predicting solvation energetics for spherical ionic species have been applied for the metallocene complexes.[15,54,55] Shortcomings and criticisms of the electrostatic model are discussed in light of the experimentally derived estimates.

Throughout this work, several important objectives are examined. The evaluation of accurate ionization and reduction potentials and detailed analyses of the data for prototypical organometallic complexes are important objectives of this work. For example, temperature-dependence studies have been determined to evaluate entropy and enthalpies of ionization for several metallocene complexes.[16] Comparisons of the experimental work to spectroscopically derived thermodynamic parameters revealed specific contributions of the ionization process. Thus, the thermodynamic origins of the ionization processes are critically analyzed.

The application of thermodynamics to predict reaction mechanisms and reactivity is another major objective of this work. The thermodynamic parameters presented in this work may be applied to other areas of research that utilize the myriad of characteristics of organometallic complexes. Existing parameterization schemes[52,53] for predicting reactivity have been successfully used to correlate thermodynamic data for the metallocenes.[16,19] Where established models fail to correlate, schemes have been developed for predicting thermodynamic values for metallocene-type complexes.[20] The application and development of the parameterization schemes for understanding and predicting chemical reactivity are discussed in detail.

A significant portion of this work is devoted to deriving and understanding metallocene/metallocenium solvation effects. Relatively little is known concerning the solvent effects for organometallic complexes. Solvation data reported here may help to further develop a foundation for understanding solvation effects for other organometallic complexes.

The development of methods for fully characterizing the thermodynamics of organometallic complexes was explored. Fourier transform mass spectrometry has proven to be a powerful tool towards fulfilling this goal. Electron-transfer equilibrium techniques are an effective means of determining thermodynamic parameters. When complimented by electrochemical studies[34] and photoelectron spectroscopy,[35] FTMS studies allow for the full characterization of redox properties for organometallic complexes. Further, the development of temperature-dependence techniques establishes FTMS as a technique for deriving reaction entropies and enthalpies for metal systems.

CHAPTER 2
ADIABATIC IONIZATION ENERGIES, BOND DISRUPTION ENTHALPIES, AND SOLVATION FREE ENERGIES OF GAS-PHASE METALLOCENES AND METALLOCENIUM IONS

Introduction

The majority of data concerning metallocene oxidation-reduction potentials is in the form of vertical ionization energies measured by photoelectron spectroscopy[34] and electrochemical potentials.[35] Several experimental limitations of these two techniques can cause uncertainty in the determination of thermodynamic reduction-oxidation potentials. Many organometallic complexes have irreversible electrochemical oxidation/reduction potentials[35] which can lead to uncertain assignments for $E_{1/2}$ values. Vertical ionization energies may differ from adiabatic potentials if the equilibrium geometries of the ion and the neutral are dissimilar.[27,36] If the equilibrium geometry of the ion and the respective neutral are similar, then the vertical potential will closely approximate the adiabatic potential which is referenced at 0 K.[27] However, even if photoelectron studies can accurately determine an adiabatic potential, values for the ionization free energy or reduction and respective enthalpy changes referenced at other temperatures must be estimated from statistical thermodynamic analyses. Spectroscopic data, which include vibrational and structural characterization, for metal complexes frequently do not exist for metal complexes.[16]

Electron-transfer equilibrium, ETE, is a powerful method for determining thermal oxidation and reduction potentials for organic and inorganic species at ambient temperatures.[15,16,39,41] Kebarle and coworkers have used pulsed high pressure mass spectrometry, PHPMS, to determine the free energies of electron attachment, $\Delta G_a°$, for organic compounds in the 0-3 eV range.[42] In the Kebarle studies, the electron attachment free energy of SO_2 was used as the reference compound to anchor the $\Delta G_a°$ values derived from electron-transfer equilibrium studies. An accurate value for the electron affinity of SO_2 has been determined from photodetachment studies by Celotta et al.[56] Additionally, sufficient spectroscopic data for SO_2 exist for complete statistical mechanical analyses of the enthalpy and entropy for electron attachment.[57] Thus, all $\Delta G_a°$ values reported from Kebarle's laboratory are referenced to $\Delta G_a°(SO_2)$ at 423 K.

In this work, Fourier transform ion cyclotron resonance mass spectrometry[44-47] has been used to determine the free energies of ionization for some first transition row metallocenes, ruthenocene, and osmocene. Derived $\Delta G_i°$ values are represented by equation 2-1, where L denotes a Cp ligand or a substituted Cp ligand.

$$L_2M(g) \rightarrow L_2M^+(g) + e^- \qquad (2\text{-}1)$$

Ionization free energies for the compounds studied in this chapter have been previously reported.[13,18] However, the derived $\Delta G_i°$ values for the metallocenes reported here differ from values of the previous study due to refinements in the free

energies of ionization for the organic reference compounds and more extensive electron-transfer studies.[16]

Entropies and enthalpies of ionization for the metallocenes have been estimated from investigating the temperature-dependence of the equilibrium constants for selected metallocene reaction couples. Statistical mechanics has been used to estimate the intramolecular entropy change for ferrocene. Available spectroscopic data for Cp_2Fe and Cp_2Fe^+, in addition to new vibrational frequency data for the ferrocenium cation, were used to estimate values for the total $\Delta S_i°$ at several different temperatures. Mautner has used PHPMS to determine the ionization free energy of ferrocene by electron-transfer equilibrium in which alkylaniline compounds were used as reference compounds.[43] Additionally, Mautner was able to assess values for the entropy and enthalpy of ionization by studying the temperature dependence studies of the measured equilibrium constants. Thermodynamic parameters for ferrocene determined in this work are compared to values reported by Mautner.

Thermochemical cycles were used to estimate differential solvation free energies and bond disruption enthalpies.[15,16,18] Values for heterolytic and homolytic M-Cp bond cleavage have been previously presented.[13] However, since bond enthalpies derived from thermochemical cycles are dependent on $\Delta G_i°$ values, new estimates are included which reflect refined $\Delta G_i°$ data in addition to more accurate thermochemical analyses. Differential solvation free energies are derived from direct comparison of $\Delta G_i°$ values in the gas phase and solution.[15,16,54] Estimates for

differential solvation free energies for several metallocene couples are compared to values predicted by a simple electrostatic model.[58]

The effects of attached substituents to cyclopentadienyl and arene ring systems have been studied previously by electrochemistry and photoelectron spectroscopy. An earlier study demonstrated that free energies of ionization for alkylferrocene derivatives correlate well with alkylbenzene analogues.[13] In the present work, $\Delta G_i°$ values derived from electron-transfer equilibrium studies for the alkylferrocene complexes are correlated with alkyl substituent parameters. Alkyl substituent parameters have been shown to correlate well with $\Delta G_i°$ data for organic compounds and chromium coordination complexes,[51] but have only recently been applied to metallocenes.[16,32] These data may prove beneficial for the interpretation and prediction of physical properties for organometallic complexes such as ionization energies or optical transition energies useful to photochemistry.[49]

Reevaluation of Metallocene Free Energies of Ionization Based on Electron-Transfer Equilibrium Studies

Electron-transfer techniques have been described elsewhere.[15,16,39,42] The general electron-transfer equilibria shown in equation 2-2 were studied where L_2M represents a metallocene and R denotes a reference compound with known $\Delta G_i°$ value. Ionization free energies for the reference compounds used in this work are typically $\pm$ 1 to 2 kcal mol^{-1}.[27,40,59]

$$L_2M + R^+ \rightleftharpoons R + L_2M^+ \qquad (2\text{-}2)$$

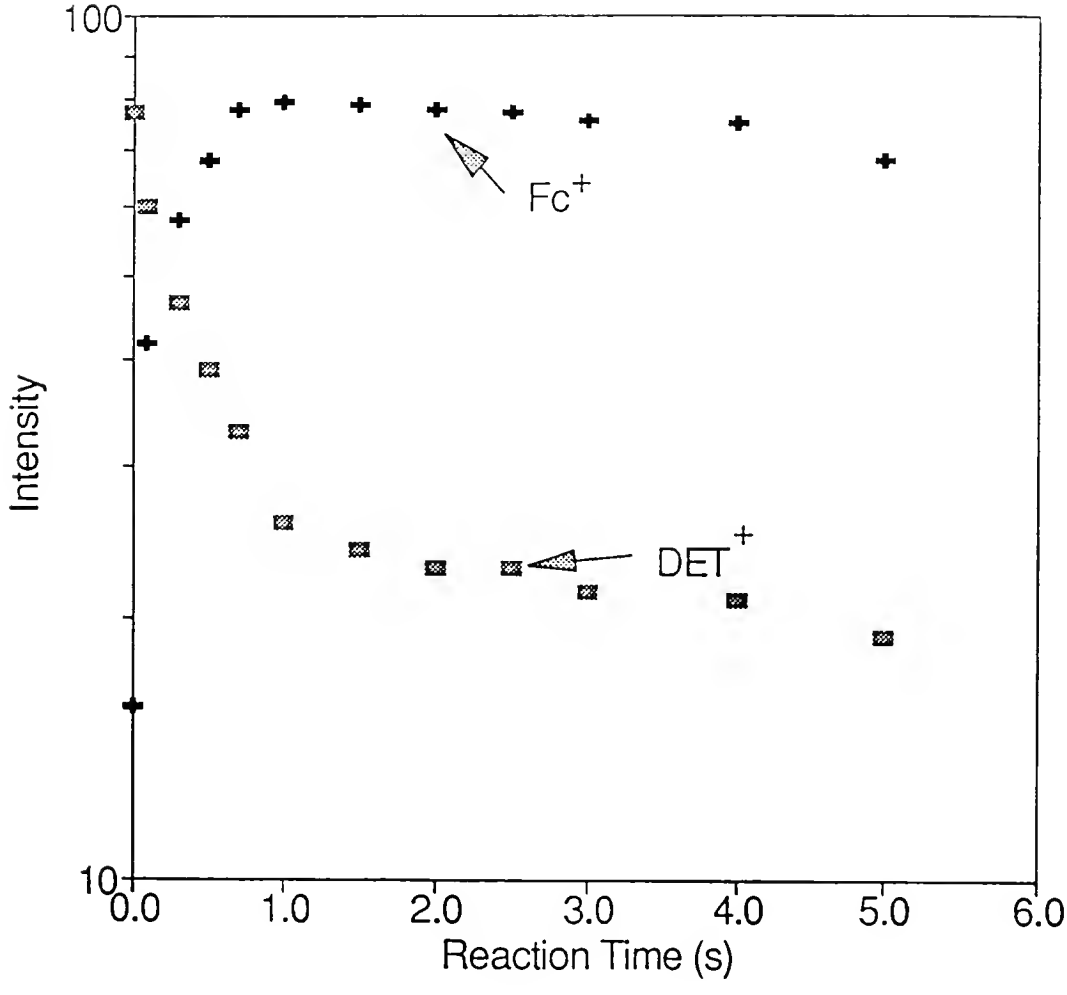

Figure 2-1 Log plot for the electron-transfer reaction of $Cp_2Fe + DET^+ = DET + Cp_2Fe^+$. Ion intensity units are arbitrary. DET = N,N-diethyltoluidine and Fc = ferrocene.

Figure 2-1 is an example of typical electron-transfer equilibrium reaction, the ferrocene/N,N-diethyltoluidine couple in this example. The decay of ion signal over time is due to diffusive loss of ions from the reaction cell of the mass spectrometer. Equilibrium constants and subsequently electron-transfer reaction free energies, ΔG_{et}°, can be determined (equation 2-3) if the difference in the ionization free energies of the two compounds is ≤ 4 kcal mol^{-1}.[10] In equation 2-3, P denotes the partial pressure and I represent the parent ion intensity for species in reaction 2-2.

$$\Delta G_{et}^{\circ} = -RT \ln K_{eq} = -RT \ln [(P(R)/P(L_2M)) * (I(L_2M^+)/I(R^+))] \qquad (2\text{-}3)$$

Equilibrium between parent ions can actually be monitored for reactions with ΔG_{et}° values approaching 5 kcal mol^{-1};[60] however, the partial pressure ratios must exceed 100, leading to large experimental uncertainties. The pressure of the minor component would only be slightly above the background pressure (ca. 1-2 x 10^{-8} Torr). Since the ΔG_{i}° value for R is known, the free energy of ionization of the metallocene at temperature T can be determined from equation 2-4. Determination of ΔG_{et}° values over a range of temperatures yields estimates of ΔH_{et}° and ΔS_{et}°.

$$\Delta G_{et,T}^{\circ} = \Delta G_{i,T}^{\circ}(L_2M) - \Delta G_{i,T}^{\circ}(R) \qquad (2\text{-}4)$$

If the enthalpy and entropy of ionization of the reference compound are known, corresponding values for the metallocenes can be derived for the appropriate

temperature range. All reactions temperatures in the present work used to derive $\Delta G_{et}°$ values are 350 K unless otherwise stated.

Reference Compounds Used in Electron Transfer Equilibrium Studies.

Appropriate reference compounds for ETE studies in the 6-7 eV range have been studied by PHPMS and ion cyclotron resonance mass spectrometry.[39,59] Lias et al. have used ETE methods to determine the ionization energies of several aniline derivatives which are used as reference compounds in the present work.[59] Reference compounds are anchored to the ionization potential value of N,N-dimethylaniline, DMA, at 350 K.[59] The ionization energy of DMA is anchored to the ionization potentials of benzene and NO_2,[39] which have been determined spectroscopically. Values of $\Delta S_i°$ for benzene and NO_2 have been estimated from statistical mechanic analyses;[39] subsequently, accurate values of $\Delta G_{i,350}°$ have been determined.

Reevaluation of the ionization thermodynamics for the reference compounds was necessary in order to determine $\Delta G_{i,350}°$ data for the metallocenes. Ionization thermodynamics used in this work for the reference compounds are based on several important assumptions:

(i) $\Delta H_i°$(DMA) = 7.12 ± 0.02 eV (164.2 ± 0.5 kcal mol^{-1}).[27]

(ii) $\Delta S_i°$ for azulene results from ΔS_{elec}. Therefore $\Delta S_i° = R \ln g$ = 1.38 cal $mol^{-1}K^{-1}$.[40] The ionization of azulene is a singlet to doublet transition in which g = 2.

(iii) Based on the reported $\Delta S_{et}°$ value from ETE studies by Nelsen and Mautner involving DMA and azulene, the ionization entropy for DMA is 2.3 cal $mol^{-1}K^{-1}$.

(iv) Based on the structural similarity, the $\Delta S_i°$ values for the aniline derivatives used as reference compounds are equal to $\Delta S_i°$(DMA).

(v) Changes in the integrated heat capacities of the reference compounds and their neutrals are negligible and will cancel. Therefore, derived $\Delta H_i°$ values are assumed to be independent of temperature in the 350-500 K range.[39]

Assumption i has been used in other studies in which N,N-dimethylaniline has been used as a reference compound.[40,43] The $\Delta G_i°$ value used here is within ± 0.01 eV of the literature value[27] and in agreement within experimental uncertainty of the $\Delta G_i°$ value used by Nelsen and Mautner. Assumption ii is quite reasonable considering the small vibrational changes expected for the ionization of azulene. Azulene and its cation are expected to be structurally similar,[16,40] therefore vibrational and rotational contributions to the ionization entropy will be negligible. Translational entropy changes for ions and their parent neutrals will be negligible since the two species differ only by the mass of an electron. Aniline derivatives are also expected to have small vibrational and rotational contributions to the total entropy change, and $\Delta S_i°$ = 2.3 cal $mol^{-1}K^{-1}$ (assumptions iii and iv) represents the electronic entropy change (singlet to doublet process, g = 2) with some contribution for ΔS_{vib} and ΔS_{rot}. Based on previous studies the $\Delta S_{et}°$ for the azulene/DMA couple[40] was reported to be

0.9 cal $mol^{-1}K^{-1}$ which results in $\Delta S_i°$(DMA) = 2.3 cal $mol^{-1}K^{-1}$. The minor effects of ΔC_p on $\Delta H_i°$ are not unreasonable especially for larger molecules. For example, $\Delta H_{i,350}$ - $H_{i,0}$ for benzene, determined from statistical mechanics, is only 0.2 kcal mol^{-1} which is negligible when compared to the much larger $\Delta H_i°$ value.[39] As will be shown later, assumption v holds true for the metallocenes.

Ionization Energetics Data for Some Metallocenes

Figure 2-2 is an electron-transfer equilibrium ladder displaying all reaction investigated in this chapter. This ladder is similar to an equilibrium ladder previously reported.[13] The $\Delta G_i°$ values in Figure 2-2 differ from those of an earlier study due to the assumptions outlined above and more extensive ETE studies. Details involving individual ETE have been discussed elsewhere.[16] Several ETE reactions performed with respect to an earlier report[13] include the following reactions couples: Cp_2V/Cp_2Fe, (EtCp)CpFe/Cp_2Fe, (EtCp)CpFe/(n-butylCp)CpFe, and temperature dependent studies of the equilibrium constant for Cp_2Fe/DET and (EtCp)CpFe/Cp_2Fe couples. Numbers adjacent to arrows in Figure 2-2 denote $\Delta G_{et,350}°$ values for individual ETE reactions. Reactions involving only reference compounds are included in the equilibrium ladder to serve as checks on the literature values.[59] Values in parentheses are unchecked literature values. Table 2-1 lists the revised $\Delta G_i°$ values for the Cp_2M compounds in addition to the vertical ionization energies measured by PES.[35] An experimental error of ± 1.5 kcal mol^{-1} is assigned to each $\Delta G_i°$ value based on experimental uncertainties of the reference compounds and errors in the

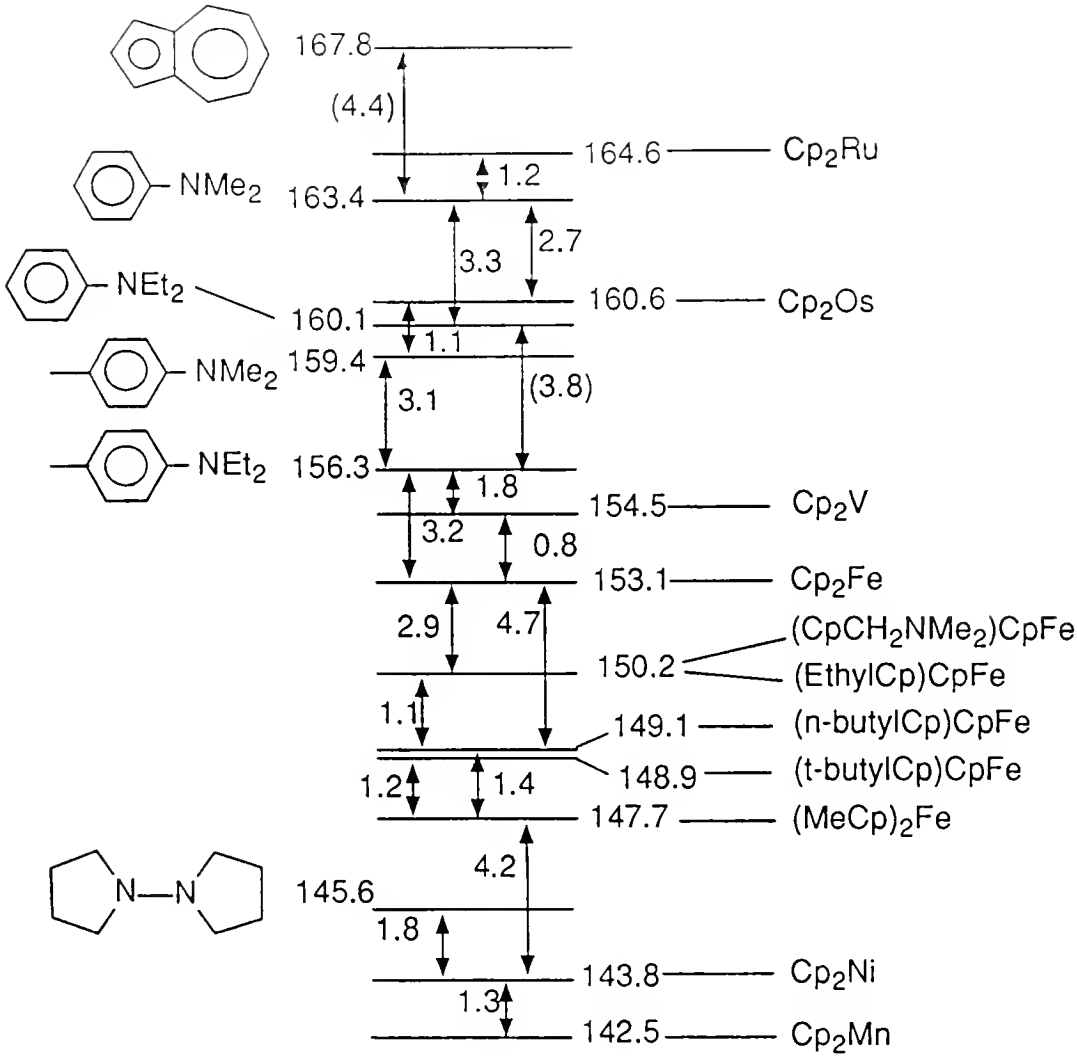

Figure 2-2 Free energy of ionization ladder for some metallocenes. Values of $\Delta G_{et}°$ lie adjacent to arrows and $\Delta G_{i}°$ values are next to the compound. All values are in kcal mol^{-1} .

Table 2-1. Ionization Energetics Data for Some Metallocenes.

Cp_2M	$\Delta G_i^{\circ a,b}$	$\Delta H_i^{\circ a}$	$\Delta S_i^{\circ c}$	vIP (PES)[a]
Cp_2V	154.5	~154	~0 ± 0.3[d]	155.7[e]
Cp_2Fe	153.1	157.2	11.6[f]	158.2[g]
Cp_2Mn	142.5	-	-	159.3[g]
Cp_2Ni	143.8	-	-	149.9[g]
Cp_2Ru	164.6	165.4	5.0[h]	171.8[g]
Cp_2Os	160.6	161.1	5.0[h]	164.9[i]

a. Units are kcal mol^{-1}.
b. Determined from the derived free energy of ionization and the estimated entropy of ionization at 350 K.
c. Units are cal $mol^{-1}K^{-1}$.
d. The ΔS_i° value is assumed to be equal ΔS_{elec}° only estimated from uncertain ion ground state.
e. See reference 37.
f. Determined from a van't Hoff plot for the Cp_2Fe/DET couple assuming ΔS_i°(DET) = 2.3 cal $mol^{-1}K^{-1}$.
g. See reference 35.
h. Value assumed to be equal to statiastical mechanics value for $\Delta S_{i,350}^\circ(Cp_2Fe)$.
i. See reference 36.

measured partial pressures of the neutral gases. Estimates of $\Delta H_i°$ and $\Delta S_i°$ for several metallocenes are also included in Table 2-1 when sufficient data were available.

The $\Delta G_i°$ for Cp_2Ni and Cp_2Mn were referenced to the $\Delta G_i°$ for 1,1'-bipyrrolidine which is anchored to the $\Delta G_i°$ value of DMA.[40] Nelsen has suggested a value for $\Delta H_i°$ = 146.9 kcal mol^{-1} for 1,1'-bipyrrolidine based upon PHPMS ETE studies. The $\Delta H_i°$ value chosen was used as a reference for nickelocene and manganocene in an earlier paper.[16] From temperature dependent studies performed by Nelsen and Mautner, a value for $\Delta S_i°$ = 3.2 cal $mol^{-1}K^{-1}$ was reported.[40] Based on the assumptions stated earlier concerning the reference compounds, a value for $\Delta G_{i,350}°$ = 145.8 kcal mol^{-1} has been estimated. The ferrocene derivatives help extend the equilibrium ladder from free energies of ionization of the alkylaniline compounds down to manganocene and the internal agreement is very good (± 0.3 kcal mol^{-1}).

The temperature dependence of the ET equilibrium constants are shown as van't Hoff plots in Figure 2-3 and the derived thermodynamic parameters are also presented in Figure 2-3. The ionization enthalpy and entropy values for ferrocene are based on the derived thermodynamic parameters values from the van't Hoff plots.

Insights into the Free Energy of Ionization of Ferrocene

The electron-transfer equilibrium reaction of ferrocene and N,N-diethyltoluidine, DET, has been studied by Mautner by using PHPMS; a value of $\Delta G_{et,350}°$ = -0.9 kcal mol^{-1} has been estimated for the couple.[43] Mautner's study covered a temperature range of 450 - 650 K, and $\Delta H_{et}°$ and $\Delta S_{et}°$ values have been

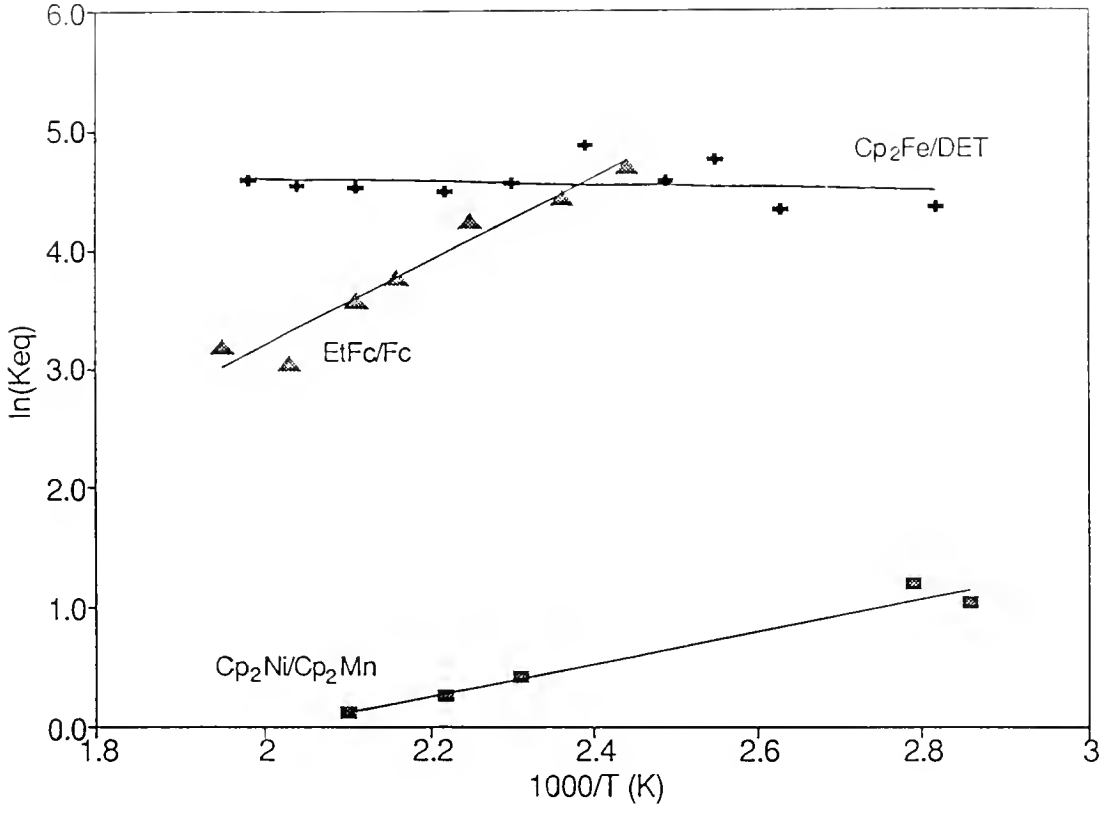

Figure 2-3 Van't Hoff plots for selected metallocene electron-transfer equilibrium couples. Values of $\Delta H_{et}°$ and $\Delta S_{et}°$ for the reaction couples are as follows. For the Cp_2Fe/DET couple, $\Delta H_{et}° = +0.05 \pm 0.47$ kcal mol^{-1} and $\Delta S_{et}° = 9.3 \pm 1.1$ cal $mol^{-1}K^{-1}$. For the EtFc/Fc couple, $H_{et}°$ and $\Delta S_{et}°$ are 3.1 ± 1.4 kcal mol^{-1} and 0.96 ± 3.6 cal $mol^{-1}K^{-1}$. For the Cp_2Ni/Cp_2Mn couple, $\Delta H_{et}° = -3.2 \pm 1.5$ kcal mol^{-1} and $\Delta S_{et}° = -5.7 \pm 3.0$ cal $mol^{-1}K^{-1}$. DET = N,N-diethyltoluidine, Fc = ferrocene, EtFc = ethylferrocene.

extrapolated to 350 K, which is the temperature at which the majority of FTMS studies were performed. From the present study, the estimated value of $\Delta G_{et,350}°$ for reaction 2-5, is -3.2 ± 0.5 kcal mol^{-1} yielding a value of $\Delta G_{i,350}°(Cp_2Fe)$ = 153.1 ± 1 kcal mol^{-1}. This value differs from a values from a previous study which reported $\Delta G_{et}°$ = -2.8 kcal mol^{-1}.[18]

$$Cp_2Fe + DET^+ \rightleftharpoons DET\ Cp_2Fe^+ \qquad (2\text{-}5)$$

The larger equilibrium constant for equation 2-5 for the FTMS study is consistent with the observation that ferrocene did not come to equilibrium with N,N-dimethyltoluidine, DMT, where an estimated $\Delta G_{et}°$ value > 5 kcal mol^{-1} is expected. The Cp_2Fe/DMT reaction couple was studied by Mautner with an estimated $\Delta G_{et}°$ = -3.9 kcal mol^{-1} at 429 K. Several electron-transfer equilibrium reactions that have been initially studied by high pressure mass spectrometry have been repeated in our laboratory with good accuracy. The electron-transfer reaction for p-cyanonitrobenzene/benzoquinone couple, (p-CNNB/BQ), equation 2-6, was studied by Grimsrud et al.[61] and $\Delta G_{et}°$ = -4.0 ± 0.8 kcal mol^{-1} was derived for the PHPMS study.

$$p\text{-}CNNB^- + BQ \rightleftharpoons BQ^- + p\text{-}CNNB \qquad (2\text{-}6)$$

The same reaction was studied by using FTMS and the derived $\Delta G_{et}°$ = -3.8 kcal mol^{-1} was determined, in good agreement with the PHPMS results.

The difference in the PHPMS and FTMS experiments for the Cp_2Fe/DET couple is much larger than expected for such comparisons and this led us to examine the reaction couple in more detail. Mautner has determined the temperature dependence of the equilibrium constants for reaction 2-5 in the 450 to 650 K range,[43] therefore the same experiment was performed by using FTMS. The thermodynamic parameters for the reaction couple derived from the PHPMS are ΔH_{et}° = -0.1 kcal mol^{-1} and ΔS_{et}° = 2.2 cal mol^{-1}K^{-1}. An FTMS temperature dependence study would serve to illustrate the origins of the differences for ΔG_{et}° between two studies and would provide thermodynamic data that would overlap in temperature with the PHPMS work.

The van't Hoff plot for the Cp_2Fe/DET couple for reaction 2-5 is shown in Figure 2-3. The temperature range in the present study is from 350 to 520 K. Consistent with the PHPMS study, the reaction displays a minor temperature dependence.[43] The derived thermodynamic values for the reaction are ΔH_{et}° = 0.05 ± 0.47 kcal mol^{-1} and ΔS_{et}° = 9.3 ± 1.1 cal mol^{-1}K^{-1} for the FTMS study. Values were determined from linear regression and are reported at the 95% confidence limit. The ΔH_{et}° value for both studies are within experimental error limits; but the ΔS_{et}° values are significantly different, the FTMS values being much more positive, and this is obviously the source of error in the ΔG_{et}° values.

Based on the assumptions outlined for the reference compounds, a value for ΔH_{i}° = 157.2 ± 1.5 kcal mol^{-1} (6.82 eV) is obtained for ferrocene. This value is 0.2 kcal mol^{-1} higher than the value obtained by Mautner because of the difference in the

chosen $\Delta H_i°$(DET). The adiabatic ionization energy obtained for both studies is well within experimental uncertainty and a value for $\Delta H_{i,0}$ can be give as 6.82 ± 0.08 eV. The vertical ionization measured by photoelectron spectroscopy by various groups is 6.88 ± 0.1 eV.[35,37,38] An adiabatic ionization potential has not been reported for ferrocene previously due to lack of vibrational fine structure in the PES valence ionization manifold. Rabalias has reported vibrational fine structure for Cp_2Fe with 35 meV separation,[62] however this has not been consistently resolved by other groups.

The source for the difference in the $\Delta S_i°$ values of the PHPMS and the FTMS studies is unclear; however, several experimental observations favor a higher value for the entropy of ionization than that reported by Mautner. The temperature dependence of other electron-transfer equilibria involving molecules and ions that have well established thermodynamic constants have been examined by using FTMS, and the entropy changes for the reaction couples are within ± 5 cal $mol^{-1}K^{-1}$ of the expected value.[10] The difference in $\Delta S_{et}°$ value for the p-CNNB/BQ reaction couple (reaction 2-6) studied by PHPMS and FTMS is ~4 cal $mol^{-1}K^{-1}$.

The temperature dependence of the electron-transfer equilibrium reaction of (EtCp)CpFe/Cp_2Fe was examined to further assess our $\Delta S_{et}°$ values for the DET/Cp_2Fe reaction. Based on the assumptions made for the reference compounds, $\Delta S_i°$(DET) = 2.3 cal $mol^{-1}K^{-1}$, therefore the $\Delta S_i°(Cp_2Fe)$ = 11.6 cal $mol^{-1}K^{-1}$. Assuming that the $\Delta S_i°$ for ethylferrocene is equivalent to that for ferrocene, the derived $\Delta S_{et}°$ for the (EtCp)CpFe/Cp_2Fe electron-transfer reaction should be ~0 cal $mol^{-1}K^{-1}$. The derived entropy change for the reaction couple was found to be approximately zero within

experimental error. Parameters for the reaction are ΔH_{et}° = 3.06 ± 1.43 kcal mol^{-1} and ΔS_{et}° = 0.96 ± 3.6 cal $mol^{-1}K^{-1}$ at the 95% confidence limit.

The organic reference compounds used in this work have ΔG_i° values that have been determined from ETE methods from PHPMS[40] and FTMS[59] studies. Mautner has determined ΔG_i° for 1,1-bipyrrolidine[40a] and the hydrazine has been linked to the alkylaniline derivatives by ferrocene and its derivatives. The internal consistency of the ladder is within 0.3 kcal mol^{-1}. Since both the PHPMS and the FTMS studies have used the same reference compounds in ETE measurements, and the internal consistency of the present equilibrium ladder is well within experimental uncertainty, the equilibrium constants obtained by FTMS for the metallocene are not expected to have large random errors.

Origins of Possible Experimental Uncertainties in the Thermodynamic Constants for Ferrocene

A possible explanation for the difference between the equilibrium constants for the ETE reaction of DET/Cp_2Fe would be inaccurate measurement of the parent ion intensity ratios due to discrepancies in the ion detection. In PHPMS studies performed by Mautner, ion sensitivities are frequently calibrated by comparing fragmentation spectra with reference spectra to insure that the mass detector is not giving biased sensitivities.[63] Reported errors due to mass detection drift in the PHPMS are ± 0.3 kcal mol^{-1} for typical ETE reactions. In FTMS experiments, mass differences between two ions can lead to differences in detection sensitivities especially if the mass difference is extremely large.[64] In this work, ion detection parameters were adjusted

to give the maximum signal for both ions. The total ion count ($I(Cp_2Fe^+)$ + $I(DET^+)$) was monitored with time and the change was determined to be small, ca. 10%. The variation of the ion intensities during the approach to equilibrium is not expected to significantly affect to the experimental uncertainties for our systems.

The most likely source of error is the measurement of the partial pressures of the neutrals. Both techniques use different methods to determine pressures of the reactant gases. It is therefore possible that systematic errors for one or both of the methods exist, leading to a difference in the equilibrium constant. The difference in the K_{eq} values for the two experiments is equivalent to a factor of 25 in the pressure ratios. Derived enthalpy changes are not dependent on pressure ratios; therefore, it is of no surprise that the $\Delta H_{et}°$ values for the two studies are in agreement. Pressures are measured directly with an ion gauge in the FTMS studies. In the PHPMS work, a solution containing known concentrations of reactants is introduced into a heated bulb and partial pressures of the reactants are calculated.[43,63] Measured partial pressures in the FTMS studies are not expected to vary by more than ± 30%, resulting in a ± 0.2 kcal mol^{-1} error in the $\Delta G_{et}°$ value.[63] In the PHPMS studies, pressures are monitored by measuring K_{eq} at various partial pressure ratios. Mautner reports that experimental error due tp pressure fluctuations are ± 0.5 kcal mol^{-1}.

Evaluation of the Electron-Transfer Reaction Rates for the Cp_2Fe/DET Couple

The rates of the ion-molecule reactions for the Cp_2Fe/DET couple were examined to further support that the source of error between the PHPMS work and the

FTMS studies stems from inaccurate pressure determinations. Electron-transfer reaction kinetics for ferrocene with DMT and DET have been investigated by using PHPMS. Mautner reports values for k_f for reaction 2-5 of 1.2 x 10^{-9} cm^3 $molec^{-1}s^{-1}$ at 461 K and 1.7 x 10^{-9} cm^3 $molec^{-1}s^{-1}$ at 429 K for the Cp_2Fe/DMT couple (reaction 2-7). By using FTMS, k_f = 2.5 ± 0.5 x 10^{-10} cm^3 $molec^{-1}s^{-1}$ for reaction 2-5 was

$$Cp_2Fe + DMT^+ \rightarrow DMT + Cp_2Fe^+ \qquad (2\text{-}7)$$

determined. The FTMS value of k_f for reaction 2-7 was determined to be 1.3 ± 0.3 x 10^{-10} cm^3 $molec^{-1}s^{-1}$. Mautner's rate constant for reaction 2-5 is slightly faster than the Langevin collision limit while the present values for k_f is ca. 25% of the Langevin collision limit. The two rate constants for reaction 2-5 differ by a factor of 5 and do not resolve the disagreement in the derived $\Delta G_i°$ values for ferrocene.

For example, if the PHPMS value for K_{eq} is assumed to be correct, then the pressure ratio determined in the FTMS work, $P(DET)/P(Cp_2Fe)$, is too large by a factor of ~25. This would lead to an overestimation of k_f by a factor of ~25, depending on the errors in the absolute partial pressures of DET and ferrocene. Thus, the k_f values for the two experiments would diverge if the pressure of ferrocene, for example, was underestimated.

By examination of equation 2-8, if the pressure for ferrocene was incorrectly underestimated, the equilibrium constant, and thus $\Delta G_{et}°$ would be too large since there exists an inverse relationship between $P(Cp_2Fe)$ and K_{eq}. Moreover, an

$$K_{eq} = \ln [(P(DET)/P(Cp_2Fe)) \times (I(Cp_2Fe^+)/I(DET^+))] \quad (2\text{-}8)$$

underestimation of the reaction pressure of ferrocene would lead to a value for k_f that is slower than determined. Reaction pressure and k_f are inversely related, therefore if the total pressure of a reaction is actually greater than measured, the rate constant for the reaction will be slower than the experimentally determined k_f value. Thus, it obvious that comparison of the rate constants for the Cp_2Fe/DET couple do not resolve the discrepancies for the two experiments.

Based on previous FTMS studies involving electron-transfer reactions of metallocenes,[14] it seems unlikely that such large errors in the measured partial pressures could occur. The same electron-transfer methods have been applied to the study of metallocene self-exchange and cross reactions.[14] Estimated reaction efficiencies for exothermic cross reactions were in the 0.5-1.5 range which suggests that partial pressure errors may be incorrect by as much as 50%. Reaction efficiencies are given by equation 2-9, where an estimate of k_L for the metallocenes, the Langevin collision rate, is 1.0×10^{-9} cm^3 $molec^{-1}s^{-1}$.[14]

$$\text{Efficiency} = k_f/k_L \quad (2\text{-}9)$$

An observed efficiency of ~0.2 is not unexpected for a reaction with low exothermicity. The reported FTMS self-exchange rate constant for $Cp_2Fe^{+/0}$ is 2.7×10^{-10} cm^3 $molec^{-1}s^{-1}$ (0.27 efficient)[14] which is consistent with the present k_f for the

DET/Cp_2Fe couple. Alternatively, large pressure errors in the PHPMS work also seem improbable since ferrocene in not susceptible to thermal decomposition in the temperature range used.[65] Although there are distinct differences in the observed forward rates for reaction 2-5, the kinetic data does not expose the origin for difference in the two experiments.

A Brief Survey of Proton-Transfer Reactions of Ferrocene

The kinetics and thermodynamics of the protonation of ferrocene have been studied by several groups by using PHPMS[43,66] and ion cyclotron resonance mass spectrometry.[67] Recently, PHPMS proton-transfer equilibria studies performed by Ikonomou and Kebarle assessed a value for $\Delta G_B°$ for ferrocene of 195.2 ± 1.0 kcal mol^{-1} at 500 K.[66] A value for $\Delta G_B°(Cp_2Fe)$ = 195.0 ± 1.5 kcal mol^{-1} at 600 K has been estimated from PHPMS data obtained by Mautner.[43] The term $\Delta G_B°$ is the gas-phase bacisity (the free energy of proton attachment), and differs from the proton affinity, which is an enthalpy change, $\Delta H_B°$, referenced at 298 K.

The proton-transfer reaction 2-10 was studied by using FTMS in order to gain additional information concerning discrepancies in the $\Delta G_i°(Cp_2Fe)$ values reported here and by Mautner. The proton-transfer equilibrium reaction 2-10 has also been studied by both Mautner[43] and Ikonomou[66] and the reported free energy changes are -1.2 and -1.9 kcal mol^{-1} respectively. A value of $\Delta G_{350}°$ = -1.5 kcal mol^{-1} was

$$PyrroleH^+ + Cp_2Fe = Cp_2FeH^+ + Pyrrole \qquad (2\text{-}10)$$

derived from FTMS studies of reaction 2-10 and this value is consistent with the two PHPMS $\Delta G°$ values. The difference in the $\Delta G°$ values for the FTMS study and the PHPMS work results in a factor of ~1.5 in the measured equilibrium constants. A factor of 25 in K_{eq} for the proton-transfer reactions, which is the difference in the K_{eq} values for reaction 2-5, would yield a value of $\Delta G_{350}°$ ~3.6 kcal mol^{-1} for reaction 2-10. As all three studies yield equivalent $\Delta G°$ values for reaction 2-10, evaluation of proton-transfer reactions does yield inforamtion concerning the discrepancies in the $\Delta G_i°$ values for ferrocene. Furthermore, the $\Delta G_B°$ estimated by Beauchamp and Stevens[67] from ICRMS experiments is consistent with all three proton-transfer studies.

Intramolecular Entropy Changes for the Ferrocene/Ferrocenium Couple

In order to further understand the uncertain entropy change for the $Cp_2Fe^{+/0}$ couple, detailed statistical mechanical analyses have been performed to provide an accurate estimate for $\Delta S_i°(Cp_2Fe)$. Table 2-2 lists values for translational, rotational, vibrational, and electronic entropies of ferrocene and ferrocenium ion at several temperatures. Complete vibrational analyses for all 57 vibrational modes of ferrocene have been reported by Bodenheimer and Low[68] and the measured frequencies were used in the vibrational entropy analysis. Although a complete vibrational analysis for the ferrocenium cation has not been performed, sufficient vibrational frequency assignments for Cp_2Fe^+ have been reported by several groups to allow for an estimate of $S_{vib}°(Cp_2Fe^+)$.[69-71] Additionally, crystal structures for both ferrocene and

Table 2-2. Calculated Entropies and Integrated Heat Capacities for Ferrocene and Ferrocenium Ion at 298, 450, and 600 K.

	Cp_2Fe (298K)	Cp_2Fe^+ (298K)	Cp_2Fe (450K)	Cp_2Fe^+(450K)	Cp_2Fe (600K)	Cp_2Fe^+ (600K)
$S°_{trans}$ [a]	41.6	41.6	43.6	43.6	45.0	45.0
$S°_{rot}$ [a,c]	24.3	24.4	25.5	25.6	26.4	26.6
$S°_{int\ rot}$ [a]	5.24	5.24	5.75	5.75	6.12	6.12
$S°_{vib}$ [a,d]	14.88	17.19	30.17	32.97	45.84	48.89
$S°_{elec}$ [a,e,f]	$^1A_{1g}$ q = 1 S° = 0	$^2E_{2g}$ q = 2.07 S° = 1.7	$^1A_{1g}$ q = 1 S° = 0	$^2E_{2g}$ q = 2.22 S° = 2.02	$^1A_{1g}$ q = 1 S° = 0	$^2E_{2g}$ q = 2.55 S° = 2.25
$S°_{total}$ [a]	86.0	90.1	105.0	109.9	123.4	128.9
$\Delta H°_T - \Delta H°_{0K}$ [b]	5.3	5.7	12.3	13.0	21.7	22.6

a. Units are cal $mol^{-1}K^{-1}$.
b. Units are kcal mol^{-1}.
c. Entropy of rotations calculated by assuming Cp-Fe behaves as a linear rigid rotor.
d. Vibrational entropy was calculated for all vibrational modes.
e. $S°_{elec,T} = -R\ln(q) + E_{therm,T}$.
f. The $^2E_{2g}$ orbitals are split due to spin-orbit coupling (~700 cm^{-1}). See reference 77.

ferrocenium cation have been reported providing information needed for determining of the rotational entropy change for the $Cp_2Fe^{+/0}$ couple.[72,73].

Low-frequency metal-ligand vibrations can contribute significantly to entropy changes of metal complex redox processes if M-L frequency shifts drastically change upon oxidation or reduction. For example, changes in the skeletal Co-N vibrations for the $Co(NH_3)_6^{2+/3+}$ redox couple result in an estimated entropy change of 12.6 cal $mol^{-1}K^{-1}$.[74] The change in the asymmetric T_{1u} vibration alone accounts for ~3 cal $mol^{-1}K^{-1}$ or ~25% of the total skeletal vibrational entropy change for the $Co(NH_3)_6^{2+/3+}$ couple.[74]

The doubly-degenerate Cp-Fe-Cp bend has not been reported previously, but the corresponding mode for ferrocene has a relatively low frequency, υ_{22} = 179 cm^{-1}.[68] Because of the importance of this low frequency skeletal mode, rather than estimate a value for υ_{22}, the Cp-Fe-Cp frequency for ferrocenium ion was measured. Our far-infrared studies have conformed υ_{22} for ferrocene and tentatively assign a value of 135 cm^{-1} for $\upsilon_{22}(Cp_2Fe^+)$. The Fe-Cp distance increases upon oxidation, and this distance increase is expected to result in a lowering of the frequency for the υ_{22} metal-ligand bending mode.[72] This single shift in the bending mode contributes 1.0 cal $mol^{-1}K^{-1}$ to the $\Delta S_i°(Cp_2Fe^{+/0})$ at 298 K. The results of the far-IR studies for several ferrocenium salts are given in Table 2-3.

An estimate of $\Delta S_{et}°$ for the electron-transfer equilibrium reaction at 450 K can be determined by combining the calculated entropy of ionization for ferrocene (4.9 cal $mol^{-1}K^{-1}$) with the assumed value of $\Delta S_i°$(DET) = 2.3 cal $mol^{-1}K^{-1}$ giving a value for

Table 2-3. Vibrational Frequencies For Various Ferrocenium Salts

Compound	Frequency (υ_{22}) Cp-Fe-Cp Bend	$S°(\upsilon_{22})^a$ cal $mol^{-1}K^{-1}$
$(Cp_2Fe^+)(Cl^-)$	135 cm^{-1}	5.7
$(Cp_2Fe^+)(BF_4^-)$	140 cm^{-1}	5.6
$(Cp_2Fe^+)(PF_6^-)$	130 cm^{-1}	5.8
Cp_2Fe	179 cm^{-1}	4.7

a. Contribution of υ_{22} doubly degenerate mode to the vibrational entropy at 298 K.

ΔS_{et}° = 2.8 cal $mol^{-1}K^{-1}$ for reaction 2-5. Assuming that the statistical mechanics calculations provide a good estimate for $\Delta S_i^{\circ}(Cp_2Fe)$, this analysis supports the PHPMS temperature dependence study of reaction 2-5. However, use of solid-state vibrational frequencies for gas-phase ferrocenium ion may not be valid, therefore the estimated value for ΔS_i° may be different from the true value. Gas-phase vibrational frequencies for metal-ligand modes may be significantly shifted to lower frequencies relative to the solid-state since crystal lattice stabilization is lost in the gas-phase.

Vibrational Entropy Calculations for the Ferrocene/Ferrocenium Couple

Since only a limited number of published vibrational frequencies for Cp_2Fe^+ exist, several frequencies for the cation were estimated from the known vibrational frequency changes of ferrocene and ferrocenium. From known vibrational frequencies of the ion and neutral that were measured (Table 2-4), the percent change in the vibrational force constant was calculated. It was assumed that for a specific vibrational mode, the percent change for an anologous mode which has not yet been measured would be equivalent. For example, the symmetric ring-distortion mode, υ_{28}, for both the cation and the neutral have been measured,[68] where υ_{28} is 597 cm^{-1} for ferrocene[68] and 471 cm^{-1} for Cp_2Fe^+.[69] The corresponding force constants are 3.26 mdyne $Å^{-1}$ and 2.04 mdyne $Å^{-1}$ respectively. Equation 2-11 was used to determine vibrational force constants from measured frequencies where υ is converted to energy, E, μ is the reduced mass for the vibrational mode, k is the vibrational force constant, and h is Plank's constant.[75]

$$E = (h/2\pi)*(k/\mu)^{1/2} \quad (2\text{-}11)$$

Thus, as demonstrated by the scheme below, an estimate for the vibrational force constant for the unsymmetrical υ_{34} mode, which is the asymmetric analogue to υ_{28}, was calculated. Note that the υ_{34} and the υ_{28} modes correspond to degenerate low-energy ligand distortions perpendicular to the principle molecular axis.

$k(Cp_2Fe)$ for υ_{28} = 3.26 mdyne $Å^{-1}$

$k(Cp_2Fe^+)$ for υ_{28} = 2.04 mdyne $Å^{-1}$

Δk_{28} = 0.63 and assume $\Delta k_{28} \approx \Delta k_{34}$ (degenerate modes)

$k(Cp_2Fe)$ for υ_{34} = 2.97 mdyne $Å^{-1}$

$k(Cp_2Fe^+)$ for υ_{28} = (0.63 * 2.97) mdyne $Å^{-1}$ = 1.86 mdyne $Å^{-1}$

From equation 2-11, $\upsilon_{34} \approx 450$ cm^{-1}.

Vibrational entropy contributions for individual frequencies were calculated from equation 2-12. The value of u is dependent on the frequency of the vibration and the absolute temperature, shown in equation 2-13. From equation 2-12, entropies for all vibrational frequencies were calculated for ferrocene and ferrocenium ion. Table 2-4 lists the frequencies used in the vibrational entropy calculations; literature

$$S_{vib}^\circ = R[(u/eu - 1) - \ln (1 - e^{-u})] \quad (2\text{-}12)$$

$$u = 1.4387(\upsilon/T) \quad (2\text{-}13)$$

Table 2-4 Vibrational Frequency Data for Ferrocene and Ferrocenium Cation

No.[a]	$Cp_2Fe(\upsilon)$[b]	$Cp_2Fe^+(\upsilon)$	Cp_2Fe^+ Reference
1	3110	3110	Estimated
2	814	805	Estimated
3	1102	1102	Estimated
4	309	304	Ref. 70
5	1255	1258	Estimated
6	c	c	c
7	1250	1250	Estimated
8	3103	3100	Ref. 69
9	820	782	Ref. 69
10	1110	1110	Ref. 69
11	478	418	Ref. 69
12	3068	3068	Estimated
13	998	1005	Estimated
14	844	833	Estimated
15	1410	1412	Estimated
16	389	398	Ref. 70
17	3077	3100	Ref. 69
18	1005	1017	Ref. 69
19	855	846	Ref. 69
20	1410	1420	Ref. 69
21	492	490	Ref. 69
22	179	135	d
23	3100	3100	Estimated
24	1191	1192	Ref. 69
25	1058	1058	Ref. 69
26	1356	1356	Estimated
27	897	874	Ref. 69
28	597	471	Ref. 70
29	3085	3085	Estimated
30	1189	1192	Ref. 69
31	1055	1055	Ref. 69
32	1351	1351	Estimated
33	885	874	Ref. 69
34	569	450	Estimated

a. Vibrational frequency assignments from reference 68.
b. All Cp_2Fe vibrational frequencies from reference 68.
c. Torsional vibration determined as internal rotation.
d. Measured frequency.

sources are included when available. All frequencies for ferrocene used in this work were measured by Bodenheimer and Low.[68]

Vibrational entropy calculations based on spectroscopic data assume that molecular vibrations behave as harmonic oscillators, therefore the displacement force is equal to the restoring force.[55] Atomic systems typically deviate from harmonic conditions and corrections for anharmonicity must be considered for more complete calculations. However, the harmonic formula is an accurate first approximation for $S_{vib}°$ quantities.

Translational and Rotational Contributions to the Entropies

The translation entropy of an ideal gas is dependent on the molecular weight and the temperature of the species. For ionization processes, the molecular weight of the ion and the neutral are essentially equal, therefore the translational contribution at temperature T to $\Delta S_i°$ is 0 cal $mol^{-1}K^{-1}$. In order to report accurate $\Delta S_i°$ estimates for Cp_2Fe and Cp_2Fe^+, translational entropies were determined for completeness. The Sackur-Tetrode equation[76] (equation 2-14) was used to estimate $S_{trans}°$ values, where

$$S_{trans}° = R(3/2 \ln M + 5/2 \ln T) - 2.315 \text{ cal mol}^{-1}\text{K}^{-1} \qquad (2\text{-}14)$$

M is the molecular weight, R is the ideal gas constant, and T is the temperature.

Rotational entropies were calculated by assuming that ferrocene behaves as a linear rigid rotor and that the Cp rings are point masses of 65 a.m.u. Rotational

entropies are dependent on the moments of inertia I of the molecule, therefore by choosing the Fe atom to lie at the center of gravity of the molecule, the moments of inertia for Cp_2Fe were calculated. Since the Fe atom is defined to lie at the origin of the cartesian axes, I_x and I_y are equal (corresponding to rotations perpendicular to the principle axis). The rotational moment of inertia along the principle axis was defined as I_z. Here, the Cp rings where considered as mass with five-fold rotational symmetry rather than point masses. The product of the three principle moments of inertia yields a determinant D which is used in estimating S_{rot}° (equation 2-15).[55] The symmetry number σ for ferrocene is 10 based on D_{5d} molecular symmetry.[72] Note that D_{5h} symmetry, for an eclipsed structure, will also yield $\sigma = 10$.

$$S_{rot}^\circ = R(1/2 \ln D \times 10^{117} + \ln T - \ln \sigma) - 0.033 \qquad (2\text{-}15)$$

Because of the low energy barrier, the Cp rings of ferrocene freely rotate at ambient temperatures.[72] Therefore, rather than consider rotation of the Cp ligands as a torsional vibration, the internal rotational entropy was estimated as a restricted internal rotation. The potential barrier of rotation $V = 0.9$ kcal mol^{-1}.[72] The moment of inertia for the system is given as $I_r = (I_z)^2/2I_z$, where I_z is the rotational moment of inertia along the principle axis. Therefore, using the method outlined by Brewer and Pitzer,[55] S_{int}° for was estimated. The internal rotational entropy for a restricted rotation is calculated from the entropy of free rotation along the principle axis minus

the restriction energy associated with rational barrier. Since I_z for both ferrocene and ferrocenium are equal, $\Delta S_{int} = 0$ cal mol^{-1}K^{-1}.

Electronic Entropy Considerations for the Ferrocene/Ferrocenium Couple.

The electronic energy level separations of a molecule are usually large, and at ambient temperatures only the ground state is thermally populated.[55] The electronic partition function q is used to determine S_{elec} values where $q_e = g$, the spin degeneracy of the ground state. Thus, in the absence of thermally accessible energy levels, the electronic entropy is given by $S = R \ln(g)$. In the case of ferrocene, the spin multiplicity is 1 and $S_{elec} = 0$ cal mol^{-1}K^{-1}. Ferrocenium is a ^{2}E complex, however the ^{2}E state is spit due to spin-orbit coupling with ~700 cm^{-1} separation.[77] Since the split states are thermally accessible in the 298 - 600 K range, the value of q_{elec} was evaluated which includes the theraml energy of the split electronic states. The electronic entropy of Cp_2Fe^+ is given as $S_{elec,T} = E_{therm,T} + R \ln(g)$, where $E_{therm,T}$ is the energy of the thermal population of the split states at temperature T.

Ionization Free Energies of Ruthenocene and Osmocene

Discussion of the ionization free energies of ruthenocene and osmocene has been reported previously.[16] The observed trend in $\Delta G_i°$ values for the iron triad is consistent with vertical ionizations[35,78] (IP $Cp_2Fe < Cp_2Os < Cp_2Ru$).

Lichtenberger and Copenhaven were able to obtain vibrational fine structure for the first ionization manifold of osmocene.[78] An average spacing of 42.1 meV for the

spacing of vibrational energy levels in the first ionization manifold for the cation was used to determine the adiabatic ionization energy for osmocene of 161.1 kcal mol^{-1}. Assuming the $\Delta S_i°$ for osmocene is equal to $\Delta S_i°(Cp_2Fe)$ estimated from statistical mechanics, the estimated osmocene aIP for Cp_2Os is 162 kcal mol^{-1}. Thus the two techniques are within experimental error.

Free Energies of Ionization for Vanadocene, Manganocene, and Nickelocene

The sharpness of the first ionization band in the PES of vanadocene indicates that the difference in the equilibrium geometries of the ion and neutral are small.[37,38] A recent PES of Cp_2V assigns the vIP = 155.7 ± 0.1 kcal mol^{-1}.[16] As the first ionization manifold is a sharp band (width = 0.19 eV), the aIP is closely approximated by the vIP. The $\Delta G_i°$ value from ETE studies is 154.5 ± 1.5 kcal mol^{-1}. Assuming $\Delta S_i°$ is predominately the electronic entropy change for vanadocene (ΔS_{vib} ~0 based on the PES) the $\Delta H_i°$ is estimated at 154 ± 2 kcal mol^{-1}. The estimated $\Delta H_i°$ value is slightly less than the estimated aIP but lies within the band envelope.

The $\Delta G_i°$ for nickelocene is in agreement with PES data; however,[35] the $\Delta G_i°$ of manganocene is ~18 kcal mol^{-1} lower than the reported vIP values.[35,37,38] The relaxation energy for Cp_2Mn is large compared to other metallocenes. Manganocene exists as a high-spin complex with only a small percentage of the complex in a low-spin configuration.[79] From PES studies the vIP of the low-spin complex has been assigned (~144 kcal mol^{-1}) and is in agreement with the $\Delta G_i°(Cp_2Mn)$.

The temperature dependence of the Cp_2Mn/Cp_2Ni ETE reaction couple was investigated to assess the expected negative intramolecular entropy change for the $Cp_2Mn^{+/0}$ couple. The van't Hoff plot in Figure 2-3 indicates that the Cp_2Mn/Cp_2Ni ETE reaction couple is strongly temperature dependent with a negative $\Delta S_{et}°$. Details of the Cp_2Mn/Cp_2Ni ETE couple have been presented elsewhere.[13] The origin of the large negative entropy change is primarily attributed to $\Delta S_i°(Cp_2Mn)$. The estimated change in the metal to ring-centroid distance for Cp_2Mn/Cp_2Mn^+ is ~0.25 Å[80] resulting in a large change in vibrational and rotational entropy for the $Cp_2Mn^{+/0}$ couple. The Mn-C distance will decrease upon oxidation leading to a negative $\Delta S_{vib}°$. As spin degeneracy is conserved, $\Delta S_{elec}(Cp_2Mn^{+/0})$ is essentially zero. However, due to spin orbit coupling of the ^3E state of the ion, ΔS_{elec} for manganocene will be greater than that of manganocenium ion. This is consistent with a net negative entropy change expected for $Cp_2Mn^{+/0}$. The rotational entropy change is estimated to contribute 0.6 cal $mol^{-1}K^{-1}$ to $\Delta S_i°$ based on the estimated change in the Mn-Cp distance accompanying ionization. Thus estimated vibrational, rotational, and electronic entropy changes for manganocene are all negative and are consistent with the negative $\Delta S_{et}°$ observed for the Cp_2Mn/Cp_2Ni ETE couple.[16]

Substituent Effects in Ferrocene Derivative Oxidations

Although extensive photoelectron spectroscopy studies of the ionization energetics of metallocenes have been reported,[35] little is known concerning the effects substituents have on metallocene thermochemistry. Therefore, various ferrocene

derivatives have been studied by ETE methods in order to assess the effect alkylation of the cyclopentadienyl rings has on the ionization potentials of metallocenes. Free energy of ionization data for several alkylferrocene complexes have been reported earlier[16] and a ΔG_i° value for ethylferrocene is reported here. Values of ΔG_i° differ from other values previously reported[13] due to modifications in the ΔG_i° values of the reference compounds.

It is known from PES data that dimethylation or permethylation of metallocenes lower the ionization energies.[35] The vertical ionization energy of ferrocene (6.88 eV) is ~0.2 eV greater than the vIP of 1,1'-dimethlyferrocene[35] and 1 eV more endoergic than the vIP of decamethylferrocene.[37] Attachment of alkyl groups on the metallocene rings stabilizes the molecular cation relative to the neutral compound, thus lowering the free energy of ionization of the derivative relative to the parent metallocene.[32,35] Electron-transfer equilibrium results for alkylferrocene derivatives studied in the present work are shown in Figure 2-2.

Molecular ionization potentials of organic[81] and organometallic compounds[32,51] have been correlated previously with Taft substituent parameters. The aliphatic σ_I parameters were derived originally for substituted acetic acids, and they have been used successfully to correlate IP data.[51,52,81] For example, a plot of IP for benzene-R chromiumtricarbonyl derivatives versus σ_I(R), where R is an attached substituent, shows a strong correlation line.[51] The equation used by Levitt and coworkers for the Taft analyses is given in eq 2-16, where IP(M-R) and IP(M) are the ionization potentials for the derivative and the parent compound respectively, σ_I is the Taft

$$IP(M\text{-}R) = a_I\sigma_I(R) + IP(M) \qquad (2\text{-}16)$$

parameter for R, and a_I is the slope of the line. The Taft parameter for H is zero thus the substituent effects are referenced to hydrogen.[5] The slope a_I indicates the sensitivity of the ionization process to the change in substituents.[81]

A plot employing equation 2-16 for the ferrocene derivatives is shown in Figure 2-4. The slope of the line is 57 ± 6 kcal mol^{-1} which can be compared to that for the $(RBz)Cr(CO)_3$ compounds, a_I = 34.6 kcal mol^{-1}, and alkylbenzenes, a_I = 109.3 kcal mol^{-1}.[51] Therefore, alkylferrocene ionization energies are nearly twice as sensitive to changes in alkyl substituents as the chromium arene complexes but are less affected than the alkylbenzenes.[51] The $\Delta G_i°$ data here is consistent with the results of Matsumura-Inoue and coworkers who correlated PES data of Cp_2Fe derivatives with Taft parameters.[32] The differences in substituent effect sensitivity for various parent compounds can be rationalized by several factors, including proximity of substituents to the site of ionization.[81] Additionally, electronic coupling between the alkyl σ orbitals and the ionized molecular orbital may direct changes in the ionization potentials with respect to the parent compound.[16] It should be noted that although the observed substituent effects in alkylferrocenes follow the trend of expected "electron-releasing" ability of the alkyl substituents, the observed sensitivity of ionization energies to substitution will not necessarily hold for other metallocenes.[16,19] Electron loss originates from different valence molecular orbitals for the metal complexes.[35]

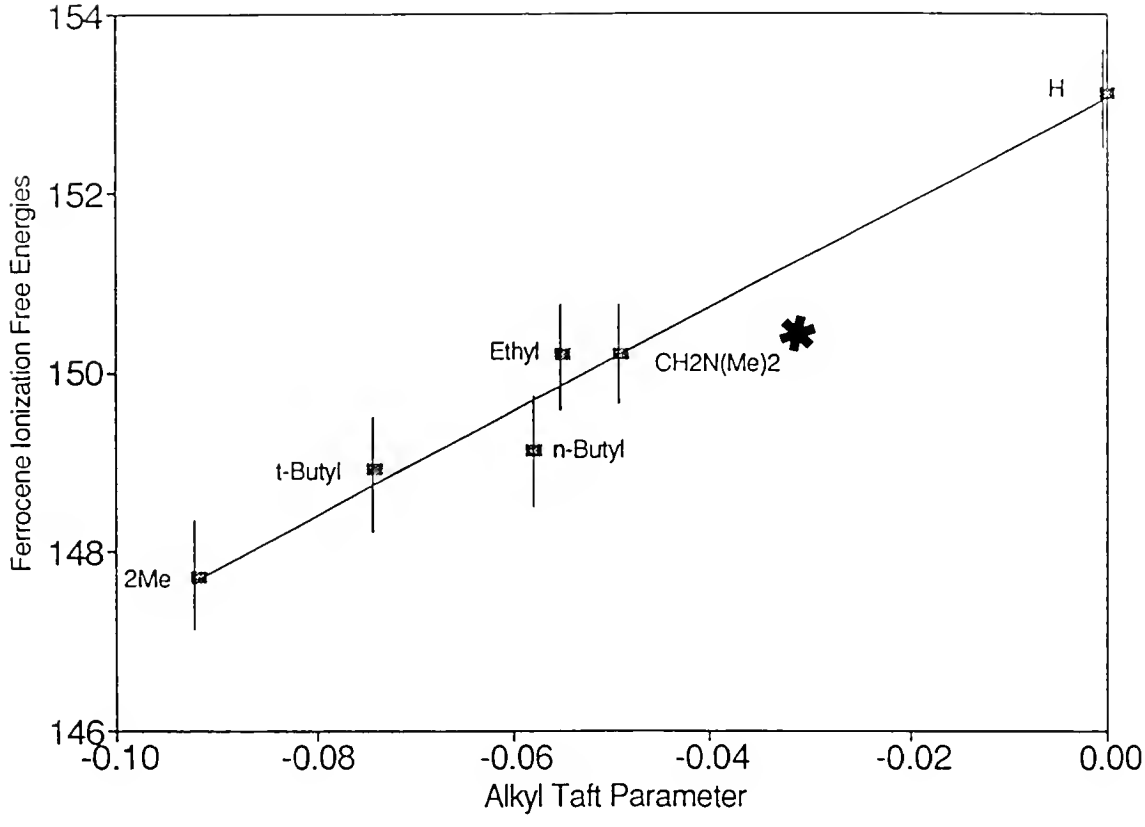

Figure 2-4 Plot of $\Delta G_i°$ values (kcal mol^{-1}) versus alkyl Taft parameters (σ_I) for several ferrocene derivatives. Asterisk indicates new Taft parameter for $CH_2N(CH_3)_2$.

Further, the electron-releasing character of the alkyl groups observed for the ionization of neutral metallocenes does not necessarily apply in other circumstances. For example, the substituent effects for electron attachment to neutral metal complexes has been shown to be different than for ionization process.[19,82]

With respect to the construction of Taft parameter correlations such as that in Figure 2-4, it is notable that parameters for substituents with low ionization potentials can be derived from the data for ferrocene derivative ionizations. For R = CH_2NMe_2, the first ionization of the benzene derivative removes an electron from the nitrogen lone-pair orbital and not from the benzene ring, which would be a more endoergic process. The ionization of benzene is 9.25 eV,[27] which is significantly more endoergic than the ionization potential of N,N-dimethylaminobenzene (7.69 eV).[27] However, in the case of $(CpCH_2NMe_2)(Cp)Fe$, the ionization occurs at the same site as in the other alkylferrocenes, thus allowing derivation of a σ_I parameter for the substituent (-0.049 ± 0.013).

Heterolytic and Homolytic Metal-Ligand Bond Disruption Enthalpies for Metallocenes and Metallocenium Ions

Bond disruption enthalpies for several metallocenes have been reported previously[16] therefore only a brief discussion concerning M-Cp bond enthalpies will be give here. Thermochemical cycles have been used to derive estimates of M-Cp bond disruption enthalpies.[10,16] Since $\Delta H°$ values depend on ionization energetics data, M-Cp bond enthalpies reported here differ from previously reported[13] values due to more accurate free energy of ionization data for the metallocenes and more accurate

assessment of auxiliary thermochemical data.[16] Additionally, more detailed error analysis was performed for the heterolytic and homolytic bond disruption enthalpies and in most cases error limits were found to be lower than previously reported.[13]

Application of Thermochemical Cycles to Derive Estimates for Metallocene and Metallocenium Bond Disruption Enthalpies

Thermochemical cycles for ionization processes of the metallocenes and their corresponding ions used to derive bond enthalpies data are shown in Figure 2-5. The bottom portion of the figure is a cycle used to derive solvation energetics for the metallocenes which will be discussed later. Similar cycles have been used by Buckingham and Sargeson to derive crude estimates for metal complex thermodynamic quantities.[83] Related thermodynamic quantities have recently been derived for coordination complexes and complex ions by use of analogous thermochemical cycles.[84] In Figure 2-5, the term $\Delta X°$ represents any thermodynamic function therefore entropy, enthalpy or free energy data can be incorporated in the cycles to derive thermodynamic values.

In this work, average heterolytic bond disruption enthalpies, half the $\Delta H°$ expressed in reactions 2-17 and 2-18, will be denoted as $\Delta H_{het}°$. Homolytic metal-ligand bond cleavage will be denoted as $\Delta H_{hom}°$ and represents $\frac{1}{2}\Delta H°$ for reactions 2-19 and 2-20. From the thermochemical cycles used here only average bond

$$Cp_2M(g) \rightarrow M^{2+}(g) + 2Cp^-(g) \qquad (2\text{-}17)$$

$$Cp_2M^+(g) \rightarrow M^{3+}(g) + 2Cp^-(g) \qquad (2\text{-}18)$$

$$Cp_2M(g) \rightarrow M(g) + 2Cp(g) \quad (2\text{-}19)$$

$$Cp_2M^+(g) \rightarrow M^+(g) + 2Cp(g) \quad (2\text{-}20)$$

disruption enthalpies can be obtained. Further, enthalpy values for M-Cp bond cleavage for consecutive ring cleavage will not be equivalent. For heterolytic cleavage, removal of the first Cp^- ligand will be less endothermic than removal of the second ligand due to an increase in the electrostatics between the positively charged metal center and the anionic Cp ligand. Similarly, $\Delta H_{hom}°$ for the first M-Cp homolytic cleavage will not be equal to $\Delta H_{hom}°$ for the second M-Cp cleavage.

Homolytic bond energies for ferrocene have been studied by pyrolysis techniques.[85] The activation energy for the decomposition of ferrocene, reaction 2-21, was monitored and based on the measured E_a, the first bond dissociation bond

$$Cp_2Fe \rightarrow CpFe + Cp \quad (2\text{-}21)$$

enthalpy was estimated to be 95 kcal mol^{-1}.[85] Consequently, removal of the second Cp ring is less endothermic by approximately 30 kcal mol^{-1} than removal of the first ligand. Faulk and Dunbar have used photodissociation methods to arrive at a value of 85 ± 7 kcal mol^{-1} for the first homolytic cleavage of Cp_2Fe^+. Therefore, the $\Delta H_{hom}°$ for the second cleavage is more endothermic than the first dissociation. Increased electrostatic attraction for the second Fe^+-Cp cleavage accounts for an increase in the second $\Delta H_{hom}°$ for Cp_2Fe^+.[86]

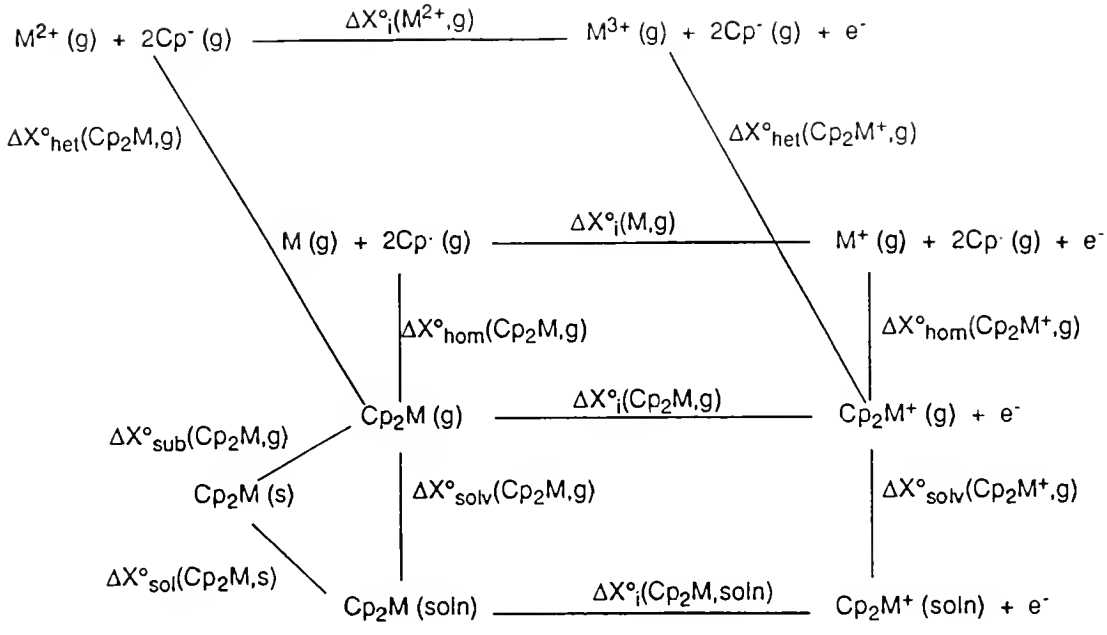

Figure 2-5 Thermochemical cycles used to determine bond disruption enthalpies and differential solvation free energies for metallocenes. The upper portion of the cycle yields estimates for the average homolytic and heterolytic bond disruption enthalpies for M-Cp cleavage. Comparison of $\Delta G_i°$(g) and $\Delta G_i°$(soln) in lower portion of the cycle yields estimates of differential solvation energies, $\Delta\Delta G_{solv}°$, for $Cp_2M^{+/0}$ couples.

Combining Free Energy and Enthalpy Data in Thermodynamic Cycles

Free energy of ionization data has been used to derive heterolytic and homolytic bond disruption enthalpies for metallocenium ions. The validity of combining ΔG_i° data for the metallocenes with enthalpy data referenced at other temperature, i.e. 0 or 298 K, is dependent on the accuracy of substituting $\Delta G_{i,350}^\circ$ values for $\Delta H_{i,298}^\circ$. This approximation relies on the premise that the entropy of ionization is small with respect to the larger values of ΔH° at temperature T. Manganocene is expected to have the largest $|\Delta S_i^\circ|$ of the metallocenes studied in this work.[16] Assuming $|\Delta S_i^\circ|$ = 12 cal $mol^{-1}K^{-1}$, the entropy contribution to the free energy of ionization at 350 K is 4 kcal mol^{-1}. Furthermore, even with such a large entropy change, the error estimated for manganocene is not expected to exceed 2 kcal mol^{-1} per bond. Generally, the assumption that $\Delta G_{i,350}^\circ \approx \Delta H_{i,298}^\circ$ for the other metallocenes is acceptable since entropy contributions will be small with respect to the larger values for the free energy of ionization. When compared to the absolute values for heterolytic and homolytic dissociation, the error introduced by assuming $\Delta G_{i,350}^\circ \approx \Delta H_{i,298}^\circ$ will small, ca. 2-3% for the homolytic bond enthalpies and less than 1% for the heterolytic enthalpies.

Heat capacity corrections are also expected to be small on going from 350 to 298 K. The heat capacity terms for ferrocene has been determined by statistical mechanics and the difference in the ΔH_i° values is only 0.1 kcal mol^{-1} from 350 to 298 K.[16]

Heterolytic and Homolytic Bond Disruption Enthalpies for Metallocenes and Metallocenium Ions

Bond disruption enthalpies for the Cp_2V, Cp_2Mn, Cp_2Fe, and Cp_2Ni have been reported previously.[13] However, as mentioned earlier, values reported here have been refined due to more accurate $\Delta G_i°$ values and auxiliary data. Derived bond enthalpies for the metallocenes are presented in Table 2-5. Auxiliary data[16] used in the thermochemical cycles are presented in Table 2-6. Error limits for homolytic and heterolytic dissociations take into account errors in the heats of formation of the neutral[27] and ionic species[16] and errors in the free energies of ionization. Bond enthalpies for ruthenocene, osmocene, and the substituted metallocenes are not reported due to lack of reliable thermochemical data for $\Delta H_f°$ of the neutral organometallics and the alkylated cyclopentadienyl compounds.

Differential Solvation Free Energies for Metallocene Redox Couples

Differential solvation free energies, $\Delta\Delta G_{solv}°$, for several metallocene redox couples have been determined through the application of thermochemical cycles (Figure 2-5) by combining $E_{½}$ data at 298 K to $\Delta G_{i,350}°$ values. As mentioned earlier, because of the relatively small entropy effects for the metallocene $Cp_2M^{+/0}$ oxidation couples, the errors introduced by substituting $\Delta G_{i,350}°$ for $\Delta G_{i,298}°$ are expected to be less than 1 kcal mol^{-1}. Values for $E_{½}$ have been used to derive $\Delta G_i°(Cp_2M)(soln)$; from Figure 2-5, values of $\Delta\Delta G_{solv}°$ have been derived from the lower thermochemical

Table 2-5 Mean Bond Disruption Enthalpies for Some Metallocenes.

Cp_2M	$\Delta H_{het}[M^{2+}\text{-}Cp^-]^a$	$\Delta H_{het}[M^{3+}\text{-}Cp^-]^a$	$\Delta H_{hom}[M\text{-}Cp^\cdot]^a$	$\Delta H_{hom}[M^+\text{-}Cp^\cdot]^a$
V	303 ± 3	563 ± 4	95 ± 2	95 ± 3
Mn	286 ± 3	604 ± 5	59 ± 2	74 ± 4
Fe	318 ± 3	593 ± 4	79 ± 1	91 ± 3
Ni	326 ± 3	659 ± 4	67 ± 2	83 ± 3

a. Units are kcal mol^{-1}

Table 2-6. Auxiliary Thermochemical Data Used in Thermochemical Cycles.

Process	V	Mn	Fe	Ni
$\Delta H_f°[Cp_2M]^b$	49 ± 2[a]	66 ± 2	58 ± 1	85 ± 1
$\Delta H_f°[M]^c$	123 ± 2	67 ± 2	99 ± 2	103 ± 2
$\Delta H_f°[M^+]^c$	278 ± 2	238 ± 2	281 ± 2	279 ± 2
$\Delta H_f°[M^{2+}]^c$	616 ± 2	599 ± 2	654 ± 2	698 ± 2
$\Delta H_f°[M^{3+}]^c$	1292 ± 2	1376 ± 2	1361 ± 2	1509 ± 2

$\Delta H_f°[Cp]^b$ = 58 ± 1

$\Delta H_f°[Cp^-]^b$ = 19.6 ± 4

a. Units are kcal mol^{-1}.
b. See reference 27.
c. See reference 8.

cycle. A negative value of $\Delta\Delta G_{solv}^{\circ}$ represents decreased exoergicity for the reduction of a metallocenium ion in solution compared to the gas phase. An analysis of the estimation of absolute electrode potentials for redox couples in solution has been given earlier,[54] and a similar approach has been used for the derivation of $\Delta\Delta G_{solv}^{\circ}$ quantities in this work. Specifically, a value of 4.44 V has been used for the absolute potential of the standard hydrogen electrode, E_{NHE}°, and no corrections for liquid junction potentials have been applied to the $E_{1/2}$ data for the metallocenes.[54] Thermochemical cycles were used in the derivation of the absolute potential of the normal hydrogen electrode. The largest source of error introduced in the derivation of E_{NHE}° was the free energy change for the solvation of the proton, ΔG_{solv}°, which can not be measured directly.[87] The value used for $\Delta G_{solv}^{\circ}(H^{+})$ is based on electrochemical experiments and the reliability of this value has been discussed elsewhere.[54,84] In addition, the stationary electron convention is used for both the gas-phase and solution thermochemistry, although near 298 K the thermal electron convention yields similar results for ΔG_{i}° values.[88]

The electrochemical $E_{1/2}$ values used in the estimates of $\Delta\Delta G_{solv}^{\circ}$ values are shown in Table 2-7. Equation 2-22 was used to derive estimate for ΔG_{i}°(soln) for the metallocenes. The value E_{ref}° is the potential of the reference electrode relative to the normal hydrogen electrode, n is the number of electrons transferred in

$$\Delta G_{i}^{\circ}(Cp_2M)(soln) = -nF[(E_{1/2}(Cp_2M) + E_{ref}^{\circ} + E_{NHE}^{\circ}] \qquad (2\text{-}22)$$

Table 2-7. Electrochemical $E_{½}$ Data and Differential Solvation Energies for Some Metallocenes $Cp_2M^{+/0}$ couples.

$Cp_2M^{+/0}$	$E_{½}$[a] (solvent)	$\Delta G_i°$(soln)[b]	$-\Delta\Delta G°_{solv}$[b]
V	-0.55[c,d] (THF)	95	60
Cr	-0.67[c] (CH_3CN)	92	36[e]
Fe	0.31[c] (CH_3CN)	115	38
Co	-0.94[c] (CH_3CN)	86	38[e]
Ni	-0.09[c] (CH_3CN)	106	38
Ru	1.03[f] (CH_2Cl_2)	131	33
Ru	0.78[d,g] (CH_3CN)	126	38
Os	0.86[f] (CH_2Cl_2)	127	34
Os	0.75[d,g] (CH_3CN)	125	36
Mn	(0.13)[h]	(105)[h]	(38)[h]

a. Values reported in volts using 0.1 M Bu_4NPF_6 as supporting electrolyte against SCE, except ruthenocene in 0.1 M Bu_4TFPB against Ag/AgCl and osmocene in 0.1 M Bu_4NBF_4 against SCE.
b. Units are kcal mol^{-1}. Estimated error limits ± 4 kcal mol^{-1}.
c. See reference 89.
d. Irreversible oxidation potential.
e. Estimated from $\Delta G_i°$ values. See Chapter 5.
f. See reference 90.
g. See reference 92.
h. Estimated from data in Figure 2-6 and reported against SHE.

the electrochemical process (1e$^-$ oxidations for the metallocenes) and F is Faraday's constant. Most of the $E_{½}$ values were obtained from a single literature source[89] and were measured under common experimental conditions. The solvent is acetonitrile for all quoted $E_{½}$ values except for vanadocene (THF) and ruthenocene and osmocene (CH_2Cl_2).[90,91] Values of $E_{½}$ for ruthenocene and osmocene are also reported in CH_3CN.[92] Table 2-7 presents the derived differential solvation energies for the metallocenes and the corresponding solution free energies of oxidation for comparison to the gas-phase ionization energies. Differential solvation free energies were calculated from equation 2-23, which originates from the thermochemical cycles in Figure 2-5. A plot of free energy of ionization data versus the first transition row

$$-\Delta\Delta G_{solv}^{\circ}\ (Cp_2M^{+/0}) = \Delta G_i^{\circ}(Cp_2M)(g)\ -\ \Delta G_i^{\circ}(Cp_2M)(soln) \qquad (2\text{-}23)$$

metallocenes is presented in Figure 2-6 and serves to demonstrates the periodic trends for $\Delta G_i^{\circ}(Cp_2M)$ in solution and the gas-phase. The average value for $\Delta\Delta G_{solv}^{\circ}$ for the first transition row metallocenes is -38 ± 2 kcal mol^{-1}, excluding vanadocene. The $\Delta\Delta G_{solv}^{\circ}$ values for cobaltocene and chromocene were based on ΔG_i° values determined from FTMS ETE studies and are discussed in Chapter 5. The obvious exception to the observed trend in differential solvation energies (Figure 2-6) is noted for Cp_2V oxidation,[89] which has a $\Delta\Delta G_{solv}^{\circ}$ value more negative by ~20 kcal mol^{-1} relative to the other first transition row metallocenes. This additional stabilization of the cation can be attributed to inner sphere coordination

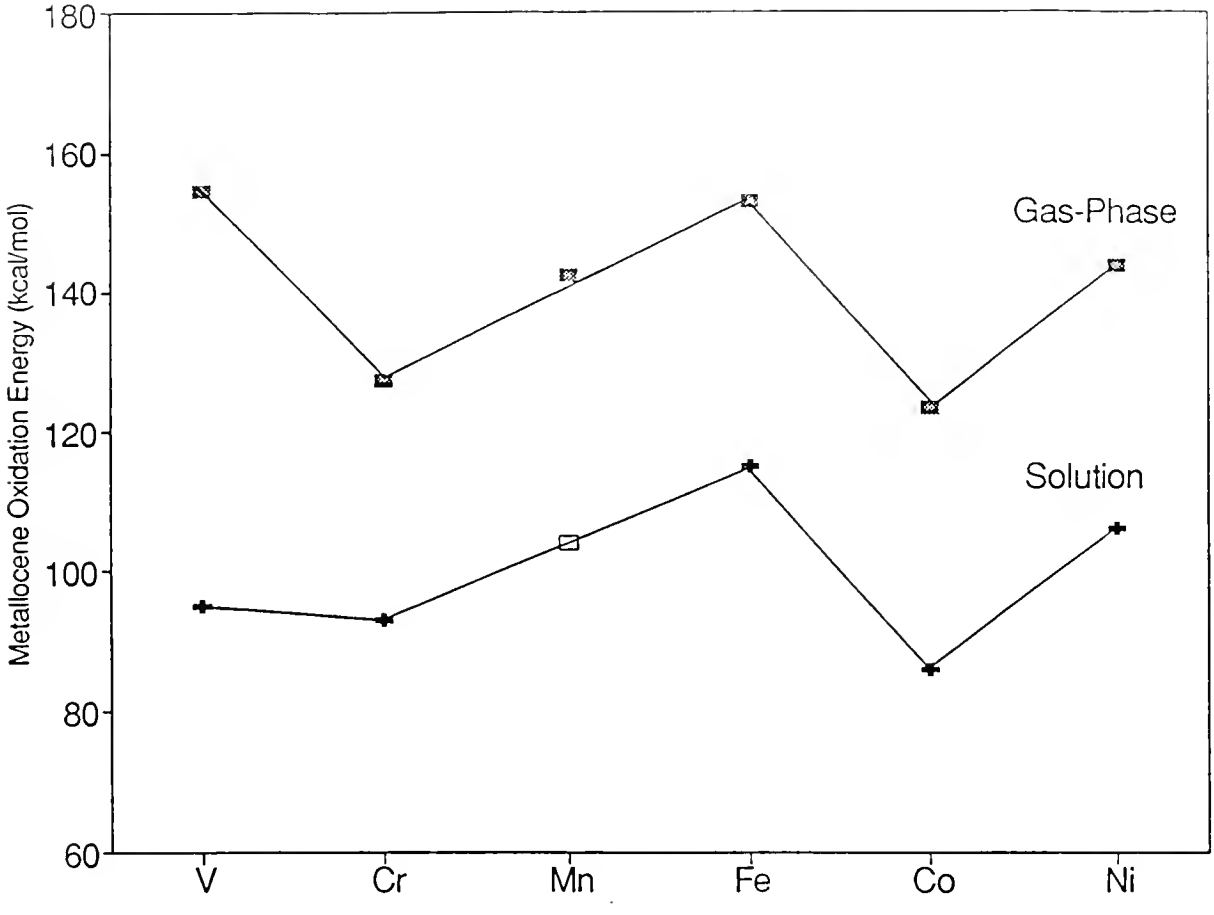

Figure 2-6 Plot demonstrating the periodic trend of ionization energies for the first transition row metallocenes. Gas-phase data (filled squares) include $\Delta G_i°$values from this work. Solution $\Delta G_i°$ values (crosses) were determined through thermochemical cycles. The solvent is CH_3CN except for Cp_2V in THF. An estimate of $\Delta G_i°$(soln) for manganocene (versus SCE) is included (open square).

of solvent following oxidation.[89] From the trends in Figure 2-6, a prediction can be made for the unknown $E_{1/2}$ for Cp_2Mn, -0.13 V vs. SCE.

Gieger has reported that electrochemical oxidation of Cp_2V is quasi-reversible in tetrahydrofuran, THF, which is consistent with there being no significant structural changes in going from a d^3 to d^2 metal complex.[89] However, the correlation of $\Delta G_i°$(g) versus $\Delta G_i°$(soln) clearly indicates that Cp_2V lies outside the fit; thus, a structural variation can not be ruled out. A structural change, similar to that shown in Figure 2-7, could explain the lack of correlation for Cp_2V. It can be rationalized that in an attempt to increase the electron density around the electrophilic metal

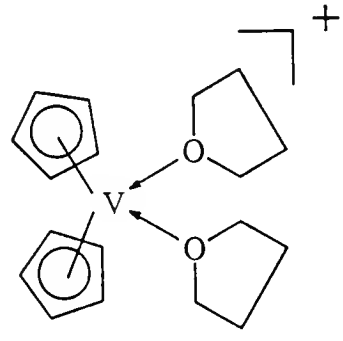

Figure 2-7 Structure of an $18e^{-1}$ vanadocenium-THF complex

center, polar solvent molecules coordinate to the metal complex. The addition of two THF molecules, for example, would lead to the formation of an 18 e^- cationic $Cp_2V{\cdot}2THF$ complex.

A comparison of $\Delta\Delta G_{solv}°$ results to values predicted by dielectric continuum theory suggests that the solvation thermochemistry of $Cp_2M^{+/0}$ couples can be adequately modelled by the Born charging model.[54] The Born equation determines

the change in electrostatic free energy, ΔG_{el}° when a charge on an electrostatic sphere of radius r_{eff} is transferred in a vacuum to a sphere of equivalent volume in a solution of dielectric constant D. For equation 2-24, the Born equation, *z* denotes fundamental charge of the ion (here 1+). The definition of the Born equation is directly comparable to the concept of differential solvation energy defined by equation 2-23.[54]

$$\Delta G_{el}^{\circ} = (-166z^2/r_{eff})(1 - 1/D) \text{ kcal mol}^{-1} \qquad (2\text{-}24)$$

The Born model neglects the actual work required for an ion to pass from a vacuum through the solvent barrier. However, this work is usually quite small compared to the values for the differential solvation free energy.[55]

From crystallographic data, the radii for Cp_2Fe and Cp_2Ni are estimated to be 3.9 and 3.7 Å respectively.[72] The r_{eff} value obtained from the Born equation for a ΔG_{el}° = -38 kcal mol^{-1} in acetonitrile is 4.3 Å. From another point of view, the structural model radius (3.9 Å) predicts a $\Delta\Delta G_{solv}^{\circ}$ value of -41 kcal mol^{-1}. This close agreement between the structurally estimated radii and the thermochemical radii is consistent with relatively small specific interactions between solvent and metal complex as well as the compact structure of metallocenes. The same conclusions were obtained by Krishtalik et al. who used a ΔG_i° value of ferrocene based on the photoelectron spectrum.[93] For comparison, in the tris(acetylacetonate) metal complexes, where polar solvent molecules can interpenetrate between the chelating bidentate ligands, the experimental solvation energy is approximately twice the value

predicted from the structural model. The Born model predicts a value for r_{eff} of 2.9 Å for $Ru(acac)_3^{0/-}$ based on a value of 57.5 kcal mol^{-1} for $\Delta\Delta G_{solv}°$.[84] However, the crystallographic radius (maximum radius taken from Ru metal center to furthest ligand proton) for the ruthenium complex is ~6 Å. A shortcoming of the Born model is that it assumes the charge is evenly distributed over the entire sphere which is not necessarily true, especially for large metal complexes

Equation 2-24 predicts that $\Delta\Delta G_{solv}°$ will be increased by ~3 kcal mol^{-1} for r_{eff} = 3.9 Å when acetonitrile, D = 36, is replaced by methylene chloride, D = 9. From the reversible potentials for ferrocene, ruthenocene, and osmocene in CH_2Cl_2 given by Hill et al.,[90] lower solvation energetics for $\Delta\Delta G_{solv}°$ values (-34 ± 1 kcal mol^{-1}) are estimated for the three couples. However, the difference in the $\Delta\Delta G_{solv}°$ values derived in the different solvents are in good agreement and are consistent with experimental $\Delta\Delta G_{solv}°$ values determined through thermochemical cycles.

Conclusions

Free energies of ionization have been determined for a number of gas-phase metallocenes. These ETE data complement and extend information on the oxidation energies of metallocenes obtained previously by electrochemistry[34] and photoelectron spectroscopy.[35] Further, the $\Delta G_i°$ values for the metallocenes are in agreement with the vertical ionization energies measured by PES by several groups.[37,38,78] The free energy of ionization for manganocene is in agreement with the vIP for the low-spin complex. The temperature dependence of the Cp_2Ni/Cp_2Mn couple is consistent with

a large negative entropy change for the manganocene ionization process. Comparison of ETE data with PES spectra for Cp_2V and Cp_2Os yield the same values for adiabatic ionization potentials within experimental error.[16,78] Overall, the good agreement of $\Delta G_i°$ data with PES data indicates that large experimental errors do not exist for the ETE studies. With the exception of vanadocene, correlation $\Delta G_i°$ values in the gas phase and solution for the first transition row metallocenes is linear. Inner-sphere solvent coordination can be used to rationalize the disparity of the vanadocene couple relative to the other metallocenes.[89] An estimate for $E_{½}$ for manganocene has been made based on $E_{½}$ values for the other first transition row metallocenes.

Detailed investigations of the ionization free energy for ferrocene support a value of $\Delta G_i° = 153.1 \pm 1.5$ kcal mol^{-1}. Temperature dependent ETE studies on selected equilibria have established experimental enthalpy and entropy of ionization values for ferrocene. Although the present data establish a relatively large value of $\Delta S_i°(Cp_2Fe)$, statistical mechanical analyses and previous PHPMS results[43] suggest that a smaller $\Delta S_i°$ value (~4-5 cal mol^{-1}K^{-1}) is appropriate. The positive entropy change for ferrocene ionization can be attributed to roughly equal contributions from intramolecular vibrational entropy changes and changes in electronic entropy. The vibrational contribution to the entropy change accounts for over 50% of the total $\Delta S_i°$ at 298 K for the $Cp_2Fe^{+/0}$ couple. Temperature dependent investigation of the ETE reaction couple EtFc/Cp_2Fe indicate that the $\Delta S_{et}°$ is ~0 cal mol^{-1}K^{-1} which indicates that the $\Delta S_i°$ for ethylferrocene and ferrocene are equivalent. The ETE reaction couple

Cp_2V/Cp_2Fe indicates that the $\Delta G_i°$ of ferrocene is less than vanadocene which supports the lower $\Delta G_i°(Cp_2Fe)$ value.

The $\Delta G_i°$ data have been incorporated into thermochemical cycles to allow estimations of bond disruption enthalpies for selected gas-phase metallocenium ions. Estimates of differential solvation energies for several $Cp_2M^{+/0}$ couples have also been derived from thermochemical cycles. An average value of $\Delta\Delta G_{solv}°$ for the metallocenes is -38 ± 2 kcal mol^{-1} with CH_3CN as the solvent. Solvation of a gas-phase metallocene decreases the ionization energy by a relatively constant amount (~1.6 eV with acetonitrile as solvent). Solvation is therefore secondary to metal ligation in determining the potential of $Cp_2M^{+/0}$ couple relative to the ionization of the corresponding M^{2+} (g) ion (ligation of M^{2+} by two Cp^- ligands reduces the ionization energy by ca. 13 ± 1 eV).

The Born equation, used for deriving estimates of differential solvation energies, has been applied to the metallocenes. Values of $\Delta G_{el}°$ are in agreement with $\Delta\Delta G_{solv}°(Cp_2M^{+/0})$ values which demonstrates that the metallocenes have compact molecular structures. Specific solvent interactions such as inner-sphere coordination of solvent are minimal for the metallocenes.

Experimental Methods

Electron-Transfer Equilibrium Studies

Electron-transfer equilibrium studies were performed by using a Nicolet FT/MS 1000 Fourier transform ion cyclotron resonance mass spectrometer as previously

described.[15-20] Briefly, the pressure of each compound was adjusted to establish a workable pressure ratio to allow equilibria to be monitored. The time dependence of parent ions formed from neutral molecules of known partial pressure was monitored as the molecular ions underwent electron transfer with neutrals. Reactions were typically followed to ca. 5 or more seconds. Apparent equilibrium was generally attained in less than two seconds.

Reference compounds were sublimed into the FTMS high vacuum chamber through a precision leak valve. The vapor pressure of most metallocene samples was sufficient to allow for direct introduced into the high vacuum chamber through a second leak valve. Ruthenocene, Cp_2Ru, and osmocene, Cp_2Os, were introduced by using a heated solids probe positioned adjacent to the reaction cell. The FTMS reaction cell was typically 350 K as measured by an Omega RTD thin film detector. Positive ions were produced by electron impact at 9-12 eV with beam times ranging between 5 and 25 ms. Ionization of metallocenes and organics occurs with some fragmentation of the molecular ion (vide infra); other unwanted ions are formed by ion-molecule reactions. Prior to study of electron-transfer reactions, several ion ejections were required in order to select only the parent ions.

Since reactions were followed for at least 5 s, all ions formed as a result of EI were assumed to be effectively thermalized through ion-molecule collisions. At a neutral pressure of 10^{-6} Torr at 350 K, a typical metallocenium ion will undergo ca. 30 collisions s^{-1}, which is believed sufficient to remove much of the excess rotational and vibrational energy present due to the ionization process.[14,16] Approach to

equilibrium was followed from endoergic and exoergic directions. Prior to reaction, one of the parent ions was ejected from the reaction cell and the population change of both parent ions was monitored at set time intervals. Equilibrium was deemed to have been achieved when the ratio of the two parent ion populations reached a constant value within experimental error.

Partial pressures of the various neutrals were determined by using an ion gauge calibrated with an MKS baratron capacitance manometer (in the 10^{-5} torr range) extrapolated to experimental conditions. In order to approach dynamic pressure equilibrium throughout the vacuum chamber, the 300 L s^{-1} pumping speed of the diffusion pump connected to the high vacuum chamber was reduced to ca. 75 L s^{-1}. Neutral gas pressures were calibrated for all reactants in open (75 L s^{-1}) and closed (no pumping) systems. It has been shown that partial pressure is independent of neutral gas leak rate. A calibrated ion gauge connected to a Granville-Phillips controller was positioned at the site of the reaction cell with the magnetic field off, thus providing a field free vacuum system. The pressure measured at the middle of the vacuum chamber where the reaction cell is located, was equivalent to metallocene pressures determined at the remote ion gauge following pressure calibrations.[94]

Temperature Dependence Studies

The temperature dependencies of electron-transfer equilibria were investigated by using a customized cell heater designed to heat a 1" x 1" x 1¾" analyzer cell. The heater consisted of two Macor plates (1½" x 2" x ¼") attached to the long sides of the

reaction cell. Macor sheets (6" x 6"x ¼") were purchased from Astro Met Inc. Ni-Cu wire (0.015" diameter, purchased from Omega Industries) was wrapped around the external Macor plates and was resistively heated by using an Omega digital temperature controller (maximum output current (~5 A) resulted in temperatures of ~520 K). Cell temperatures were measured using an Omega RTD thin film detector fastened to the analyzer cell. Additionally, the entire high vacuum chamber was heated by using the vacuum bake-out system in order to minimize radiative temperature loss to the vacuum chamber walls.

Following the measurement of K_{eq} at a set temperature, the cell heater and bake-out were allowed to cool to a lower temperature and the entire system was allowed to equilibrate at the new temperature for 30 min. Experimental reproducibility was tested by following the temperature dependence of K_{eq} as the reaction cell temperature was increased from 350 to 500 K.

The cell temperature was measured before and after each reaction and usually fluctuated ± 2 K during a single experiment. Typically, reactions were repeated three times at a single temperature. Linear regression and statistical analyses of the all measured equilibrium constants provided error limits at the 95% confidence level for reported $\Delta H_{et}°$ and $\Delta S_{et}°$ values.

Metallocenes and Reference Compounds

Metallocenes were purchased through Strem Chemicals except for ferrocene and ruthenocene (Aldrich). No further purification was required except for Cp_2Mn

which was resublimed prior to use. For temperature dependence studies, a sublimed sample of ferrocene was used. Organic reference compounds were purchased from Aldrich except N,N'-diethyl-p-toluidine (Alfa Chemicals). A sample of 1,1'-bipyrrolidine[40a] was donated by Professor Stephen Nelsen from the University of Wisconsin. Organic reference compounds were used without further purification. Liquid samples were degassed through several freeze-pump-thaw cycles prior to use.

Far-infrared Spectroscopy.

Ferrocene salts in Table 2-3 were prepared according to literature procedures.[95] The hexafluorophosphate and the tetrafluoroborate salts were prepared by dissolution of pure ferrocene in concentrated sulfuric acid, followed by dilution of the dark blue solution with water. The solution was filtered and then an aqueous solution of Bu_4NX was added, where X = PF_6 or BF_4. The precipitate was filtered and washed with water until the washings were clear. The chloride salt was obtained by distilling ferrocene in concentrated HCl for several days. The blue precipitate was filtered and washed with water. Infrared spectroscopy in the 400 - 3200 cm^{-1} region confirmed the compounds to be ferrocenium salts.[69-71] The samples were prepared as dilute 13 mm polyethylene pellets. Far-infrared spectra were recorded using a Bruker IFS 113V spectrophotometer in the 50 - 750 cm^{-1} spectral region.

CHAPTER 3
SUBSTITUENT EFFECTS IN THE GAS-PHASE AND SOLUTION IONIZATION AND ELECTRON ATTACHMENT ENERGIES OF ALKYLNICKELOCENES.

Introduction

Alkyl substituent effects have been studied extensively in organic chemistry with emphasis towards understanding acidities,[30a] basicities,[30b] and reactivity of organic systems.[5,53] The correlation between structure and reactivity of alkyl substituents has led to detailed explanations and an interpretation of chemical reactivity and chemical equilibria.[2-5] Methods that correlate structure-reactivity relationships allow for quantitative interpretation of various electronic perturbations of substituents relative to a parent molecular-frame. Subsequently,[5] chemical transformations for yet unknown species can be determined based on known substituent effects.

Gas-phase investigations have been very effective in evaluating intrinsic substituent effects.[16,19,20,32,37,91] Specific electronic effects may be masked in condensed-phase; therefore, intrinsic effects observed in solution studies may be significantly modified or even reversed relative to gas-phase studies.[5] Additionally, the results may vary from solvent to solvent. Nonpolar solvents may yield approximations of intrinsic substituent electronic effects, while strongly coordinating

solvent may inhibit substituent electronic effects altogether.[5,53] To truly resolve substituent effects in various solvents, gas-phase data must be used as a reference.

Relatively few gas-phase studies of alkyl substituents effects of metal complexes have appeared,[16,18,35,91] and little is known concerning the relative alkyl effects in the thermochemistry of metal complex redox couples.[32,34] Comparisons of the gas-phase and solution results address solvent effects of metal redox couples, and allow for estimates of differential solvation energetics of metal complexes to be made.[15,16] Additionally, such studies help extend parameterization schemes derived from organic systems to the area of inorganic chemistry.

From photoelectron spectra[35] and electrochemical studies,[32,34] it is commonly assumed that alkyl groups on coordinated ligands are electron-donating in metal complex redox processes. Specifically, alkyl groups stabilize the oxidized form of a complex relative to the reduced species. In order to further explore and understand alkyl substituent effects for transition metal compounds, gas-phase electron-transfer equilibrium studies have been performed, by using FTMS,[44-47] to determined free energies of electron-attachment ($\Delta G_a°$) and ionization ($\Delta G_i°$) for a series of alkylated nickelocene complexes.[19] The results indicate, similar to organic systems,[2,3] that alkyl groups are not always electron-donating in organometallic redox processes.[19] Models that include polarizability effects, in addition to more traditional inductive effects, must be used to interpret the data.[5,52,53]

Nickelocene is a useful parent compound for these studies because it forms stable anions and cations in the gas-phase[18,19] and solution.[34,89] Furthermore,

oxidation and reduction of nickelocene involves the same e_{1g}^* set of molecular orbitals.[96] A two-electron oxidation process for negative nickelocene ion is shown in Figure 3-1 with accompanying molecular orbital diagrams of the 3d valence orbitals for the $Cp_2Ni^{+/0/-}$ complexes. A one-electron model suggests, because the same molecular orbital of nickelocene is both oxidized and reduced, perturbations in the orbital energies due to alkyl substitution on the Cp rings are expected to be similar for the ionization and electron attachment processes. That is to say, the difference in the ionization energies and electron affinities of an alkylated complex relative to nickelocene should be comparable.[36] However, this is not the case and an a more flexible model must be used to explain the trends in the experimental data.

Solution phase redox studies were performed for comparison to the gas-phase data. Differential solvation energies for some alkylated nickelocene complexes have been derived from thermochemical cycles. Values for $\Delta\Delta G_{solv}°$ for the $Cp_2Ni^{+/0}$ and the $Cp_2Ni^{0/-}$ couples are discussed.

Electron-Transfer Equilibrium Studies Involving Negative and Positive Alkylnickelocene Ions

The electron-transfer equilibrium method has been discussed previously.[16,18] Procedures for determining free energies of ionization and free energies of electron attachments are similar. The equilibrium constants were determined for the reactions shown in equations 3-1 and 3-2 where RCp and R'Cp represent alkylated cyclopentadienyl ligands and X, for these examples, denotes a reference compounds

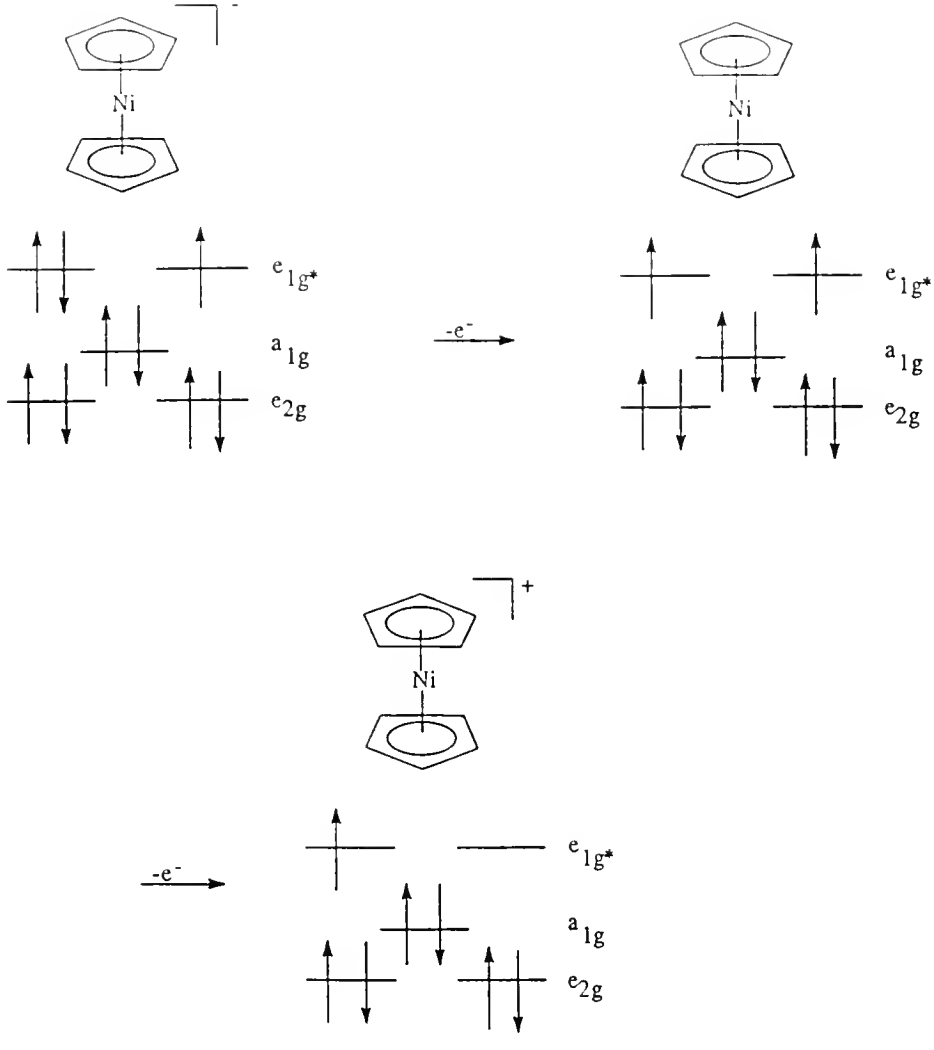

Figure 3-1 Molecular orbital diagrams for nickelocene anion, nickelocene, and nickelocene cation.

with known a $\Delta G_i°$ or $\Delta G_a°$ value. Ion intensities and partial pressures were measured directly during the ETE experiment. Thus, the equilibrium constants and reaction free energies for the reactions 3-1 and 3-2 can be determined (see equation 2-3).

$$(RCp)(R'Cp)Ni + X^+ = X + (RCp)(R'Cp)Ni^+ \quad (3\text{-}1)$$

$$(RCp)(R'Cp)Ni + X^- = X + (RCp)(R'Cp)Ni^- \quad (3\text{-}2)$$

Free energy ladders for gas-phase electron-transfer equilibria studied in this work are shown in Figures 3-2 and 3-3. Derived $\Delta G_i°$ and $\Delta G_a°$ (electron attachment free energy) values are referenced at ~350 K as measured by an RTD thin film detector. The $\Delta G_i°$ values, for the process $(RCp)(R'Cp)Ni \rightarrow (RCp)(R'Cp)Ni^+ + e^-$, in Figure 3-2 are anchored to the $\Delta G_i°$ values of nickelocene, manganocene, and bis(benzene)chromium. The $\Delta G_i°$ values for Cp_2Mn and Cp_2Ni have been reported previously.[16] Electron-attachment free energies (for the process $M + e^- \rightarrow M^-$) in Figure 3-3 are anchored to the $\Delta G_a°$ value of azulene and nickelocene.[18]

The $\Delta G_i°$ value for Bz_2Cr was based on the photoelectron spectrum which has an extremely sharp first ionization band with a peak maximum at 5.47 eV.[19] Because of the sharpness of the band, the vertical ionization energy closely approximates the adiabatic IP (see Figure 1-1B). The $\Delta G_i°(Bz_2Cr)$ = 125.7 kcal mol^{-1} was estimated by assuming aIP = vIP = 126.1 kcal mol^{-1}. An estimate for $\Delta S_i°$ was determined by assuming only the electronic entropy contribution was important. Thus, $\Delta S_{vib}° \sim \Delta S_{rot}° \sim 0$ cal mol^{-1} K^{-1}. The electronic entropy change associated

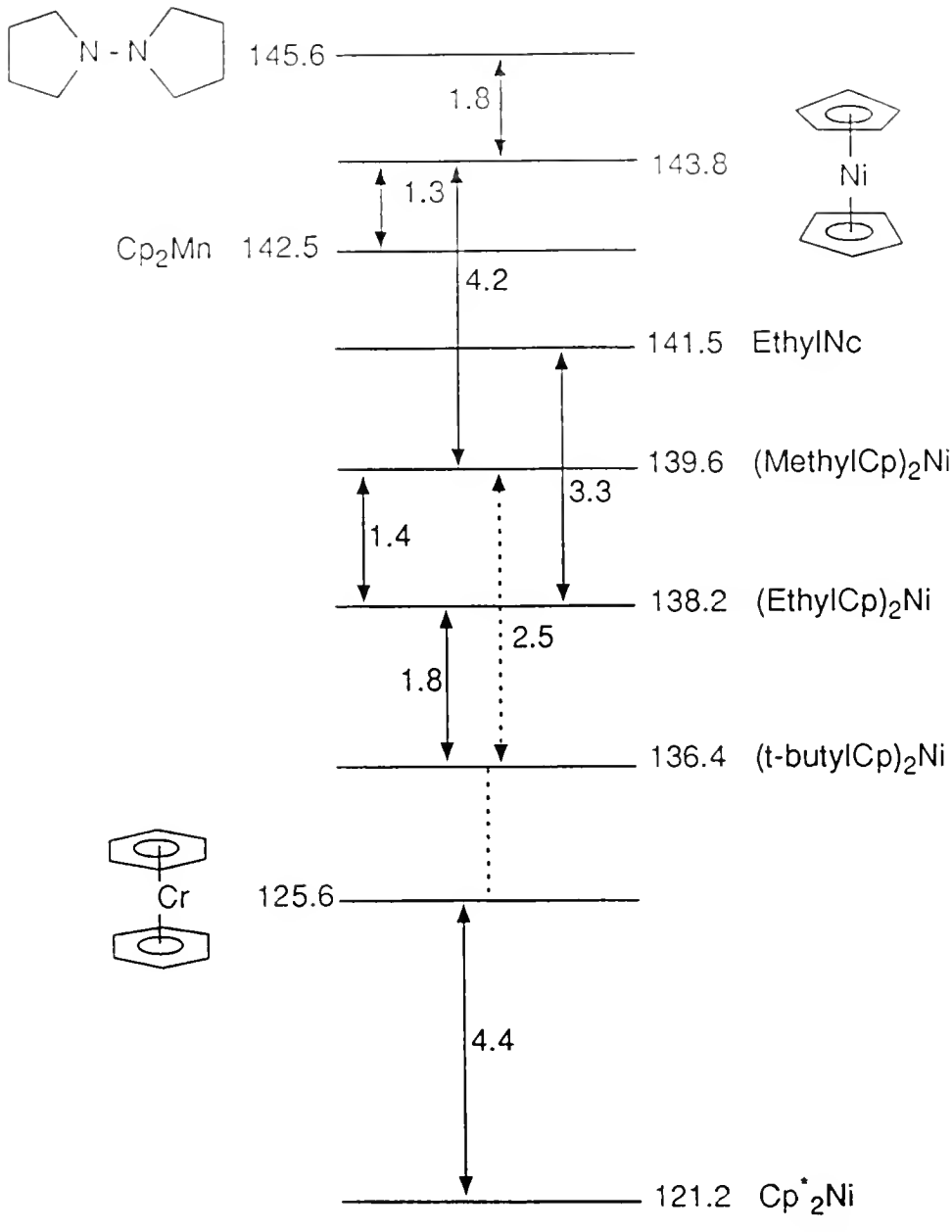

Figure 3-2 Electron-transfer equilibrium ladder for ionizations for several alkylnickelocene complexes for the process $M \rightarrow M^{+} + e^{-}$. Values of ΔG_i° ($\pm$ 1.5 kcal mol^{-1}) for the nickelocene complexes are to the right of the ladder and ΔG_{et}° values for individual ETE reaction are adjacent to the arrows. The ΔG_{et}° value for the $(MeCp)_2Ni/(t\text{-}BuCp)_2Ni$ couple is not within the expected $\pm$ 0.5 kcal mol^{-1} experimental error limit.

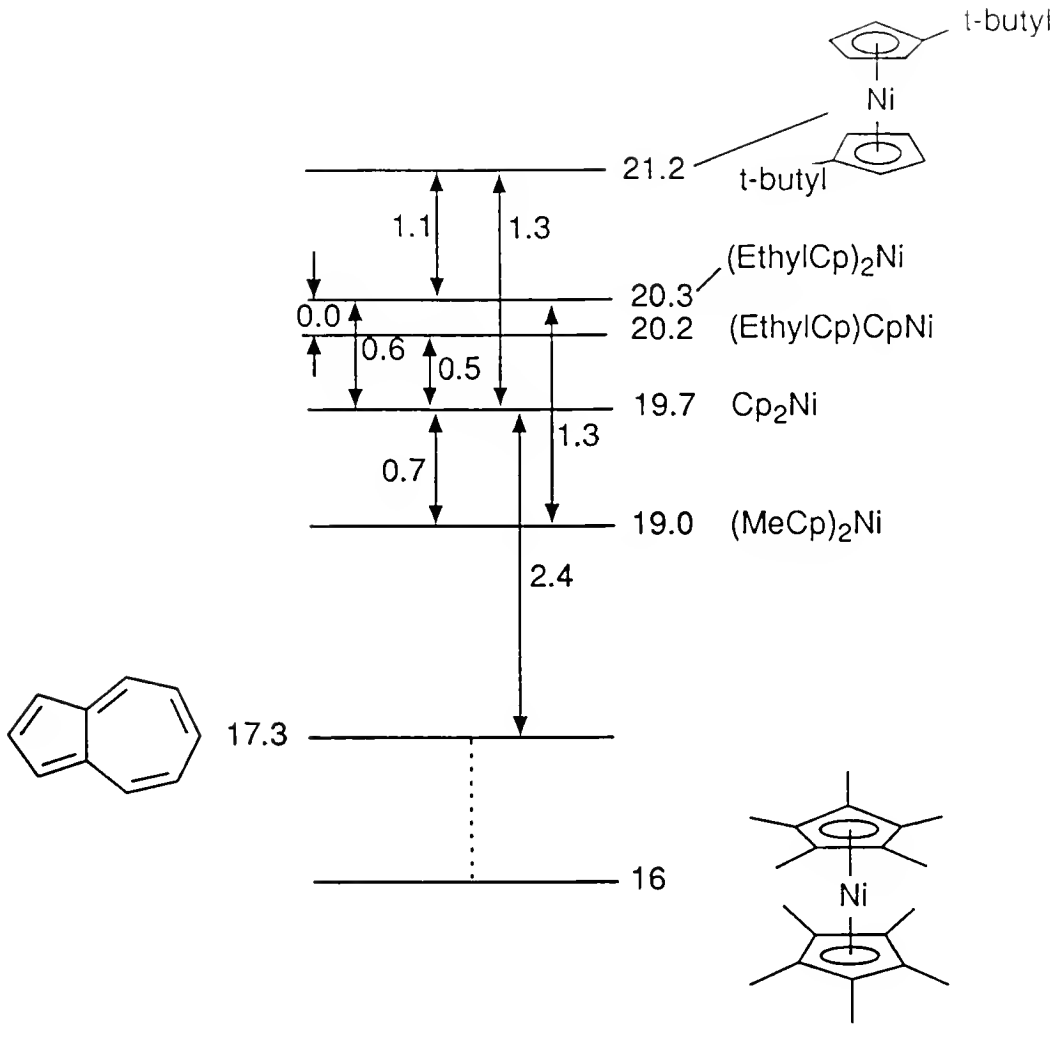

Figure 3-3 Electron-transfer equilibrium ladder for electron-attachments for alkylnickelocene complexes for the process $M + e^- \rightarrow M^-$. Values of $\Delta G_a°$ ($\pm$ 1.5 kcal mol^{-1}) for the nickelocene complexes are to the right of the ladder and $\Delta G_{et}°$ values for individual ETE reaction are adjacent to the arrows. The $\Delta G_a°$ for Cp^*_2Ni is an estimated value.

with an ^1A to ^2A transition is $\Delta S_{elec}^\circ = R \ln 2 = 1.4$ cal mol^{-1} K^{-1}. Further details concerning ΔS_i° and ΔG_i° of Bz_2Cr are discussed in Chapter 5.

Electron-transfer equilibrium reactions were repeated several times to insure reproducibility. Cross checks were performed when possible to check the internal consistency of the derived ΔG_i° and ΔG_a° values. The experimental uncertainty in the individual electron-transfer equilibrium reactions is ± 0.5 kcal mol^{-1}. Electron attachment and ionization free energies are reported with ± 1.5 kcal mol^{-1} error due largely to errors in the ΔG° values of the reference compounds.

Nickelocene is expected to have the highest electron affinity of the first transition row metallocenes since it has the lowest reduction potential.[89] This is further substantiated in the observation that no other metallocene forms negative ions in the gas phase by low energy electron impact or chemical ionization. Decamethylnickelocene could not be brought to electron-transfer equilibrium with any reference compound. Further, $Cp^*_2Ni^-$ was not observed from electron impact or chemical ionization. Attempts to ionize Cp^*_2Ni with electron-transfer reagents such as azulene (ΔG_a° = 17.3 kcal mol^{-1})[27] and C_6F_6 (ΔG_a° = 12 kcal mol^{-1})[27] were unsuccessful. The electron affinity of Cp^*_2Ni was estimated from the difference in the ΔG_a° values of $(MeCp)_2Ni$ and nickelocene by assuming that the electronic effect of the methyl groups is additive. The ΔG_a° value of Cp^*_2Ni puts it at the bottom of the equilibrium ladder for compounds that have had ΔG_a° values determined from the electron-transfer equilibrium method.[42]

Results of the ETE studies for the cations and anions are presented in Table 3-1. The $\Delta G_i°$ value for nickelocene is included as a reference for the alkylated complexes. The $\Delta G_a°$ for nickelocene was determined from ETE studies with azulene.[18] Nickelocene was brought to equilibrium with azulene eight times from both exoergic and endoergic directions and therefore serves as a second reference for ETE studies of the negative ions. It is worth mentioning for historic reasons that the author used the azulene/nickelocene negative ion couple as a training project to learn how to operate a Nocolet FT/MS-1000. The not-so-serendipitous electron-transfer equilibrium that ensued developed into a cavalcade of valuable experiments and the present dissertation.

It is clear from the data in Table 3-1 that increasing the size and number of alkyl substituents for nickelocene decreases the free energy of ionization. A similar effect was observed for the alkylferrocene derivatives.[16] In contrast to the ionization energy data, trends in the $\Delta G_a°$ values do not consistently reflect an increase in an "electron-donating" effect. Moreover, the ethyl and t-butyl groups lead to an increase in the electron affinity relative to H on the Cp rings. However, two methyl groups lower the electron affinity relative to nickelocene. The shifts in the $\Delta G_a°$ values relative to nickelocene are in general small, but appear to be significantly larger than the error estimated for the electron-transfer free energies (~0.5 kcal mol^{-1}) derived from electron-transfer equilibrium experiments. The absolute free energies have larger errors as mentioned earlier of ± 1.5 kcal mol^{-1}.

Table 3-1 Free Energies of Ionization and Electron Attachment

No.	L	L'	$\Delta G_i^{oa,b}$	$-\Delta G_a^{oa,b}$
1	Cp	Cp	143.8	19.7
2	MeCp	MeCp	139.6	19.0
3	EtCp	Cp	141.5	20.2
4	EtCp	EtCp	138.2	20.3
5	*t*-BuCp	*t*-BuCp	136.4	21.2
6	C_5Me_5	C_5Me_5	121.2	(~16)[c]

a. Units are kcal mol^{-1}.
b. Estimated error in absolute values ± 1.5 kcal mol^{-1}.
c. Estimated value.

Note that by convention, electron affinities are expressed as positive values (the affinity of an electron to be attracted to the nucleus of an atom) although they represent an exoergic property. For application in thermochemical cycles, $-\Delta G_a°$ and $-\Delta H_a°$ values are incorporated as negative values,[15] however in the discussion the electron affinities and free energies of electron attachment, the negative sign is dropped.

An increase in $\Delta G_a°$ for larger alkyl groups relative to R = Me is a well documented effect for organic systems.[98,99] For example, the electron affinities of alkoxy radicals, RO•, increase in the order R = Me < Et < n-Pr < t-Bu.[98] However, in solution the trends are reversed due to solvent effects.[5] The solution acidity of methanol is greater than that of ethanol, but in the gas phase, ethanol is more acidic than methanol and even water.[100] For *p*-benzoquinone (BQ) derivatives, the electron affinity of 2,6-di-*tert*-butyl-BQ is ~1 kcal mol^{-1} greater than that of 2,6-dimethyl-BQ. The $\Delta G_a°$ values for the series of methylated benzoquinones compounds decrease monotonically by ~2 kcal mol^{-1} per methyl group from the methyl to the tetramethyl derivative.[27] Although the alkyl effects for these systems are quite subtle relative to alkyl effects for positive ions, the gas-phase results demonstrate that large alkyl groups can stabilize anions in simple saturated and conjugated systems.[100,101] However, methyl groups tend to destabilize the electron affinities. The lower electron affinity for $(MeCp)_2Ni$ relative to nickelocene is consistent with the usual destabilization of anions by methyl substitution.[42] Thus, from the above analysis, methyl groups can be

described as intrinsically electron-donating functions, stabilizing cationic systems and destabilizing anionic complexes.

Alkyl Substituent Analyses for Positive and Negative Ions and Rationalization of the Gas-Phase Trends for the Ionization and Electron Attachments Free Energies

Numerous alkyl substituent parameter schemes have been developed to fit chemical reactivity to an electrostatic models.[4,5,52,53] The parameters are based on the premise that any substituent R in place of a reference, hydrogen for example, may alter the bonding, reactivity and overall chemical characteristics of the parent molecule.[5] Substituent schemes based on a single parameters or several parameters have been used to correlate energy perturbations for chemical systems relative to a parent reference.[50-52] The single parameter model quantitatively predicted shifts in the ΔG_i° values of the alkylferrocene complexes (Chapter 2) relative to ferrocene with $\pm$ 3 kcal mol^{-1} accuracy.[16]

The Taft model used in the ferrocene analysis employed σ_I parameters which were used to assess inductive effects of alkyl parameters. Generally, the parameters incorporate several electronic effects (i.e, field, polarizability, resonances) thus separation of the specific electronic effects are not accounted for in this model. Field effects refer to a charge/dipole, or dipole/dipole electronic interaction transmitted through space or a through polarizable bond.[5] Polarization effects pertain to a charge/induced-dipole or dipole/induced-dipole interaction. Polarization effects are

more strongly distance dependent than field effects.[5] However, the relative magnitude of the two effects are also important in understanding the overall substituent effects.

A single[5,53] and a two-parameter[102] model based on previously derived schemes were used to fit the $\Delta G_i°$ and $\Delta G_a°$ data for the alkylnickelocene complexes. Free energies of ionization and electron attachment in Table 3-1 were plotted against σ_I parameters. Figure 3-4 is a plot of the free energy data versus the alkyl Taft parameters. Equation 3-3a was used to fit the $\Delta G_i°$ data to the Taft σ_I parameters and equation 3-3b was used to fit the $\Delta G_a°$ values to the σ_I parameters. The alkyl substituents used in the correlations are shown in Table 3-2. Additivity of the parameters is assumed for the fits. The values of p_I is the sensitivity parameter for the

$$\Delta G_i°(RCp)(R'Cp)Ni = p_I(\Sigma\sigma_I) + \Delta G_i°(Cp_2Ni) \quad (3\text{-}3a)$$

$$\Delta G_a°(RCp)(R'Cp)Ni = p_I(\Sigma\sigma_I) + \Delta G_a°(Cp_2Ni) \quad (3\text{-}3b)$$

Taft analyses. All fits used in substituent parameter analyses correspond to shifts in the free energy data relative to nickelocene, where R = H, for the processes shown below. The free energies for equations 3-4 and 3-5 are the stabilization energy or destabilization energy for the substituents. Thus $\Delta G_{34}°$ is the stabilization for the

$$(RCp)(R'Cp)Ni + Cp_2Ni^+ = Cp_2Ni + (RCp)(R'Cp)Ni^+ \quad (3\text{-}4)$$

$$(RCp)(R'Cp)Ni + Cp_2Ni^- = Cp_2Ni + (RCp)(R'Cp)Ni^- \quad (3\text{-}5)$$

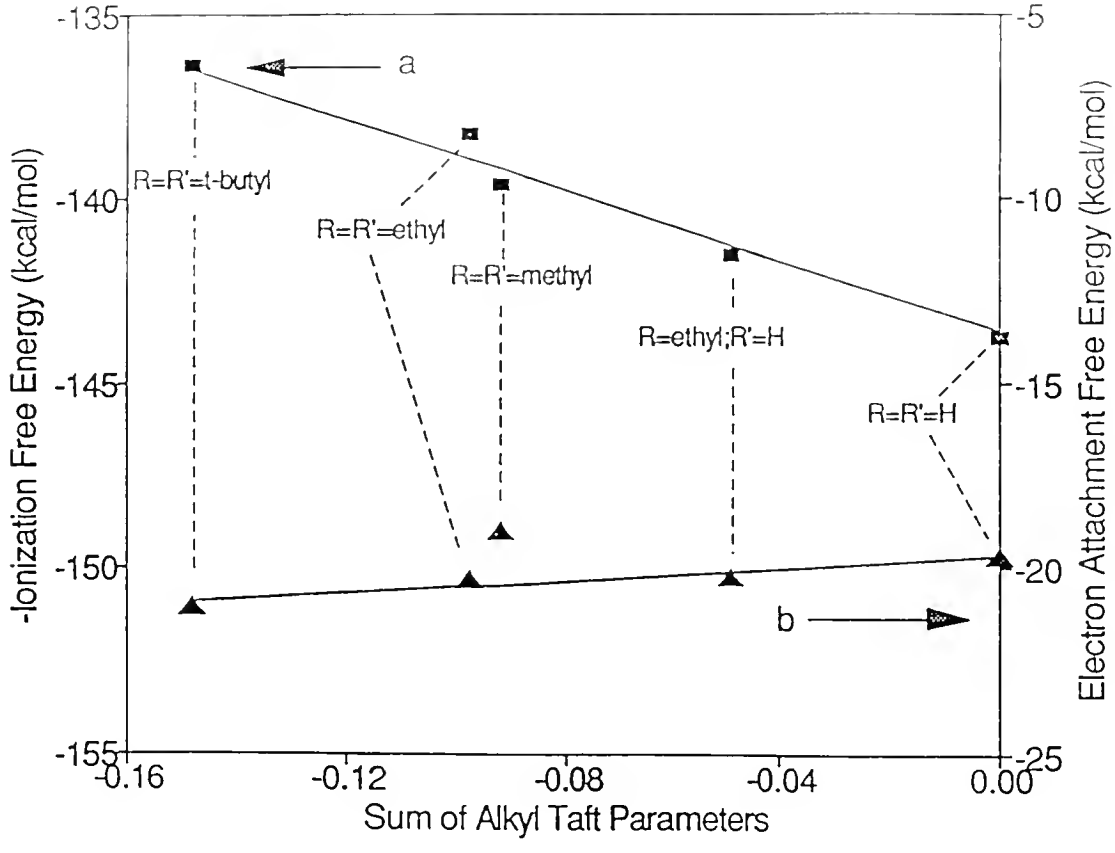

Figure 3-4 Plots of $\Delta G_i°$ and $\Delta G_a°$ data versus Taft $\Sigma(\sigma_I)$ parameters. (a) Ionization data (left scale, squares) are plotted as $-\Delta G_i°$ values for $L_2Ni \rightarrow L_2Ni^+ + e^-$. (b) Electron attachment data (right scale, triangles) are plotted for the process $L_2Ni + e^- \rightarrow L_2Ni^-$. The best fit line for the ΔG_a fit is drawn for all data except $(MeCp)_2Ni$.

Table 3-2 Alkyl Substituent Parameters for Some Alkylnickelocene Complexes and Free Energies for Reactions 3-4, 3-5 and 3-6.

No.[a]	$\Sigma\sigma_I$	$\Sigma\sigma_\alpha$	ΔG_{34}°[b,c]	ΔG_{35}°[b,c]	ΔG_{36}°[b,c]	ΣI[b,d]	ΣP[b,d]
1	0	0	0	0	0	0	0
2	-0.092	-0.70	-4.2	0.7	-4.9	2.5	1.7
3	-0.055	-0.49	-2.3	-0.5	-1.8	1.4	0.9
4	-0.110	-0.98	-5.6	-0.6	-5.0	2.5	3.1
5	-0.148	-1.5	-7.4	-1.5	-5.9	3.0	4.4
6	-0.46	-3.5	-22.5	(~3.5)	(-26)		

a. Compound numbers taken from Table 3-1
b. Units are kcal mol^{-1} .
c. Estimated error for free energy is ± 0.4 kcal mol^{-1}.
d. The derived I and P values in kcal mol^{-1} for the individual substituents are H, $I = P = 0$ (defined); Me, $I = 1.2$, $P = 0.9$; Et, $I = 1.3$, $P = 1.3$; t-Bu, $I = 1.5$, $P = 2.2$

cations and $\Delta G_{35}°$ is the stabilization energy for anions relative to nickelocene, except Me which is destabilizing. The direction of the slopes are opposite because, in general, alkylation of nickelocene stabilizes formation of the cations and anions. For the positive ions, electron-attachment becomes less exoergic as alkylation increases since the cations are stabilized relative to nickelocene. Clearly, the effects of the alkyl groups are different on the electron attachment energies compared to the ionization energies. The ionization data fit with equation 3-3a yields a good fit, with a correlation coefficient of $r = 0.997$. The parameter p_I (= 49.9 ± kcal mol^{-1}) is the slope of the line and reflects the sensitivity of nickelocene ionization potentials to alkylation. This value is comparable to p_I for the alkylferrocenes of 57 ± kcal mol^{-1}.[16] Conversely, the same parameters provide an unacceptable fit of the electron attachment data ($r = 0.51$). The lack of correlation of the methyl derivative is primarily responsible for the poor fit of the $\Delta G_a°$ data to equation 3-3b. The p_I value for the negative ion data is 6 ± 6 kcal mol^{-1}.

A single parameter model was developed by Hehre et al. based on polarizability effects,[52] σ_α parameters, of R. The σ_α parameters have been used to successfully fit the proton-transfer free energies of various cationic and neutral acids. Fits to the alkylnickelocene $\Delta G_i°$ and $\Delta G_a°$ data (Figure 3-5) result in good correlation for the ionization free energies ($r = 0.994$) but only poor correlation for the electron attachment free energies ($r = 0.63$). The σ_α parameters are included in Table 3-2. The slopes for the plots are 5.0 ± 0.4 kcal mol^{-1} for the ionization and 0.8 ± 0.6 kcal mol^{-1} for the reductions. Based on the observed lack of correlation, a single

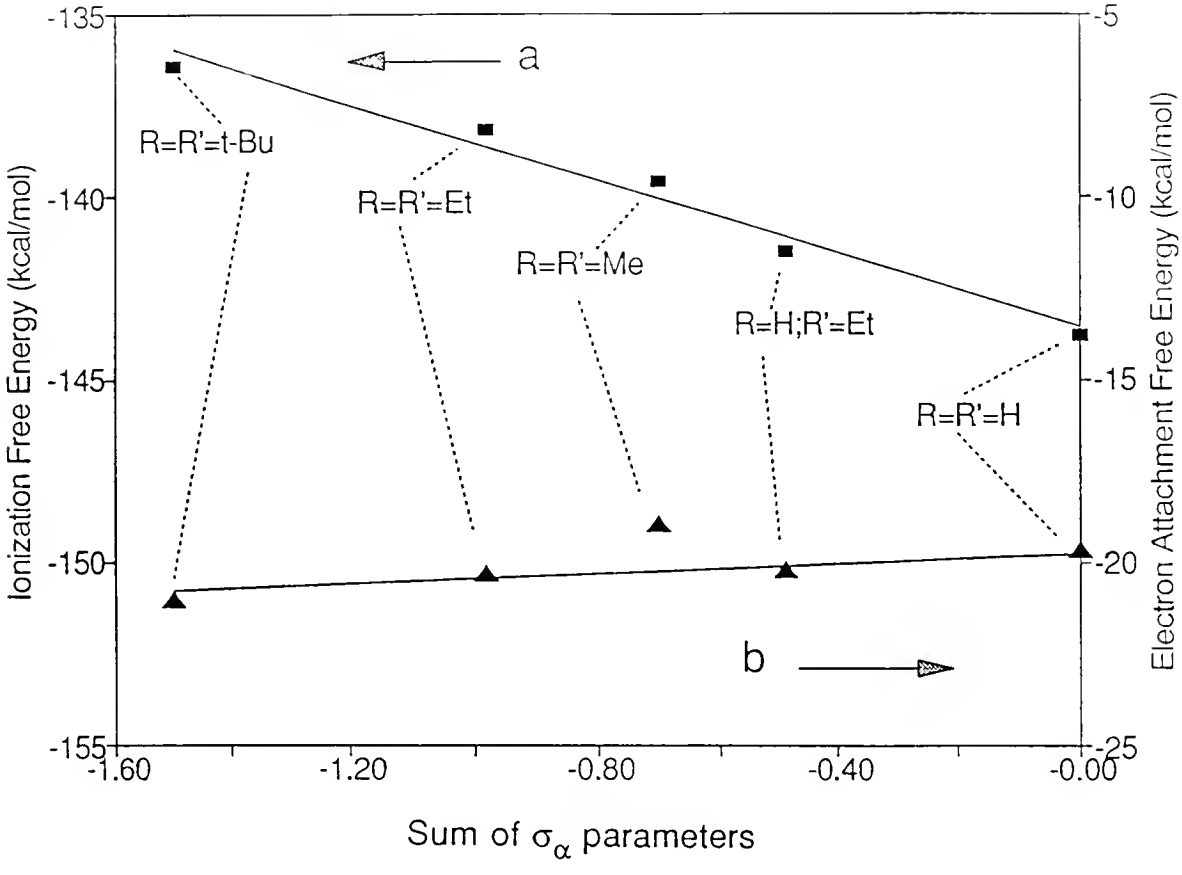

Figure 3-5 Plot of $\Delta G_i°$ and $\Delta G_a°$ data for some alkylnickelocene complexes versus $\Sigma(\sigma_\alpha)$ parameters. (a) Ionization data (left scale, squares) are plotted as $-\Delta G_i°$ values for $L_2Ni \rightarrow L_2Ni^+ + e^-$. (b) Electron attachment data (right scale, triangles) are plotted for the process $L_2Ni + e^- \rightarrow L_2Ni^-$. Plot of ΔG_a versus σ_α is drawn for all points except $(MeCp)_2Ni$.

paramter model is not adequate to correlate the alkyl effects both of the $\Delta G_i°$ and $\Delta G_a°$ values. The failure for the electron attachment data to fit with either of the single parameter models can be largely attributed to the experimentally observed effects of methyl in contrast to t-butyl and ethyl. Both σ_I and σ_α values predict the same direction of effect for all three groups.[50-53]

The trends in the free energy data require a more complex model for interpreting alkyl substituent effects for the nickelocenes than one based only on a single parameter. Apparently, more than one electronic effect is responsible for the disparity in the correlations for the $\Delta G_i°$ and $\Delta G_a°$ data with the σ_I and σ_α values. A simple alternative model combines the effects of the polarizability of the alkyl groups with the inductive effects. A quantitative model has been developed by Taft and workers to separate inductive and polarizability effects for gas-phase proton transfer equilibria involving a number of alcohols (ROH) and their corresponding bases (RO^-) and acids (ROH_2^+).[102] However, the successful application of σ_α parameters to the same data lead Hehre et al. to question the necessity of a two-parameter model.[52] The application of the two-parameter model[102] was used for a comparison to the other fits and to uncover the origin of the disparate effects for methyl relative to other alkyl groups.

The polarizability and the inductive effects relative to R = H are separated by examining the hypothetical gas-phase equilibrium reaction described by equation 3-6 where Cp_2Ni (R = H) is used as the reference compound. Furthermore, the free

energy for the hypothetical equilibria is given by the difference in the free energies of equations 3-4 and 3-5. The polarization effect (P) for R relative the H arises from

$$(RCp)(R'Cp)Ni^- + Cp_2Ni^+ \rightleftharpoons Cp_2Ni^- + (RCp)(R'Cp)Ni^+ \quad (3\text{-}6)$$

$$\Delta G_{36}^\circ = \Delta G_{34}^\circ - \Delta G_{35}^\circ \quad (3\text{-}7)$$

greater charge-induced dipole stabilization of both the cation and the anion. Polarization effects are not destabilizing since the induced-dipole interaction is brought about by a charge localization on a species remote to the substituent.[5] It is assumed that the polarizable alkyl groups will stabilize the nickelocene cations and anions equivalently. Since the same molecular orbital is both electron donor and acceptor orbital, the assumption that polarization stabilization for the positive and negative metal complex ions is the same is easily rationalized.[102] An inductive effect (I) is an electron-releasing effect and will therefore destabilize the negative ions relative to a parent (i.e. $(MeCp)_2Ni^-$ relative to Cp_2Ni^-) but stabilize cation complexes (i.e. $(MeCp)_2Ni^+$ relative to Cp_2Ni^+).[102] It is also assumed that I effects, similar to P, will be approximately equivalent for both the positive and negative ions.[102] Consequently, for the equations 3-4 and 3-5, P is considered positive, while I has opposite effects in both processes. The free energies for equations 3-4 and 3-5 can be written as $-\Delta G_{34}^\circ \simeq I + P$ and $-\Delta G_{35}^\circ \simeq -I + P$. By subtracting these two equations, $\Delta G_{36}^\circ = -2I$ for equation 3-6 is derived. The derived P and I parameters for the alkylnickelocene

compounds are shown in Table 3-2. As expected, correlation of $-\Delta G_{36}°$ values ($2I$) with σ_I parameters (Figure 3-6) yields a good fit (r = 0.995).

The resulting analysis leads to the conclusion that the inductive and polarizability contributions to shifts in the $\Delta G_i°$ and $\Delta G_a°$ values for alkylnickelocene are similar in magnitude. The relatively small changes in the $\Delta G_a°$ values can be attributed as the difference in the polarizability and inductive effects (P - I), both of which are of comparable magnitude. The polarizability and inductive effects for the positive ions are additive (P + I) resulting in a larger overall sensitivity to alkyl substitution.

The separation of polarizability and inductive effects for the acid and base equilibria of the gas-phase alkyl alcohols indicated that P effects are significantly more important than I effects in evaluating the relative gas-phase acidities and basicities of the ROH compounds.[102] For example, the P/I ratio derived for ethyl and t-butyl ROH derivatives are 5.4 and 3.7 respectively.[102] The P/I ratio for the alkylnickelocene complexes for this study are Et =0.9 and t-Bu = 1.5. The I parameters for the two gas-phase studies are equivalent, however the P values derived for the gas-phase alcohols are several times larger than P values derived for the nickelocenes. According to Hehre et al., the separation of effects may not be valid for the ROH compounds since the σ_α parameters provide and acceptable fit to the data.[53] However, it may be necessary to use a two parameter model when the magnitudes of the polarization and inductive effects are comparable.

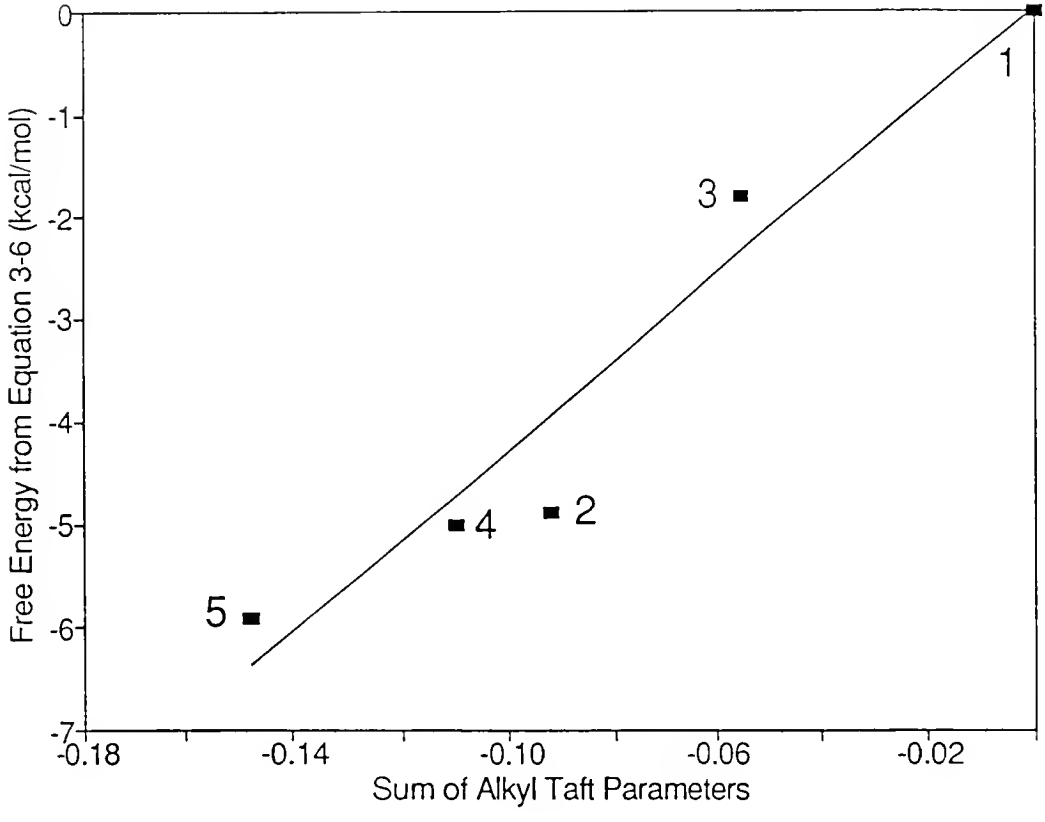

Figure 3-6 Plot of ΔG_{36}° values (kcal mol^{-1}) derived from equations 3-4, 3-5, and 3-6 versus $\Sigma(\sigma_I)$ values. Compound numbers are given in Table 3-1.

The two parameter scheme suggests that the alkyl group polarizability is much smaller for the nickelocenes than the effects of alkyl groups for the ROH compounds.[102] This can be easily rationalized for the nickelocenes because of the increased distance of the charged center to the R group (~3.3 Å)[72] in comparison to RO^-, for example. The polarizability has a $1/r^4$ effect in this case, which can be compared to a $1/r^2$ dependence for inductive effects.[5] The rapid decrease of P and I effects with increasing distance is consistent with the present results.

Solvation Energetics of Nickelocene Cations and Anions

As demonstrated in Chapter 2, $E_{½}$ values for oxidation and reduction of a compound can be related to the gas-phase free energy of ionization or electron attachment through thermochemical cycles. The gas-phase and solution values are related through the differential solvation energetics of the ion and the neutral.[16-20] The $\Delta\Delta G_{solv}°$ for the $Cp_2Ni^{+/0}$ has been discussed in the previous chapter. The $\Delta\Delta G_{solv}°$ value for the $Cp_2Ni^{0/-}$ couple has been determined and relationship of the two values is considered.

Nickelocene has an electrochemical reversible one-electron oxidation potential in various solvents.[89] The reduction of nickelocene is only quasi-reversible in DMF of THF at low temperatures.[34,89] The earlier electrochemical studies by Holloway and Geiger of nickelocene have been repeated.[89] The cathodic peak potential for the reduction of Cp_2Ni was found to be relatively insensitive to temperature over a wide temperature range (~210 to 296 K). Similarly, the E_{pc} value for $(t\text{-butylCp})_2Ni^{0/-}$ was

also found to be independent of temperature over the same temperature range. Electrochemical potentials were measured by using ferrocene as an internal standard.[103] The $\Delta E_{1/2}$ value relative to $E_{1/2}(Fc^{+/0})$ for the oxidation of nickelocene is 0.42 ± 0.1 V compared to a value of 0.40 V measured by Holloway.[89] An estimate of the $\Delta E_{1/2}$ for quasi-reversible reduction potential for nickelocene determined from $E_{1/2}(Fc^{+/0})$ - E_{pc} is 2.4 V ± 0.2 V. Decomposition of the Cp_2Ni^- species at temperatures approaching 273 K was a complicating factor that was circumvented at lower temperatures; therefore, the low temperature reduction potential (~210 K) for nickelocene were used to estimate the E_{pc} value.

From the gas-phase and solution phase data, the differential solvation energies for the 0/- couple was derived by using equation 3-8. The $\Delta\Delta G_{solv}°$ value for the $Cp_2Ni^{0/-}$ couple is -40 ± 5 kcal mol^{-1}. The $\Delta\Delta G_{solv}°$ for the $Cp_2Ni^{+/0}$ couple from Chapter 2 is -38 ± 5 kcal mol^{-1}.[16]

$$\Delta\Delta G_{solv}° = nF[E_{pc} + E_{NHE} + E_{ref}] - \Delta G_i°(g) \qquad (3\text{-}8)$$

Both values are exoergic since the solvation energy of the ion will be greater than the solvation energy of the neutral. The estimated $\Delta E_{1/2}$ from $E_{1/2,ox}$ - $E_{1/2,red}$ is ~2.0 ± 0.2 V in THF. From the gas-phase and solution data for the $Cp_2Ni^{+/0}$ and $Cp_2Ni^{0/-}$ couples, it is possible to extract the average differential solvation energy,[104] $\Delta\Delta G_{solv,av}°$ by using equation 3-9. Note that the average differential solvation free energy determined

$$\Delta\Delta G_{solv,av}^{\circ} = -\frac{1}{2}[-F(E_{ox}^{\circ} - E_{red}^{\circ}) + (\Delta G_{i}^{\circ} + \Delta G_{a}^{\circ})] \quad (3\text{-}9)$$

by equation 3-9 does not require knowledge of the absolute potential of the reference electrode.[16] The absolute potential of the normal hydrogen electrode has been a source of confusion because some of the thermodynamic quantities associated with the process $\frac{1}{2}H_2(g) \rightarrow H^+(aq) + e^-(aq)$ are not accurately known.[54] Therefore, the application of equation 3-9 allows for estimates of $\Delta\Delta G_{solv}^{\circ}$ values without detailed analyses of solvent effects or reference electrode potentials. The $\Delta\Delta G_{solv,av}^{\circ}$ value of -39 ± 3 kcal mol^{-1} obtained from the electrochemical potentials measured in this work is in agreement with the $\Delta\Delta G_{solv}^{\circ}(Cp_2Ni^{+/0})$ estimated in Chapter 2 based on an estimate of the absolute potential for the $Cp_2Ni^{+/0}$ couple in acetonitrile.[16] Thus, it appears that the $\Delta\Delta G_{solv}^{\circ}$ values for the cationic and anionic couples of nickelocene are the equivalent which is consistent with the Born model used in Chapter 2.

A similar analysis for $(t\text{-butylCp})_2Ni$ was not as easily accomplished. Although the oxidation of $(t\text{-butylCp})_2Ni$ is reversible in THF at ambient temperatures, the reduction wave was irreversible even at ~200 K. Moreover, because of the observed irreversible reduction wave, the trends in the redox responses relative to nickelocene were inconsistent with the gas-phase data. The oxidation ($\Delta E_{1/2}$ = 0.52 ± 0.1 versus $E_{1/2}$[Fc])was cathodically shifted by 100 mV, however, the reduction potential was slightly anodically shifted by ~50 mV ($\Delta E_{1/2}$ = 2.35 ± 0.2 versus $E_{1/2}$[Fc])both relative nickelocene. Increased alkylation of nickelocene is expected to shift the reduction potentials cathodically due primarily to solvent effects associated

with the t-butyl groups. The differential solvation energy for the $(t\text{-butylCp})_2Ni^{+/0}$ couple is -33 ± 5 kcal mol^{-1}. The estimated $\Delta E_{1/2}$ for $(t\text{-butylCp})_2Ni$ is 1.8 ± 0.1 V resulting in a $\Delta\Delta G_{solv,av}°$ of -37 ± 3 kcal mol^{-1}, which is in agreement with the average differential solvation energy for nickelocene.

Bond Disruption Enthalpies for Nickelocene Anion

Estimates of the average heterolytic and homolytic Ni-Cp bond disruption enthalpies for Cp_2Ni^- have been determined from thermochemical cycles as previously described.[16,18,84] Values for the heats of formation of Ni(g) and $Ni^+(g)$ and $Ni^-(g)$ were determined from known thermodynamic quantities.[8,27] The reported experimental errors include uncertainties in the $\Delta G_a°$ value for nickelocene in addition to errors in the literature values for the $\Delta H_f°$ quantities. The average bond disruption enthalpies are $\Delta H_{hom}°(Cp_2Ni^-)$ = 64 ± 3 kcal mol^{-1} and $\Delta H_{het}°(Cp_2Ni^-)$ = 126 ± 5 kcal mol^{-1}.

Conclusions

The alkylnickelocene studies have allowed the first survey of alkyl substituent effects for electron attachment and ionization energetics in which the same molecular orbital can be considered both the acceptor and donor orbital. The data for the alkylnickelocene complexes demonstrate that gas-phase electron affinities of metal complexes can be increased by increased alkylation. However, due to larger inductive effects versus polarization effects, methyl groups destabilize formation of nickelocene

negative ions. The destabilization of methylated nickelocene complexes was further demonstrated by lack of an observed ion signal for $Cp^*_2Ni^-$ and the absence of an electrochemical response for reduction of Cp^*_2Ni.[39,105] For comparison, the gas-phase $\Delta G_a°$ values for some ruthenium β-diketonate complexes[42] are consistent with the present conclusions that increased alkylation yield an increase in electron affinity. Thus, alkyl groups are not intrinsically electron-donating with respect to gas-phase redox thermochemistry of metallocenes[16,19] or coordination complex ions.[84] Specifically, electron attachment and ionization free energies are not always lowered by alkyl groups.

An electrostatic model was successfully used to rationalize the trends in the $\Delta G_i°$ and $\Delta G_a°$ values for the nickelocene complexes. Single parameter models can be used to interpret free energy of ionization data for the alkyl metallocene compounds,[5,52,53] however, electron attachment data fail to correlate using either σ_I or σ_α parameters. The separation of inductive and polarizability effects[102] revealed that the two electronic effects are comparable in magnitude for the nickelocene complexes. Furthermore, *I* and *P* effects are additive when considering shifts in the $\Delta G_i°$ values relative to nickelocene but the effects approximately cancel for the negative ions. Overall, the shifts in the $\Delta G_i°$ values relative to nickelocene are greater than comparable shifts in the $\Delta G_a°$ values.

Analysis of the differential solvation free energies for one-electron oxidation and reduction of nickelocene shows that both couples have similar differential solvation energies. The $\Delta\Delta G_{solv,av}°$ values estimated for $(t\text{-butylCp})_2Ni$ is -37 ± 5

kcal mol^{-1}, and is consistent with the similar value for nickelocene (-39 ± 5 kcal mol^{-1}). The difference in solvation relative to nickelocene can be rationalized due to the lipophilicity of the t-butyl groups. The similar $\Delta\Delta G_{solv}°$ values for the nickelocene +/0 and 0/- redox couples are consistent with the Born model. According to the Born model, $\Delta\Delta G_{solv}°$ values are dependent on ionic charge (q^2) and ionic radius (r) in addition to the dielectric constant of the solvent.[54] Since both the size and charge parameters are equal for the $Cp_2Ni^{+/0}$ and $Cp_2Ni^{0/-}$ couples, the differential solvation energies, according to the Born model should be equal in the same solvent.

Experimental Procedures

Positive and negative ion electron-transfer equilibrium studies were performed on a Fourier transform ion cyclotron resonance mass spectrometer as previously described.[14-20] The methods for positive and negative ion studies are similar with a few important exceptions. Most obvious is that positive trapping potentials were used for positive ion studies and negative trapping potentials were employed for the study of negative ions. Electron impact energies ranged from 8 - 12 volts for the positive ions studies however negative ions were generated from low energy electron impact.

Cyclic voltammetry studies were performed with a PAR system (Models 173/175). A platinum button working electrode and a KCl saturated Ag/AgCl reference electrode were used. Electrochemical experiments were performed in THF containing 0.1 M Bu_4NPF_6 and solutions were freshly prepared prior to each experiment. Tetrahydrofuran was distilled from Na/benzophenone. The supporting

electrolyte Bu_4NPF_6 was recrystallized several times from an acetone/ethanol mixture and dried in vacuo overnight. Electrolytic solutions containing the nickelocenes were either prepared in an inert atmosphere glove box or by injecting millimolar solutions of a nickelocene/THF solution directly into the cell through a septum. Sublimed samples of ferrocene and nickelocene were used.

Low temperature electrochemical studies were performed by submerging the entire electrochemical cell into solvent/CO_2 baths: acetone (-72 °C), isopropanol (-55 °C), CCl_4 (-23 °C), and ice water. By varying the solvent/CO_2 ratio, intermediate temperatures were obtained. The electrochemical cell was allowed to equilibrate at a temperature for several minutes before scans were recorded. Typically, temperature variation of ± 5 K during each individual scan were measured by using a low temperature alcohol thermometer.

Azulene was purchased from Aldrich chemicals and used without further purification. Nickelocene and Bz_2Cr were purchased from Strem Chemicals and were purified by vacuum sublimation. The alkylated nickelocene complexes were prepared according to literature methods[106] and purified by preparative HPLC.

CHAPTER 4
GAS-PHASE AND SOLUTION OXIDATION POTENTIALS OF RUTHENOCENE DERIVATIVES

Introduction

Variation of the ligand environment around a metal center is an effective means of evaluating the electronic effects of ligands with respect to a parent compound.[107] Modifications of Cp ligands of a metal complex can lead to modifications in reactivity. For example, substitution of Cp* for Cp is well-known for increasing the steric congestion around a metal center and therefore influence the reactivity of the complex;[107] however, Cp* substitution for Cp will also alter the electronic character metal complex.[105,108] Since steric effects have little influence on the oxidation-reduction potential of molecular species when variations are small, determined $\Delta G_i°$ or $\Delta G_a°$ changes can be attributed to the effect of the supporting ligands. Electrochemistry and photoelectron spectroscopy have been used to investigate the electronic effects of varying Cp ligation for metallocenes and metallocene derivatives. However, as mentioned earlier, the effectiveness of these two techniques for evaluation of metal complex oxidation-reduction energies can be limited by several influencing factors. Electrochemical potentials for metal complexes may be irreversible therefore the measured $E_{½}$ values may not be accurate assessments of the thermodynamic potential. Vertical ionization energies measured by photoelectron

spectroscopy are only accurate assessments of the adiabatic ionization if the equilibrium geometry of the ion and the neutral are small.[27]

In Chapter 2, the thermal free energy of ionization for ruthenocene was reported (ΔG_i° = 164.6 ± 1.5 kcal mol^{-1}) at 350 K.[16] This value of ΔG_i° differs from a previously reported value[13] due to corrections made for ΔS_i° values for the reference compounds. The electrochemical oxidation of ruthenocene is irreversible under most experimental conditions.[91] For example, an irreversible $2e^-$ process is observed for Cp_2Ru in CH_3CN containing 0.1 M TEAP and in CH_2Cl_2 containing 0.1 M Bu_4NPF_6.[91] Recently, Mann and coworkers have reported a reversible oxidation potential for ruthenocene in CH_2Cl_2 containing tetrabutylammonium tetrakis(3,5-bis(trifluoromethyl)phenyl)borate, $Bu_4N^+TFPB^-$. The ruthenocene cation is extremely susceptible to secondary reaction in common solvent/electrolyte systems thus the extremely weakly noncoordinating anion $TFPB^-$ reduces the susceptible to secondary nucleophilic reactions of Cp_2Ru^+.[90] The majority of ruthenocene derivatives demonstrate irreversible electrochemical oxidation potentials in common electrochemical solvent systems.[91] A reversible oxidation for decamethylruthenocene has been reported in CH_2Cl_2 containing 0.1 M Bu_4NPF_6 by several workers.[90,91,92]

The lack of reversible electrochemical oxidations for most ruthenocene derivatives dictates the need for accurate thermochemical ionization potentials. Electron-transfer equilibrium techniques[15-20] have been used to determine the free energies of ionization for a broad series of ruthenocene derivatives by using Fourier transform mass spectrometry.[44-47] Electron-transfer equilibrium methods have been

described in the previous chapters. Free energies of ionization for the ruthenocene derivatives are represented by equation 4-1 and are reported at 350 K.

$$Cp_2Ru \rightarrow Cp_2Ru^+ + e^- \qquad (4\text{-}1)$$

Ruthenocene derivatives were of the type LL'Ru where L and L' are cyclopentadienyl ligands. Ligand variations for the ruthenocene derivatives include perhalogenation of a Cp ring, attachment of electronic withdrawing groups (i.e. NO_2 and CF_3) and fused-ring systems.

Cyclic voltammetry was used to reevaluate the oxidation potentials for many of the ruthenocene derivatives.[91] Oxidation $E_{1/2}$ values reported to be irreversible for several of the ruthenocenes were observed to quasi-reversible under our experimental conditions. Additionally, $E_{1/2}$ values for several ruthenocene complexes are reported for the first time. Several solvent/electrolyte systems were used for selected complexes in order to carefully characterize the electrochemical oxidation potentials.

Comparison of the free energies of ionization and electrochemical oxidations potentials leads to insight concerning solvent effects of the ruthenocene oxidation potentials. Thermochemical cycles which incorporate $\Delta G_i°$ values in both the gas phase and solution have been used to determine differential solvation free energies,[16,20,54,84] $\Delta\Delta G_{solv}°$, for the ruthenocene complexes. Values for $\Delta\Delta G_{solv}°$ are compared to an electrostatic model for predicting solvation energetics.[20,54]

Direct comparison of $\Delta G_i°$ values for the series of ruthenocene LL'Ru complexes with $\Delta G_i°(Cp_2Ru)$ has lead to information concerning the electronic effects of the various Cp derivatives. Ligand effects have been quantified through the development of a new set of Cp ligand parameters which use Cp and Cp* as references.[20] Implications for use of such a parameter scale for predicting metal complex reactivity are considered.

Results of the Electron-Transfer Equilibrium Reactions

Details concerning electron-transfer equilibrium techniques have been given in Chapter 2. Reactions were followed for 5-10 s to confirm ETE and were monitored from both endoergic and exoergic directions to insure that equilibrium was independent to the approach to ETE. The general electron-transfer equilibrium reaction is given in 4-2 was studied, where LL'Ru denotes a ruthenocene complex

$$LL'Ru + R^+ = R + LL'Ru^+ \qquad (4\text{-}2)$$

and R denotes a reference compound with a known $\Delta G_i°$ value. Figure 4-1 is an electron-transfer equilibrium ladder displaying all reactions involving the ruthenocene complexes. Similar to other ladders in this work, values adjacent to arrows represent $\Delta G_{et,350}°$ values for individual ETE reactions. All $\Delta G_i°$ values lie adjacent to the compound in Figure 4-1 and are also summarized in Table 4-1. Compound

abbreviations used throughout this chapter are also given in Table 4-1 and Cp ligand abbreviations are given in Table 4-2.

The ruthenocene derivatives exhibit a wide range of $\Delta G_i°$ values spanning over 2 eV. Various organic compounds and metallocenes were used as reference compounds for ETE studies.[16,27,39,40,59] Details concerning the $\Delta G_i°$ values of the reference compounds used for ruthenocene ETE studies are given in Chapter 2. Aniline and benzene derivatives used as reference compounds have ionization potentials that are anchored to the $\Delta G_{i,350}°$ values of N,N-dimethylaniline (DMA)[40,59] and benzene[27,39] which are 163.4 ± 0.5 and 212.4 ± 0.5 kcal mol^{-1} respectively. The free energies of ionization of the metallocene reference compounds were determined from ETE studies and are anchored to DMA. The $\Delta G_i°$ for ruthenocene (**1**) has been reported previously[16,20] and is used here for comparison to other ruthenocene $\Delta G_i°$ values.

In several cases, compounds were brought to equilibrium with more than one reference compound or another metallocene as a check on the internal consistency of the ladder. In general, the consistency throughout the ladder is good. For example, **1** and **5** were both brought to equilibrium with DMA and each other; it can be observed from the ladder that the expected difference in the $\Delta G_i°$ values of the ruthenocene complexes is obtained from the ETE study. In another example, bis(indenyl)ruthenocene **8** was brought to ETE with ferrocene and ethylferrocene. The difference in the $\Delta G_i°$ values for the ferrocene compounds was previously determined[16] to be 2.9 ± 0.5 kcal mol^{-1} and the observed difference from the two ETE

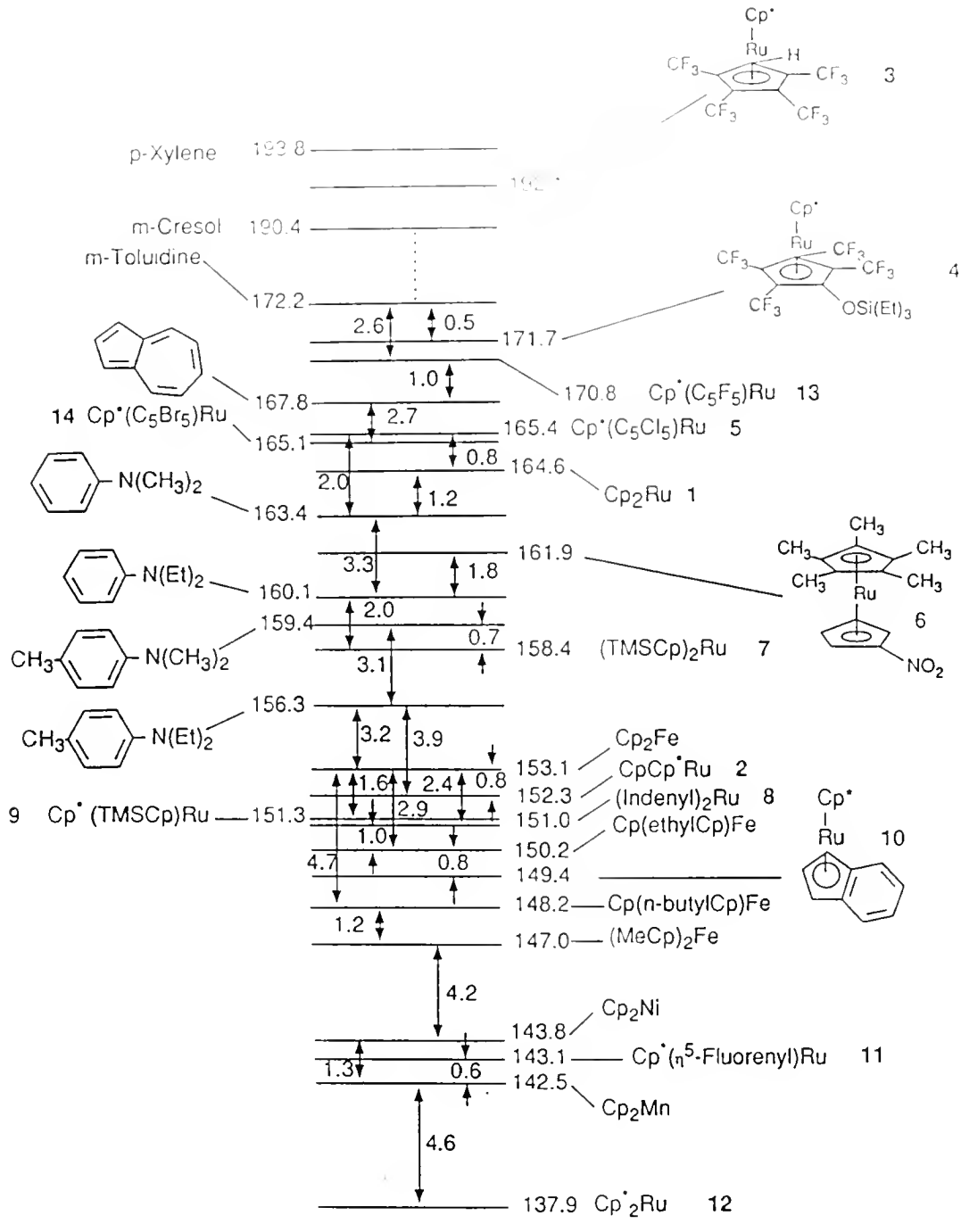

Figure 4-1 Electron-transfer equilibrium ladder for several ruthenocene derivatives for the process $M \rightarrow M^{+} + e^{-}$. Values adjacent to arrows denote ΔG_{et}° values at $T = 350$ K for individual ETE couples. Ruthenocene ΔG_{i}° values (kcal mol^{-1}) are anchored to ΔG_{i}°(DMA) and ΔG_{i}° of benzene. The ΔG_{i}° value for 3 is a bracketed value.

Table 4-1 Values $\Delta G_i°$ for Ruthenocene Derivatives and Other Data

LL'Ru[a]	No.	$\Delta G_i°$(exp.)[b,c]	XPS[d]	$\Delta G_i°$(eq 4-9)[b,e]
(Cp)(Cp)Ru	**1**	164.6	280.7	164.6
(Cp)(Cp*)Ru	**2**	152.3	280.2	151.6
(TTFMH)(Cp*)Ru	**3**	192		192
(TTFMOSi)(Cp*)Ru	**4**	171.7		171.7
(C_5Cl_5)(Cp*)Ru	**5**	165.4	280.8	165.4
(NO_2Cp)(Cp*)Ru	**6**	161.9		161.9
(TMSCp)(TMSCp)Ru	**7**	158.4		160.2
(Ind)(Ind)Ru	**8**	151.0		153.9
(TMSCp)(Cp*)Ru	**9**	151.3		149.4
(Ind)(Cp*)Ru	**10**	149.4	280.1	146.4
(Flu)(Cp*)Ru	**11**	143.1	279.6	143.1
(Cp*)(Cp*)Ru	**12**	137.9	279.9	138.6
(C_5F_5)(Cp)Ru	**13**	170.8		170.8
(C_5Br_5)(Cp)Ru	**14**	165.1		165.1

a. Ligand abbreviations given in Table 4-2.
b. Units are kcal mol^{-1}.
c. Error limits are ± 2 kcal mol^{-1} except **3** (± 5 kcal mol^{-1}).
d. Core binding energies measured by XPS are taken from reference 91.
e. Only equation 4-9 data shown. Values of $\Delta G_i°$ predicted from equation 4-8 will be exactly equal to the experimental $\Delta G_i°$ values.

Table 4-2 Ligand γ^* and γ Parameters

Ligand	Abbreviation	$\gamma^*(L)^a$	$\gamma(L)^a$
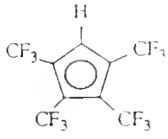	TTFMH	2.76	3.10
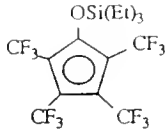	TTFMOSi	1.31	1.55
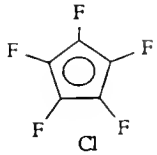	C_5F_5	1.28	1.47
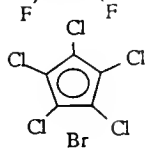	C_5Cl_5	0.91	1.06
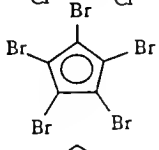	C_5Br_5	0.89	1.03
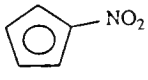	NO_2Cp	0.67	0.79
	Cp	0	0
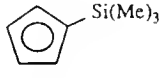	TMSCp	-0.07	-0.17
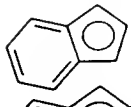	Ind	-0.20	-0.41
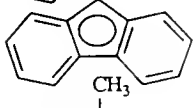	Flu	-0.64	-0.65
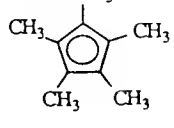	Cp^*	-1	-1

a. Ligand parameters for Cp and Cp* are 0 and -1 respectively by definition.

studies involving **8** is 3.4 kcal mol^{-1}, within the ± 0.5 kcal mol^{-1} experimental error. It was not always possible to do cross checks since many of the organometallics had to be introduced into the mass spectrometer by use of a heated solids probe. Therefore, only reference compounds that were sufficiently volatile to be sublimed via a heated leak valve were used for checks of internal consistency.

For the ruthenocene derivatives, error limits of ± 2 kcal mol^{-1} in the $\Delta G_i°$ values are reported. Errors in the free energies of ionization originate from two sources in the experiment. Error limits in the reference compounds, which are typically ± 1 kcal mol^{-1} for the organic reference compounds,[27,39,40,59] although some compounds have errors as high as ± 2 kcal mol^{-1}, and ± 1.5 kcal mol^{-1} for the metallocene reference compounds.[16] Since the majority of $\Delta G_i°$ values used in the equilibrium studies are referenced to other compounds, errors are propagated throughout the system as the accuracy of the reference compounds decreases. Errors in the measured K_{eq} values for individual ETE experiments are the second source of experimental uncertainty. Neutral partial pressure measurements of the reactant gases and ion detection measurements introduce errors in the K_{eq} quantities of approximately ± 0.5 kcal mol^{-1} (this represents an error of 50% in the measured equilibrium constant). The partial pressure measurements account for the largest experimental uncertainty in evaluation of K_{eq} values. However, an error as large as 30% in the partial pressure of the neutral gases is only a ± 0.2 kcal mol^{-1} error in K_{eq} values. Errors in the measured ion intensities are not expected to exceed 10%. Considering all

possible sources of error in the evaluation of ΔG_i° values for the ruthenocene derivatives, an overall ± 2 kcal mol^{-1} uncertainty is reported [20]

All free energy values in Figure 4-1 were obtained from direct ETE reactions involving at least one reference compounds. However, definitive equilibrium for Cp*(TTFMH)Ru (**3**) could not be established with either *m*-cresol or *p*-xylene. Therefore, a bracketed value for ΔG_i° of **3** is reported with ± 5 kcal mol^{-1} error. The bracketed value for **3** was obtained from sequential exothermic electron-transfer reactions as demonstrated by equations 4-3 and 4-4. Both reaction were observed

$$p\text{-xylene}^+ + \mathbf{3} \rightarrow \mathbf{3}^+ + p\text{-xylene} \qquad (4\text{-}3)$$

$$\mathbf{3}^+ + m\text{-cresol} \rightarrow m\text{-cresol}^+ + \mathbf{3} \qquad (4\text{-}4)$$

to completion in that no significant back electron transfer in the endothermic direction was conclusively observed. From the electron-transfer bracketing experiments the ΔG_i° value of **3** is estimated from the average ΔG_i° values of the two organic compounds. The reaction rate of **3** with *m*-cresol was slow (k_f for reaction 4-4 was 4.7 ± 1.4 x 10^{-11} cm^3 molec^{-1}s^{-1}) and this may explain why electron-transfer equilibrium was not observed.[61,80] For comparison, compound **4** was brought to equilibrium with *m*-toluidine and the rate constant reaction 4-5 of is 4.8 x ± 1.4 10^{-10} cm^3 molec^{-1}s^{-1}.

$$\mathbf{4} + m\text{-toluidine}^+ \rightarrow m\text{-toluidine} + \mathbf{4}^+ \qquad (4\text{-}5)$$

Evaluation of the Gas-Phase Free Energies of Ionization for a Series of Ruthenocene Derivatives

As all of the neutral ruthenocene complexes are d^6 metal compounds with $^1A_{1g}$ ground states,[35] variation in the ionization potentials of the derivatives with respect to **1** is due solely to shifts in the molecular orbital energies resulting from electronic effects of the ancillary Cp ligands.[20] Therefore, comparison of the $\Delta G_i°$ values for the series of compounds need only include electronic effects of the substituents or the ligands since all the ruthenocene complexes are electronically degenerate.[35] As the substituents become more electron withdrawing, the energy of the valence orbitals will decrease, i.e. harder to remove an electron from a molecular orbital.[5,53] Conversely, as substituents become more electron donating, the energy of the valence molecular orbitals are raised, thus the complexes will be more easily oxidized.[5,53]

Overall, the experimentally derived free energies of ionization for the ruthenocene complexes follow the expected trends in that compounds bearing electron-withdrawing substituents such as -Cl, -F, or $-CF_3$ have $\Delta G_i°$ values greater than ruthenocene and compounds with electron-donating substituents have lower $\Delta G_i°$ values.[5,20,50-53] The observation for electron-withdrawing groups to increase the ionization potential with respect to the parent ruthenocene has been observed by Burk and coworkers[109] and by Gassman and Winter.[91] Burk measured the oxidation potentials of **3** and **4** by using cyclic voltammetry and observed the oxidation potentials to be anodically shifted relative to ruthenocene;[109] however, the compounds demonstrated irreversible electrochemistry. Gassman and Winter measured the Ru 3d

core binding energies by using X-ray photoelectron spectroscopy (XPS) of a series of ruthenocenes and noted the Cp*(C_5Cl_5)Ru 3d core binding energy is 0.1 eV greater than that for ruthenocene.[91] Alternatively, Gassman also observed that ruthenocenes with electron-donating functions on the Cp rings had lower Ru 3d core binding energies than ruthenocene. For example, the binding energy of ruthenocene is 280.7 eV while the binding energy of decamethylruthenocene is 279.9 eV. The core binding energies are reported to be accurate within 0.01 eV.[91]

Ionization Free Energies of Ruthenocenes with Electron-Withdrawing Ligands

The compounds studied that bear electron withdrawing groups are Cp*(TTFMH)Ru (**3**), Cp*(TTFMOSi)Ru (**4**), and Cp*(NO_2Cp)Ru (**6**). The halogenated complexes Cp*(C_5X_5)Ru, where X = F, Cl, Br will be discussed in a separate section. The fluorinated complexes **3** and **4** have $\Delta G_i°$ values greater than ruthenocene.[20] Although the $\Delta G_i°$ value for **6** is lower than $\Delta G_i°$(Cp_2Ru), Cp*(NO_2Cp)Ru possesses an electron-withdrawing NO_2Cp ligand, which is countered by the polarizable pentamethylcyclopentadienyl ligand.

Complexes **3** and **4** both possess extremely electron-withdrawing trifluoromethyl groups.[109,110,111] A survey of reported ionization potentials for several benzene derivatives demonstrates that the CF_3 group is generally more electron-withdrawing than -CN or fluorine. The ionization potential of $CF_3C_6H_5$ = 223.3 kcal mol^{-1} which is 1.5 kcal mol^{-1} greater than cyanobenzene and 11 kcal mol^{-1} greater than fluorobenzene.[27]

Burk and workers first prepared the TTFMH ligand in the interest of developing highly electrophilic oxidative-resistent metal complexes.[109,112] Additionally, the solubility and reactivity of fluorinated complexes is quite different with respect to the nonfluorinated analogues.[109] Gassman and Winter prepared the first metallocene bearing the trifluoromethyl function as $(CF_3Cp)_2Fe$ and demonstrated the powerful electron-withdrawing nature of the complex by using X-ray PES.[110] The Fe 2p core binding energy of $(CF_3Cp)_2Fe$ is 708.6 eV compared to the binding energy of Cp_2Fe = 708.0 eV.[111] Recently, Gassman and workers prepared the novel ligand tetramethyl(trifluoromethyl)Cp and demonstrated that electronically, Me_4CF_3Cp is equivalent to Cp. Specifically, the Ru 3d core binding energies of $(Me_4CF_3Cp)CpRu$ and ruthenocene are equal. Based on Gassman's data, one CF_3 group is as electron withdrawing as four methyl groups are electron donating, when the functions are bonded to a coordinated ligand.[111]

Gassman's results are consistent with the $\Delta G_i°$ value of **3**. The TTFMH ligand is approximately three times more electron withdrawing as the Cp* ligand is electron donating. Therefore, a methyl group lowers the ionization potential of ruthenocene by ca. 2.5 kcal mol^{-1} per group, based on $\Delta G_i°$ data for CpCp*Ru and Cp^*_2Ru. Thus, if four methyl groups have the opposite effect to one CF_3 group, a CF_3 function on a Cp ring of ruthenocene should increase the $\Delta G_i°$ relative to Cp_2Ru by ~10 kcal mol^{-1}. Therefore, the TTFMH ligand of **3** should increase the $\Delta G_i°$ relative to ruthenocene by ~40 kcal mol^{-1} and the Cp* ligand is expected to decrease $\Delta G_i°$ ~13 kcal mol^{-1}; an

estimated $\Delta G_i°$ value for **3** of 192 kcal mol^{-1} which is the equal to the $\Delta G_i°$ value estimated from electron-transfer bracketing experiments of **3**.

The free energy of ionization of **4** is lower than $\Delta G_i°(3)$ by ~20 kcal mol^{-1}. The addition of the triethylsiloxyl function in place of the a hydrogen for TTFMOSi accounts for the lower ionization potential. The siloxyl group is electron donating and counters the electron-withdrawing nature of the CF_3 groups.[109]

The $\Delta G_i°$ value of **6** is less endoergic than ruthenocene due to the strong destablizing inductive effect of the nitro group. The $\Delta G_i°$ value of CpCp*Ru is 10 kcal mol^{-1} less than $\Delta G_i°(6)$ indicating that the NO_2 groups is as electron withdrawing as a CF_3 group. Both functions stabilize ruthenocene towards oxidation by ~10 kcal mol^{-1}.

Ruthenocenes Bearing a Perhalogenated Cyclopentadienyl Ligand

Three ruthenocene derivatives with a supporting perhalogenated Cp ligand have been studied. The pentafluorocyclopentadienyl complex, which represents the first metal complex possessing the η^5-C_5F_5 ligand, was recently synthesized by Hughes and Curnow.[114] The bromo complex was prepared by Winter and coworkers[114] by successive permercuration/perbromination of Cp. Compound **5** was prepared by the method of Gassman and Winter.[91] The interest in perhalogenated cyclopentadienyl ligands is in their electron-withdrawing properties, in addition to novel solubility and reactivity relative to Cp.[109,113] Little is known concerning the electronic properties of perhalogenated Cp ligands,[91,109,115] thus electron-transfer equilibrium methods can be

used to quantify the effects these ligands have on the physical and chemical properties of metal complexes.

In all three cases, the perhalogenated ligand stabilizes the ruthenocene complexes towards oxidation. The electronic effects of the bromo and chloro ligands are equivalent,[3,5] as $\Delta G_i°$(**5**) = 165.4 ± 2 kcal mol^{-1} is only slightly greater than that of $\Delta G_i°$(**14**) = 165.1 kcal mol^{-1}. For comparison, the ionization potential chlorobenzene is 2 kcal mol^{-1} more endoergic than the IP of bromobenzene.[27,39] The perhalogenated bromo and chloro ligands are essentially opposite in electronic effects to Cp*. Since the $\Delta G_i°$ values of complexes **5** and **14** are similar to $\Delta G_i°(Cp_2Ru)$, it can be concluded that the electron-donating nature of the Cp* ligand is countered by the electron-withdrawing character of the halogenated ligands.

The measured $\Delta G_{et}°$ values for electron-transfer equilibrium of Cp*(C_5F_5)Ru with reference compounds azulene ($\Delta G_i°$ = 167.8 ± 1.0 kcal mol^{-1}) and *m*-toluidine ($\Delta G_i°$= 172.2 ± 1.5 kcal mol^{-1}) are +2.6 and -1.0 kcal mol^{-1}. The $\Delta G_i°$ value for the for complex **13** was determined to be 170.8 ± 1.5 kcal mol^{-1}.

The perfluoro ligand was found to have electronic effects comparable to the perchlorocyclopentadienyl ligand. Replacing Cl for F results in an increase in $\Delta G_i°$ by ~1 kcal mol^{-1} per F. Compared to Cl, F is expected to increase the ionization potential due it lower polarizabilty, however π-resonance effects of F compensate[53] for the polarizabilty in the case of ruthenocene complexes. Resonance donation of the F lone-pair electrons into the Cp ring diminishes the expected large positive inductive

effect. The overall result is that the $\Delta G_i°$ values for the chloro and fluoro compounds are equivalent.

Structurally, the metal complexes bearing perhalogenated ligands are ostensibly comparable to ruthenocene and decamethylruthenocene. In both Cp_2Ru and Cp^*_2Ru, the Cp rings are eclipsed and crystal structure data for **5** demonstrates that the methyl groups and the chlorides are also eclipsed; however, an indication of the electron-withdrawing ability of the C_5Cl_5 ligand can be inferred from the ruthenium-to-ring-centroid distance. The metal center is unsymmetrically displaced closer to the electron-withdrawing ligand. The Ru-Cp* distance is 1.82 Å while the Ru-C_5Cl_5 distance is 1.78 Å.[91] This indicates that Ru is being held closer to the more electron-deficient ligand, possibly as a result of the electron-donating ability of Cp*.

Free Energies of Ionization of Ruthenocenes Derivatives with Fused-Ring Systems and Electron-Donating Ligands

Gassman and Winter noted that Cp*FluRu was more easily oxidized than Cp^*_2Ru based on electrochemical measurements and Ru 3d core binding energies measured by XPS; thus, Flu was determined to be more electron donating than Cp*.[91] Because the reported electrochemistry of **11** is irreversible,[91] and the core binding energies may not reflect valence ionization potentials, their conclusions are in doubt. Comparison of the free energies of ionization of the two compounds indicates that **12** has a lower $\Delta G_i°$ value than **11**, which is inconsistent with Gassman's findings. Moreover, decamethylruthenocene has the lowest $\Delta G_i°$ value of all the ruthenocene compounds studied. Based on the adiabatic ionization potentials, Flu does not

stabilize formation of Cp^*RuL^+ to the extent that Cp* does. The reported electrochemical potentials[91] may follow a different trend due to different solvation energies of **11** versus **12** or because of the irreversible electrochemistry of **11** does not yield an accurate assessment of the true thermodynamic potential. Definitive interpretation of the XPS results with the electron-transfer equilibrium data is not possible to due the limited amount of data that can be compared. Figure 4-2 is a plot of XPS binding energies[91] and $\Delta G_i°$ data for several ruthenocene complexes. It is obvious from the plot that the correlation fails for Cp* and Flu.

Electron-transfer equilibrium of Cp*FluRu and Cp^*_2Ru (reaction 4-6) was attempted but the reaction was exothermic favoring Cp^*FluRu^+ even at pressure

$$Cp^*_2Ru + Cp^*FluRu^+ \rightarrow Cp^*_2Ru^+ + Cp^*FluRu \qquad (4\text{-}6)$$

ratios approaching 100. The entropies of ionization for these two compounds have not been determined. Significant differences in the $\Delta S_i°$ values could realistically reverse the trend in the $\Delta H_{i,350}°$ values. However, in order to account for a 5 kcal mol^{-1} difference in the $\Delta H_i°$ values, a difference in the $\Delta S_i°$ values of ~15 cal mol^{-1} K^{-1} is required. There is no obvious reason for an entropy difference this large. The thermal ionization free energies reported here probably reflect the electronic effects that would be expected in chemical reactions of metal complexes with these supporting ligands.

The $\Delta G_i°$ values of CpCp*Ru and Cp^*_2Ru are consistent in that the electronic effects of the Cp* ligand are additive. Thus the $\Delta G_i°$ value for **2** is ~12 kcal mol^{-1}

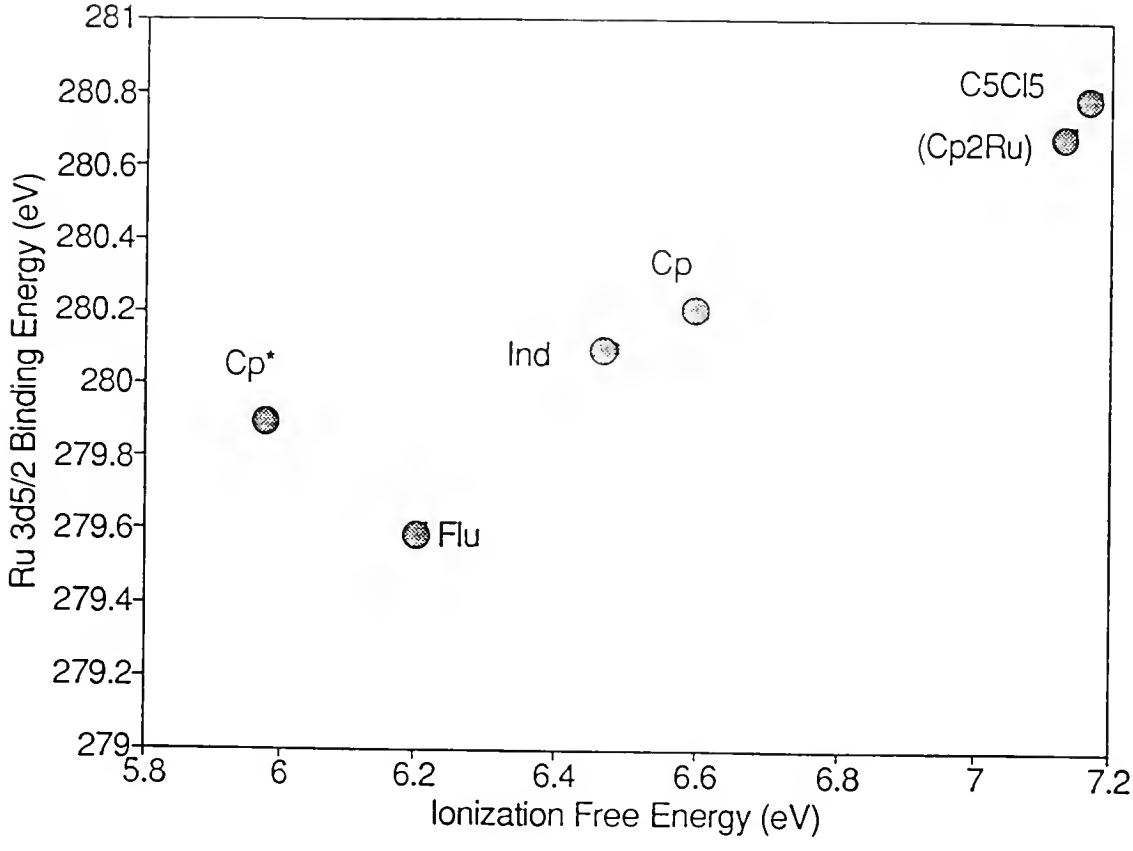

Figure 4-2 Plot of Ru 3d binding energies from reference 91 versus ETE $\Delta G_i°$ values for several Cp*Ru-L complexes and ruthenocene.

less than ruthenocene and the $\Delta G_i°$ value of **12** is ~26 kcal mol^{-1} less than ruthenocene. From these data an electron-donating effect of ca. 2.5 kcal mol^{-1} per methyl group can be estimated.

The $\Delta G_i°$ of Cp*IndRu is only 3 kcal mol^{-1} less than that of **2** indicating that the indenyl ligand stabilizes a positive charge only slightly more relative to Cp. The $\Delta G_i°$ for $(Ind)_2Ru$ confirms that the indenyl ligand is only moderately electron donating. Gassman and Winter concluded that the electronic properties of the indenyl species were between cyclopentadienyl and pentamethylcyclopentadienyl[91] and the $\Delta G_i°$ data for compounds **8** and **10** is consistent with their results.

Electron-transfer equilibrium for **7** was established with N,N-diethylaniline and N,N-dimethyltoluidine with good internal consistency (0.6 kcal mol^{-1} difference in the measured $\Delta G_{et}°$ value and the expected $\Delta G_{et}°$ value, based on published $\Delta G_i°$ data for the reference compounds). Electron-transfer equilibrium for **9** was established with ferrocene and ethylferrocene. Similar to the indenyl and permethyl ruthenocene derivatives, compounds with TMSCp ligation demonstrate an additive electronic effect. From the $\Delta G_i°$ data for **7** and **9**, a trimethylsilyl group is estimated to be roughly as electron donating as a methyl group. The electronic effects of other $(TMS)_nCp$ ligands, where n= 1, 2, or 3, are consistent with the present observations.[116]

Attempted Correlation of Ruthenocene Ionization Free Energies with Taft σ_I Parameters

Levitt has demonstrated that correlation of ionization potentials with Taft inductive substituent constants exhibits a linear free-energy relation.[50,51] Correlation

of PES ionization energy data for chromium arene complexes $(C_6H_5R)Cr(CO)_3$ with Taft inductive parameters (r = 0.996)[51] and chromium acetylacetonato $Cr(acac)_3$ complex with Hammett substituent constants (r = 0.998)[50] generated excellent fits. This allows the ionization energies of compounds that do not form stable gas-phase species or are difficult to isolate or purify to be calculated fairly accurately from a simple linear function.

Correlation of $\Delta G_i°$ values for alkyl ferrocene[16] and nickelocene[19] derivatives were demonstrated in earlier chapters. The fits of the $\Delta G_i°$ data to the established σ_I parameters showed strong correlation (r = 0.997 for ferrocene and r = 0.994 for nickelocene) however a similar fit for the ruthenocene complexes was not as successful. An attempt to correlate several of the ruthenocene complexes with σ_I parameters with is shown in Figure 4-3. A correlation of the entire series was not possible because σ_I parameters do not exist for all the substituents such as $OSiEt_3$ and the fused-ring systems. The poor correlation of $\Delta G_i°$ values in Figure 4-3 indicates that these parameters are not suitable for predicting Cp ligand effects in the ruthenocene derivative ionizations. As expected from pervious correlations, the alkylated derivatives Cp_2Ru, CpCp*Ru and Cp^*_2Ru yield a linear fit; however, compounds with electron-withdrawing groups ($Cp^*(NO_2Cp)Ru$, $Cp^*(C_5Cl_5)Ru$, and $Cp^*((CF_3)_4C_5H)Ru$, for example) do not increase the ionization energy relative to ruthenocene to the extent that is predicted by the σ_I parameters. The line drawn in Figure 4-3 is for the best fit of compounds **1**, **2**, and **12**.

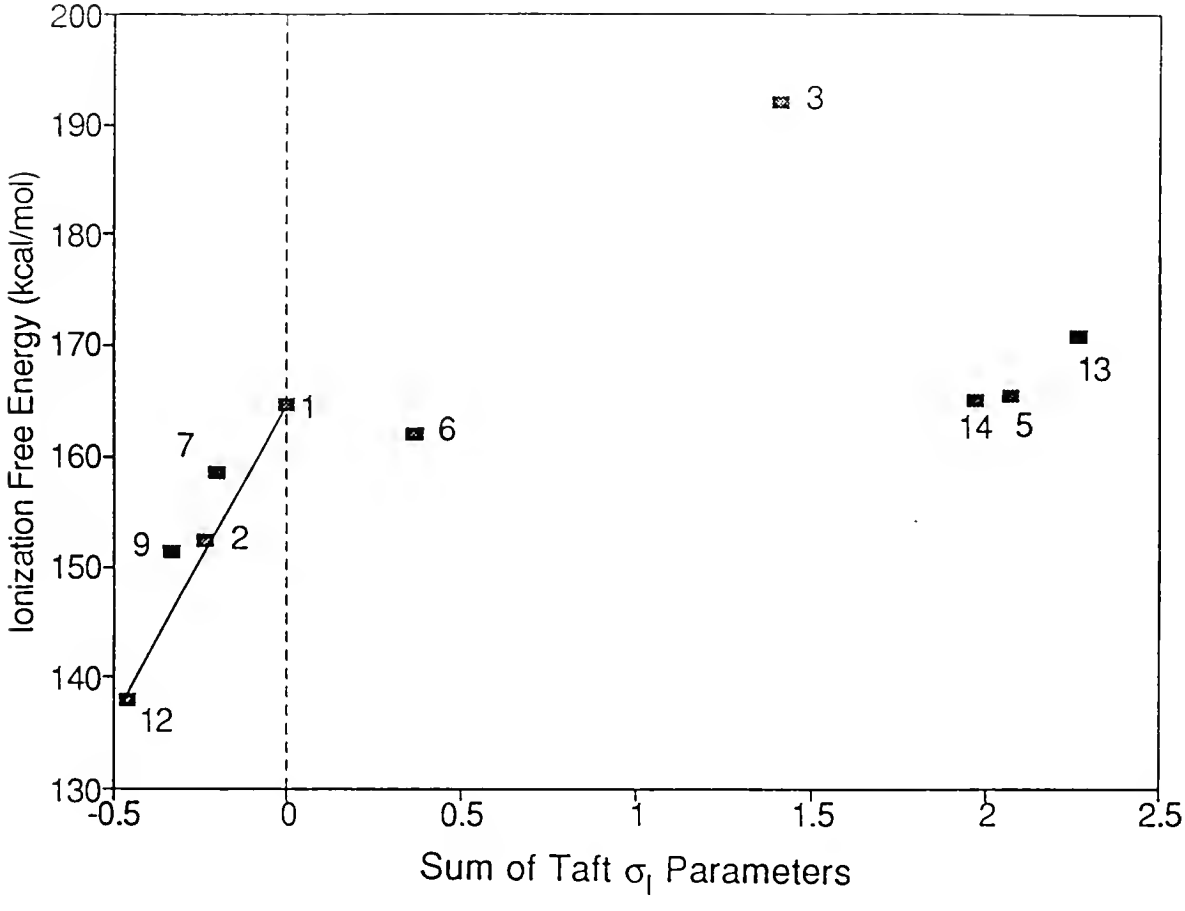

Figure 4-3 Correlation of $\Delta G_i°$ values for several ruthenocene derivatives with Taft σ_I parameters. The best-fit line is drawn for $\Delta G_i°$ values versus $\Sigma(\sigma_I)$ for the methylated complexes only (**1, 2, 12**). Compounds numbers defined in Table 4-1 and Figure 4-1

The slope of the line (the ρ value referred in equation 4-7) in Figure 4-3 is 58 ± 1 kcal mol^{-1} which is indicative of the sensitivity of ruthenocene to alkyl

$$\Delta G_i°(LL'Ru) = \rho(\Sigma\sigma_I) + \Delta G_i°(Cp_2Ru) \qquad (4\text{-}7)$$

substitution. Ruthenocene is equally as sensitive as ferrocene (ρ = 57 ± 1 kcal mol^{-1}) to alkyl substitution.

Experimental data suggest that the published value of σ_I for TMS (-0.10 - 0.11) may be too large.[3,5] The correlation of σ_I values with $\Delta G_i°$ data for Cp*(TMSCp)Ru and $(TMSCp)_2Ru$ indicates that the predicted $\Delta G_i°$ values for the TMSCp complexes are consistently lower than the experimental electron-transfer equilibrium by ~5 kcal mol^{-1}. From the estimated $\Delta G_i°$ values, a TMS function is relatively as electron-donating as a methyl group. Gassman and workers recently estimated that the TMS function is 1.25 times more electron donating than a methyl group.[116] The σ_I value for Me is -0.046, hence a σ_I value for TMS of -0.06 would predict $\Delta G_i°$ values of **7** and **9** in better agreement with the experimental $\Delta G_i°$ value and would also be more consistent with the data of Gassman and workers.[116]

The predicted $\Delta G_i°$ value for $Cp^*(C_5Cl_5)Ru$ based on the slope for the methylated compounds is 120 kcal mol^{-1} more endoergic than the $\Delta G_i°$ derived from ETE. Similarly, the value for the $Cp^*(C_5Br_5)Ru$ is also 120 kcal mol^{-1} lower than predicted from a Taft analysis. The absolute values of the Taft parameter for Cl (σ_I = 0.46) is an order of magnitude larger than the methyl parameter (σ_I = -0.046) yet the

experimental $\Delta G_i°$ values for ruthenocene and $Cp^*(C_5Cl_5)$ are equivalent. This infers that a Cl group is approximately as electron-withdrawing as a methyl group is electron-donating for the ruthenocenes. A similar comparison is also true for the bromo and the fluoro derivative. The predicted $\Delta G_i°$ value for **13** is ~125 greater than the experimental value. Note that the $\Delta G_i°$ data for compounds **5** and **14** are consistent with the relative ordering of the Taft parameters in that the σ_I for Br and Cl are +0.44 and +0.46 respectively. The $\Delta G_i°(Cp^*(C_5F_5)Ru)$ is also in agreement with the ordering of the halogen σ_I parameters. Although the Taft parameter analysis is inappropriate for these ruthenocene derivatives, the trend of the predicted order is consistent with trend of the experimental $\Delta G_i°$ data.

The small electron-withdrawing nature of the halogens is consistent with the observations of Levitt and Levitt who found that substituting Cl or Br for an arene ring proton in $(C_6H_6)Cr(CO)_3$ results in only a 0.1 eV increase in the ionization energy and F substitution results in a 0.2 eV increase. The moderate increase is attributed to lone-pair π-resonance effects which back-donate electron density to the aromatic ring. This effects has been well documented for simple benzene systems.[3,5,53]

The parameters used for fitting the gas-phase data have been described by Taft and workers and include in addition to σ_I parameters, σ_α parameters for polarizability effects and σ_{R+} used to predict π-resonance donation effects.[5] The published parameters for several substituents in Figure 4-3 are given in Table 4-3. A negative value for a parameter indicates that the electronic effect will stabilize a decrease in

electron density at a reaction center and lead to a lowering in the ionization potential. The field effects of Cl and F are essentially equal so only the polarizabilty and resonance effects will contribute to the difference of the substituents.[53] Fluorine, because of its compact size, is less polarizable than Cl, but the π resonance effect of F, which is larger than that of chlorine (Table 4-3), compensate substantially in the case of the ruthenocene derivatives. The overall result is that the ΔG_i° values for the complexes are similar. A parallel argument can be used for the bromo complex also. Note that the van der Waals radius of F is 0.5 Å smaller than of chlorine and the electronic effects are similar.[6]

It is also notable that the observed substituent effects for F (**13**) and CF_3 (**5**) are reversed from what would be predicted by the σ_I parameters. The observed shift in the ionization potentials of **3** and **6** (replacing H for CF_3 or NO_2) are also much smaller than predicted by Taft parameters but the ΔG_i° values do not deviate from experiment to the extent of the halogenated complexes. The estimated ΔG_i° values for **3** and **6** are 50 and 25 kcal mol^{-1} greater than the ETE values respectively. Neither the CF_3 group nor the NO_2 group are capable of π resonance back donation to the Cp ring ($\sigma_{R+} = 0$ for CF_3 and NO_2).[53] The larger electronic effect of CF_3 compared to F is consistent with a model of π lone-pair resonance donation for the halogens but not CF_3 or NO_2.[115] Such effects are well-known from studies of organic substituent effects. For example, the ionization potential of CF_3-C_6H_5 is 11 kcal mol^{-1} greater than for F-C_6H_5,[27] yet the σ_I parameter for F is similar to $\sigma_I(CF_3)$. The ordering of the benzene analogue ionizations is consistent with the π resonance model.

Table 4-3 Substituent Parameters for Selected Cyclopentadienyl Derivatives

Ligand	Substituent	σ_I[a]	σ_α[b]	σ_F[b]	σ_{R+}[b]
$C_5(CF_3)_4H$	CF_3	0.42	-0.25	0.44	0.0
$C_5H_4NO_2$	NO_2	0.65	-0.26	0.65	0.0
C_5F_5	F	0.5	0.13	0.44	-0.25
C_5Cl_5	Cl	0.46	-0.43	0.45	-0.17
C_5Br_5	Br	0.44		-0.25	
C_5H_4TMS	TMS	-0.1	-0.72	-0.02	0.0
Cp	H	0[c]	0[c]	0[c]	0[c]
Cp*	Me	-0.046	-0.35	0	-0.08

a. Values for parameters obtained from reference 2.
b. Values for parameters obtained from reference 5a.
b. By definition.

A New Parameter Scale for Cyclopentadienyl Substituents Based on Gas-Phase Electron-Transfer Equilibrium Studies of Ruthenocenes

Given the absence of parameters for many of the ruthenocene derivatives **1-14**, particularly the fused-ring ligands fluorenyl and indenyl, and the lack of general correlation with σ_I parameters as noted in the previous section, a new parameter scale for cyclopentadienyl derivatives has been developed.[20] The overall parameters for the Cp derivatives are based on the electronic effects of the ligand rather than the individual ring substituents. The parameters relate specifically to the stabilization or the destabilization in the oxidation of ruthenocene derivatives. It is expected that the parameters will correlate the tendency of the ligands to promote processes that involve a positive charge buildup at a metal center in metal complexes bearing these ligands.

To establish the new Cp ligand parameters, which will be denoted as γ values, the scale must be anchored to some reference values. Since the Taft parameters are anchored to Me and H,[3,5,50-55] it seems logical that the new γ parameters be anchored to the cyclopentadienyl and pentamethylcyclopentadienyl. The parameter values γ(Cp) = 0 and γ(Cp*) = -1.00 are arbitrarily assigned.[20] The negative sign indicates that the γ parameter will stabilize an increase in positive charge at a metal center or, in this case, result in a lowering of the ionization potential of the ruthenocene complex. A positive sign indicates that the parameter will destabilize an increase in positive charge at a metal center. Alternatively, the ligands may also be used for both positive and negative electronic effects however the application of γ parameters for negative ions is presently untested.

Two approaches have been used to assign ligand parameters to the various ligands. The first approach uses only data for the compounds bearing a pentamethylcyclopentadienyl ligand, Cp*RuL derivatives were L denotes the ligand for which these parameters are to be derived. The ligand parameters for this scheme are designated as γ^* value in which the asterisk corresponds to the Cp*-Ru base. Equation 4-8 was used to obtain the γ^* parameters. The value of the sensitivity

$$\begin{aligned} \Delta G_i^\circ(\text{Cp*Ru-L}) &= a^*[\gamma^*(\text{L})] + \Delta G_i^\circ(\text{CpCp*Ru}) \\ &= 14.4[\gamma^*(\text{L})] + 152.3 \text{ (kcal mol}^{-1}) \end{aligned} \tag{4-8}$$

parameter a^* = 14.4 kcal mol^{-1} is fixed by the anchored values of Cp and Cp* (0 and -1.00 respectively). The a^* value can be compared to the ρ value in a Taft analysis, as both parameters are determined from the slope of the correlation. A plot of the γ^* parameters and ΔG_i° data for the ruthenocene complexes based on equation 4-8 is given in Figure 4-4. The derived ligand parameters were presented in Table 4-2. Because of the manner in which the γ^* values were derived, all the points intrinsically yield a perfectly linear relationship. The plot is intended as graphical representation of the relative electronic effects of the Cp ligands and is not a result of two independent sets of data. The free energies of ionization for the ruthenocene were used to calculate γ^* values from equation 4-8, and not the reverse as is the case with the Taft σ_I analysis. The ligands to the right of the dashed line in Figure 4-4 destabilize the oxidation of the ruthenocene complex Cp*Ru-L relative to CpCp*Ru.

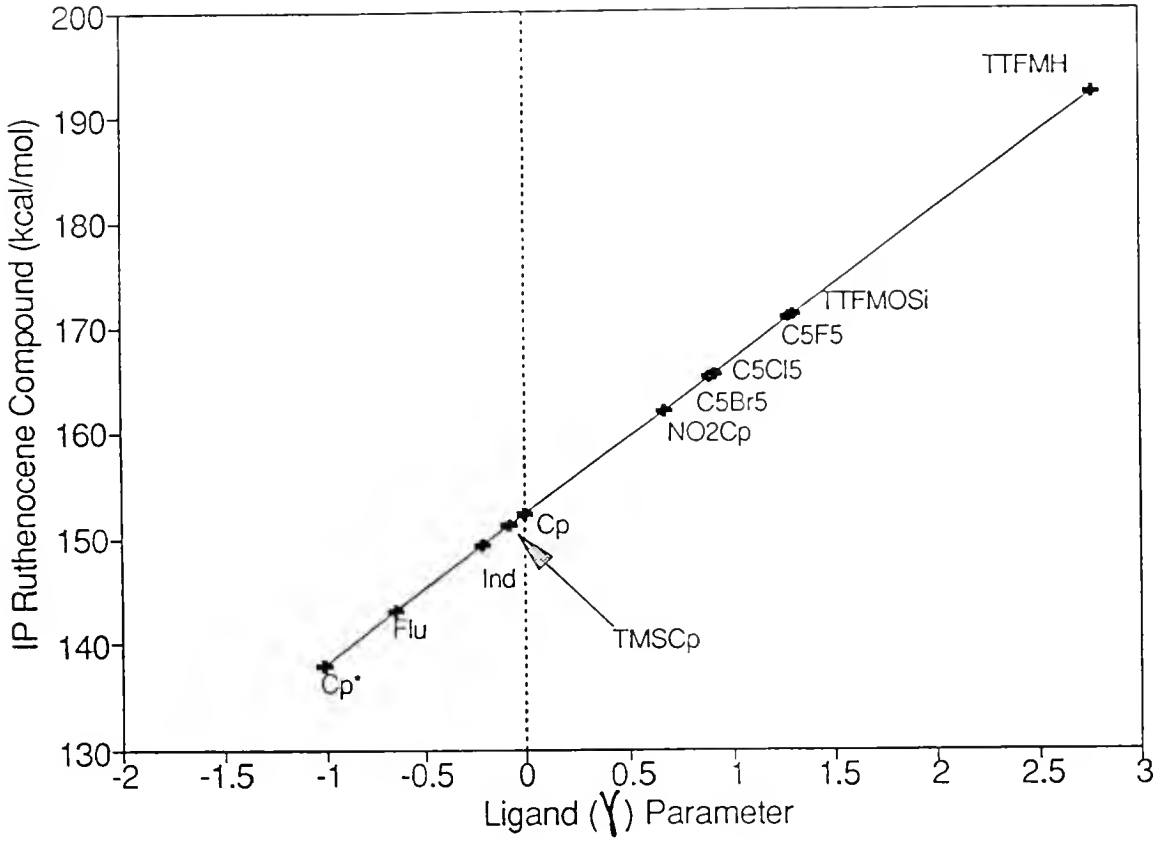

Figure 4-4 Plot of $\Delta G_i°$ values versus γ^* ligand parameters derived from the equation $\Delta G_i°(Cp^*Ru\text{-}L) = 14.4\gamma^* + \Delta G_i°(CpCp^*Ru)$ (equation 4-8).

A drawback to the above parameter scale is that the γ^* values are based on $\Delta G_i°$ values for only one system. Errors in the derived γ^* values are not obvious since the values are based solely on a single $\Delta G_i°$ value. Moreover, the additivity of the parameters has not been substantiated.

A second approach for deducing ligand parameters makes use of the homoleptic compounds (L_2Ru) in this study such as Ind_2Ru and $(TMSCp)_2Ru$. Incorporating all the gas-phase $\Delta G_i°$ values requires that the electronic effects be an additive property of the ligands. The second set of parameters derived from equation 4-9 are simply referred to as γ parameters. The utility of the parameter scheme based on equation 4-9 is that it tests the validity of ligand additivity.

$$\Delta G_i°(LL'Ru) = a(\gamma(L) + \gamma(L')) + \Delta G_i°(Cp_2Ru) \qquad (4\text{-}9)$$

The best-fit value (a = 13.0 kcal mol^{-1}) is based on the $\Delta G_i°$ values for Cp_2Ru, CpCp*Ru and Cp^*_2Ru. The experimental $\Delta G_i°$ values from Table 4-1 were then used to derive best-fit γ values for the other Cp ligands from equation 4-9. The γ values are presented Table 4-2 with the γ^* parameters. In many cases a γ value was derived from a single $\Delta G_i°$ value since the ligand appears on a single compound only. The γ parameters the indenyl and TMSCp derivatives were determined from an iterative fit of the $\Delta G_i°$ values of the metal complexes bearing these ligands. For these two ligands, the γ value was varied until the sum of the difference in the predicted $\Delta G_i°$ values and the ETE derived $\Delta G_i°$ data was minimized. The indenyl and TMSCp

ruthenocene complexes test the assumption that the electronic effects of the ligands is additive.

The correlation of $\Delta G_i°$ data with the (γ(L) +γ(L') sum for compounds **1-14** is shown in Figure 4-5. From the correlation shown if Figure 4-5 and the predicted and experimental $\Delta G_i°$ in Table 4-1, it is apparent that the ligand additivity assumptions is approximately substantiated. Predicted values of $\Delta G_i°$ are typically within 2-3 kcal mol^{-1} of experimental values. As mentioned earlier, the additivity assumption has not been tested for all of the ligands.

Included in Table 4-1 are the XPS Ru 3d core binding energies of several ruthenocene complexes measured by Gassman.[91] Comparisons of Gassman's data with electron-transfer equilibrium derived $\Delta G_i°$ values have been discussed in previous section. The general correlation, except for the reversal in the trends for **11** and **12**, of the XPS data with $\Delta G_i°$ values is good (Figure 4-2). Subsequently, because of the strong correlation in Figure 4-2, the γ parameters are also expected to correlate well with the 3d binding energies. A plot of 3d XPS data versus γ parameters for several complexes L_2ZrCl_2 complexes[116] also demonstrates good correlation (r = 0.986); therefore, the core binding energies of the Ru and Zr systems demonstrate reliable fits with the ligand parameters which indicates that ionization energetics data determined independent of this work can be correlated with the new Cp ligand γ parameters.

The γ and γ* parameters are anticipated to be useful in predicting electronic effects for different organometallic systems other than the simple metallocenes.

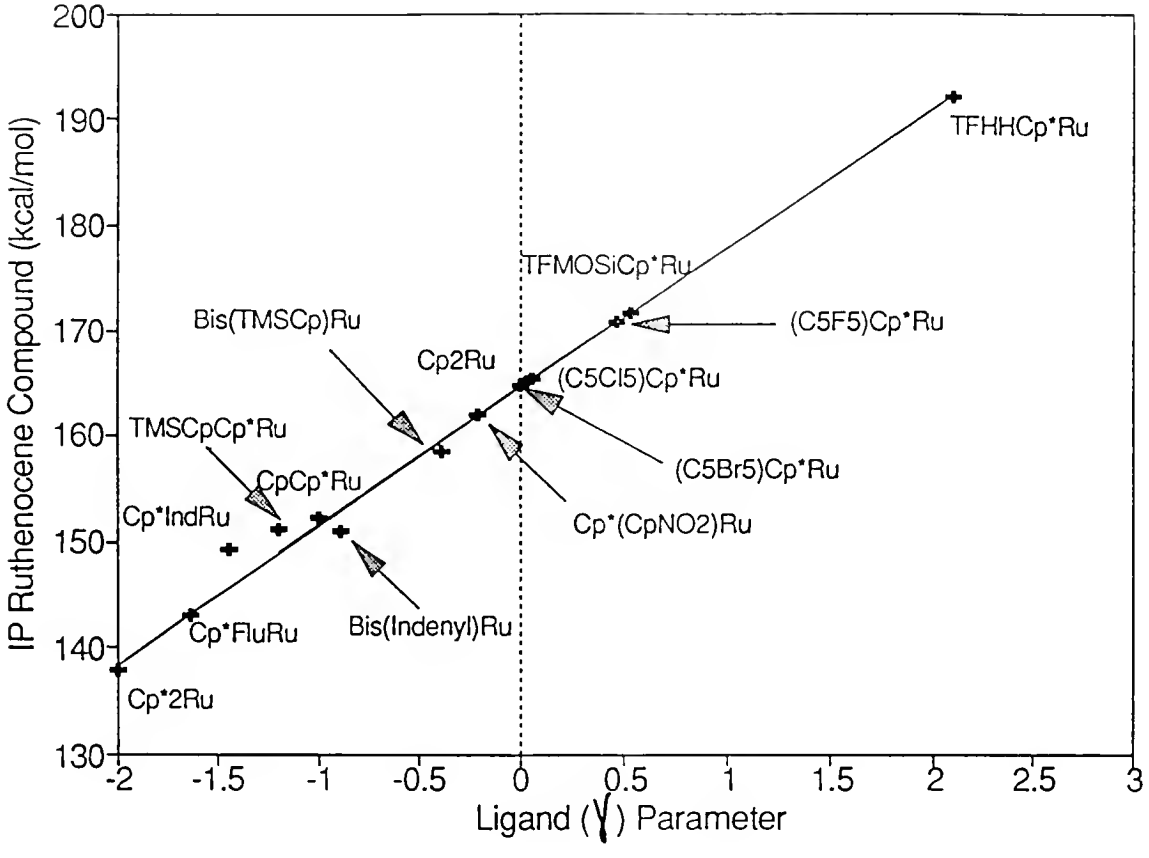

Figure 4-5 Plot of $\Delta G_i°$ values versus $\Sigma(\gamma)$ ligand parameters derived from the equation $\Delta G_i°(L_1\text{-Ru-}L_2) = 13.0[\gamma(L_1) + \gamma(L_2)] + \Delta G_i°(Cp_2Ru)$ (equation 4-9).

The application of these parameters in predicting reactivity of organometallic systems that have catalytic properties is of great interest.

Rates of Hydrogenolysis of Methylzirconocene Cations

The rates of hydrogenolysis, k_H, for methylzirconocene cation and several methylzirconocenium derivatives have been examined. The purpose of the study was to demonstrate that the Cp ligand parameters derived from free energies of ionization for ruthenocene complexes can be applied to interpret and predict chemical reactivity. The hydrogenolysis reaction for the methylzirconocene cations is convenient because steric effects are not expected to be important.[14] The insertion of H_2 into the Zr-CH_3 bond is sterically undemanding compared to other reaction involving larger substrates.[14,117] For example, reactions of $Cp^*_2ScCH_3$ with alkenes are significantly influenced by the steric effects of the Cp* ligands.[118] The general reaction shown below (reaction 4-10) was studied in the gas-phase by using FTMS. Ancillary Cp ligands are denoted by L. Methylzirconocene cations were generated from low energy

$$L_2Zr\text{-}CH_3^+ + H_2 \rightarrow L_2ZrH^+ + CH_4 \qquad (4\text{-}10)$$

electron-impact of the $L_2Zr(CH_3)_2$ neutral which eliminates CH_3.[14] The application of FTMS to study homogeneous organometallic catalysts in the gas-phase has been described by Christ et al.[14] Similar experimental procedures were used for the present hydrogenolysis studies reported here.

From the data in Figure 4-6, it is apparent that the electronic effects of supporting ligation influence the rates of hydrogenolysis of the zirconocene cationic complexes. A similar observation on the reactivity of zirconocene complexes was observed by Spaleck and coworkers.[119] In their studies, the orientation of ancillary indenyl ligands in several bis(indenyl)zirconium derivatives permitted for open coordination sites to the metal center. Subsequently, the observed rates of propylene polymerization by the Ind_2ZrCl_2 complexes were assumed to be primarily influenced by the electronic characteristics of the ligands.[119]

The rates of hydrogenolysis for only a few complexes were examined. Therefore, a meaningful correlation of k_H data with the Cp ligand parameters was not possible. However, the study serves to illustrate that their exists a measurable electronic effect for the zirconocene cationic complex reactivities.[14,119] Developing structure/reactivity relationships is fundamentally important in organometallic chemistry and further study of the gas-phase rates of hydrogenolysis for the $L_2Zr\text{-}CH_3^+$ may serve towards achieving that goal.

Comparisons of Gas-Phase Ionization Free Energies to Solution Electrode Oxidation Potentials

As the vast majority of organometallic chemistry is studied in the condensed phase, understanding the effects solvent has on the energetics of organometallic reaction is fundamentally important. Direct comparison of gas-phase and solution oxidations quantifies the effects solvent has upon the ionization process.[16,18-20,54,84]

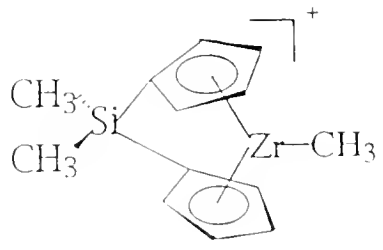

3.7E-11

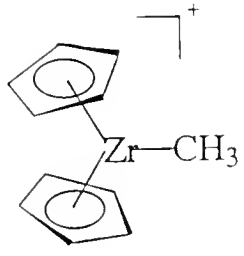

1.3E-11

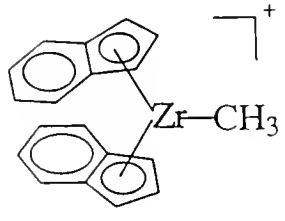

1.4E-12

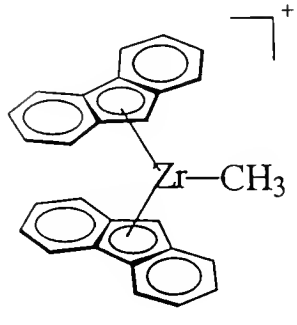

Slow/Decomposed

Figure 4-6 Gas-phase rates of hydrogenolysis for several methylzirconocene cation complexes. Numbers adjacent to structures are k_H values ($cm^3molec^{-1}s^{-1}$). Measurement of the k_H value for $Flu_2ZrCH_3^+$ was complicated by an inefficient reaction rate and thermal decomposition of the Zr complex.

In Chapter 2, thermodynamic cycles (Figure 2-5) that include $\Delta G_i°$ data in the gas phase and solution were used to determine differential solvation free energies, $\Delta\Delta G_{solv}°$ values. Similar cycles have been used here to determine the differential solvation energies for the ruthenocene derivatives.[20] Electrochemical $E_{½}$ values measured by cyclic voltammetry are compared to gas-phase $\Delta G_i°$ values determined from electron-transfer equilibrium reactions. Derived $\Delta\Delta G_{solv}°$ values from thermochemical cycles will be discussed following analysis of the electrochemical oxidation potentials.

Oxidation potentials for several of the ruthenocene derivatives have been previously reported.[90,91,109] However, as many of the reported $E_{½}$ values were based on irreversible cyclic voltammetry measurements,[90,91] reevaluation of the oxidations was performed in order to evaluate ambiguous $E_{½}$ assignments therefore electrochemical oxidation potentials for a many of the ruthenocene derivatives were measured here by using cyclic voltammetry. For complexes that are irreversibly oxidized, rather than estimate $E_{½}$ values, anodic peak potentials E_{pa} are reported. Accurate assessment of E_{pa} potentials is not possible based solely on literature $E_{½}$ values. Furthermore, in order to evaluate the $E_{½}$ data for the entire series of complexes under common reaction conditions, reevaluation of the electrode potentials was necessary in order to establish more accurate comparisons of the oxidation potentials for the series of compounds. Literature potentials were determined under various reaction conditions such as different supporting electrolytes and reference electrodes.[90,91,109] In many cases, oxidation potentials that were reported irreversible

were found to be either reversible or quasi-reversible. A quasi-reversible potential is used to refer to the situation in which the ratio of the intensities of the anodic and cathodic peaks is not unity and both cathodic and anodic waves are undoubtedly present. An irreversible potential describes an electrochemical process in which either the cathodic potential of an oxidation or the anodic potential of a reduction is not definitively observed due to decomposition of the ionized species and/or solvent complications.[120,121]

All potentials were measured against the oxidation potential of ferrocene, which was used as a $1e^-$ internal standard.[103] For aqueous electrochemistry, the normal hydrogen electrode (NHE) or saturated calomel electrode (SCE) are universally accepted reference standards.[121] Not all compounds, including the metallocenes,[89] are soluble or stable in aqueous media, therefore $E_{1/2}$ potentials must be measured in alternative solvent systems. However, for nonaqueous systems there is no universally accepted reference standard.[122] The advantage of using ferrocene as an internal standard for nonaqueous electrochemistry is that the $Cp_2Fe^{+/0}$ couple is reversible in a number of different solvent systems. Gagné and workers have demonstrated that although the formal potential for a metal redox couple may be shifted when different reference electrodes or solvent systems are used, the potential difference relative to the $Cp_2Fe^{+/0}$ couple was constant.[103] Different solvents have different junction potentials, which are usually unknown, and diverse resistivities which can result in complicated wave shapes, i.e. seemingly irreversible behavior.[103] By comparing the ΔE_p or $E_{1/2}$

value of a reaction couple to $E_{1/2}(Cp_2Fe^{+/0})$, these various experimental limitations to nonaqueous electrochemistry can be circumvented.

Table 4-4 lists electrochemical E_{pa} and $E_{1/2}$ values for compounds **1-14**. Reversible potentials were not observed for all compounds; therefore, only E_{pa} values relative to ferrocene are reported. Additionally, literature $E_{1/2}$ values are included when available for comparison. All electrochemical potentials reported here were measured in methylene chloride containing 0.1 M tetrabutylammonium hexafluorophosphate at a platinum disk electrode (working electrode) with a KCL saturated Ag/AgCl reference electrode. All values are reported versus the $Cp_2Fe^{+/0}$ couple which was observed to be reversible for all measurements. The ruthenocene oxidations are expected to proceed by a $1e^-$ process to the corresponding cation.[90] However, for cases were the oxidation was irreversible, a rapid $2e^-$ process is probable.[90,92,123] For example, ruthenocene is irreversible most solvent/electrolyte systems.[90] An observed $2e^-$ process is thought to result from the initial oxidation of Cp_2Ru^+ followed by rapid disproportionation.[90,92] It is likely that the larger metal-ring separation relative to Cp_2Fe^+ enhances the nucleophilic attack of Cp_2Ru^+ by the supporting electrolyte or solvent.

Recently, Mann and workers reported the reversible oxidation of ruthenocene in CH_2Cl_2 containing 0.1 M tetrabutylammonium tetrakis[3,5-bis(trifluoromethyl)phenyl] borate, TBA^+TFPB^-, as a noncoordinating electrolyte.[90] The reversible electrochemistry for Cp_2Ru in the presence of the strongly noncoordinating TBA^+TFPB^- is consistent with the concept that ruthenocene is susceptible to

Table 4-4 Electrode Potentials and Differential Solvation Free Energies for Some Ruthenocene Derivatives.

No.[a]	E_{pa}[b,c]	$E_{½}$[b]	$\Delta G_i°(soln)$[d,e]	$-\Delta\Delta G_{solv}°$[d,f]	δ_{Fc}[d,g]
1	0.58	0.56[h,i]	130	34	0
2	0.35	0.23[i]	126	27	+7
3		1.3[j]	148	44	-10
4		1.12[j]	144	28	+6
5	1.11	1.03[h]	141	24	+10
6	0.78		122	40[k]	-6
9	0.35		113	38[k]	-4
10	0.23	0.12[h]	123	26	+7
11	0.21		112	21[k]	+13
12	0.15	0.09[h]	120	18	+16
13	1.07		140	31[k]	+3
14	1.03	0.95[h]	139	26	+12

a. Compound numbers defined in Table 4-1.
b. Values in volts relative to $E_{½,ox}(Cp_2Fe)$.
c. Measured in CH_2Cl_2/0.1 M Bu_4NPF_6. See Experimental Methods.
d. Values are kcal mol^{-1}.
e. From equation 4-11.
f. From equation 4-12a.
g. From equation 4-12b. $\Delta\Delta G_{solv}°(Fc^{+/0}) = -34$ kcal mol^{-1} in CH_2Cl_2.
h. $E_{½}$ value reported reported for quasi-reversible potential.
i. See reference 91.
j. See reference 109.
k. E_{pp} for ferrocene used to estimate $E_{½}$ from E_{pa} value.

nucleophilic attack by coordinating anions. The oxidation of decamethylruthenocene is reversible in CH_2Cl_2 with most common electrolytes, conceivably due to steric hinderance of the metal center by the Cp* ligands. Reversible $E_{½}$ values for unsubstituted ruthenocenes are obtained with only the most noncoordinating anions. Anions such as PF_6^-, ClO_4^-, and BF_4^- contribute to irreversible electrochemical responses.[90,91]

The oxidation of $Cp^*(C_5F_5)Ru$ (**13**) was measured in CH_2Cl_2 containing 0.1 M Bu_4NPF_6 by Richardson et al. An irreversible $2e^-$ potential was observed for the **13** with E_{pa} = 1.07 V versus $E_{½}(Cp_2Fe^{+/0})$. Error limits for the oxidation potentials are given in Table 4-4. At a platinum disk electrode, the peak potential for the **13** was approximately twice that for ferrocene, consistent with a $2e^-$ process. The oxidation of **13** is also irreversible when the weakly nucleophilic tetrakis[3,5-bis(trifluoromethyl) phenyl]borate (TFPB) is the anion of the electrolyte (E_{pa} = 0.98 V). The E_{pa} value for **13** can be compared to the E_{pa} = 1.11 V for $Cp^*(C_5Cl_5)$ (**5**) in CH_2Cl_2/Bu_4NPF_6 and 1.08 V with TBA^+TFPB^- as the supporting electrolyte. Interestingly, the oxidation of **5** is quasi-reversible in methylene chloride with $E_{½}$ ~1.0 V vs. $Fc^{+/0}$ and the $\Delta E_{½}$ value was independent of supporting electrolytes used in this work. The bromo derivative also has a quasi-reversible oxidation potential in CH_2Cl_2/Bu_4NPF_6 with $E_{½}$ = 0.80 V versus $Fc^{+/0}$. The observed reversible responses for **5** and **14** support that ruthenocenes with bulky ligation prevent nucleophilic attack while unhindered ruthenocenes are more susceptible to follow-up reactions subsequent to oxidation.

The van der Waals radii of H and F are equivalent[6] and a $2e^-$ oxidation both ruthenocene and **13** is observed. The van der Waals radii of Cl is larger than that of F but slightly smaller than CH_3. Thus, the steric restrictions of a methyl group are expected to be similar to a chlorine or bromine, which may account for the observed reversible oxidation potentials for **5** and **14**. In this manner, the iodo complex, $Cp^*(C_5I_5)Ru$,[114] is predicted to give a quasi-reversible electrochemical response.

The order of the E_{pa} values for the three halogenated complexes is dissimilar to the ΔG_i° values in that the chloro derivative has a higher oxidation potential than the fluoro derivative. The irreversible oxidation of **13** however may account for the observed trend and the order of the true thermodynamic E° values may be parallel to the gas-phase ΔG_i° values.

Determination of Free Energies of Ionization in Solution from Electrochemical Oxidation Potentials

Free energies of ionization in solution have been derived previously for metallocenes[16,19,20] and coordination complex ions.[84] Half-cell potentials for the metal complex redox couples referenced to a standard aqueous reference electrode can be referenced to the absolute potential of the normal hydrogen electrode by assuming a potential for NHE.[54] From energy cycles, it can be shown that $H^+ + e^- = \frac{1}{2}H_2(g)$ has an absolute thermodynamic potential of 4.44 V. Through the Faraday relationship, $\Delta G^\circ = -nFE^\circ$, estimates of $\Delta G_i^\circ(soln)$ can be made.[54] Equation 4-11,

$$\Delta G_i^\circ(soln) = nF(E_{½} + E_{ref} + E_{NHE}) \qquad (4\text{-}11)$$

was used to estimate $\Delta G_i°$(soln) values for the ruthenocene derivatives studied. Oxidation potentials reported in Table 4-4 were corrected to include $\Delta E_{1/2}$ values relative to $E°(Cp_2Fe^{+/0})$. Therefore, the ruthenocene oxidation potentials were corrected by measuring the $\Delta E_{1/2}$ to ferrocene ($E_{1/2}(Fc^{+/0})$ = 0.46 V in CH_2Cl_2,[89,103] and then adding the potentials of the hydrogen and reference electrodes. Irreversible electrochemical potentials were used to estimate $\Delta G_i°$(soln) values for several ruthenocene complexes, accordingly E_{pa} values were used when $E_{1/2}$ data unavailable. Values of $\Delta G_i°$(soln) reported in Table 4-4 are considered absolute thermodynamic potentials for the process M(soln) = M^+(soln) + e^-, where e^- is a treated as a gas-phase electron.[54]

Differential Solvation Free Energies for Several Ruthenocene/ Ruthenocenium Couples

Differential solvation free energies, $\Delta\Delta G_{solv}°$, for the ruthenocene couples are reported in Table 4-4. Values of $\Delta\Delta G_{solv}°$ were determined from the $\Delta G_i°$(soln) estimates. In an effort to establish a reference standard for estimates of solvation free energies from metal redox couples, $\Delta\Delta G_{solv}°$ values referenced to $\Delta\Delta G_{solv}°(Cp_2Fe^{+/0})$[16] are also reported, denoted as δ_{Fc}. The ferrocene oxidation couple was chosen as reference standard for $\Delta\Delta G_{solv}°$ values for several reasons. The gas-phase[16] and solution oxidation potentials[34,89,103] are well established values, therefore $\Delta\Delta G_{solv}°(Cp_2Fe^{+/0})$ is accurately known in CH_2Cl_2 and CH_3CN. Further, as the $Cp_2Fe^{+/0}$ couple is reversible in many solvents,[103] shifts in the redox potentials for metal complexes ($\Delta E_{1/2}$) in different systems are can conveniently be compared relative

to ferrocene. Additionally, the experimental differential solvation free energy for the ferrocene couple is modeled accurately by the dielectric continuum theory indicating that ferrocene is nearly spherical in solution.[116] Thus, ion-solvent interaction for $Cp_2Fe^{+/0}$ are expected to be dependent on outer-sphere electrostatic interactions and not specific solvent interactions such as ion/solvent-dipole interactions isolated at the metal center. From this, inference to the ion-solvent interactions for metal redox couples can be made with respect to a pseudo-spherical well-modeled $1e^-$ redox couple.

Equation 4-12a was used to derive $\Delta\Delta G_{solv}^\circ$ values for the ruthenocene derivatives. From equation 4-12b, $\Delta\Delta G_{solv}^\circ$ values relative to $\Delta\Delta G_{solv}^\circ(Cp_2Fe^{+/0})$ were derived. By convention, $\Delta\Delta G_{solv}^\circ$ values are reported as negative values to indicate the amount of stabilization energy a solvated ion gains with respect

$$-\Delta\Delta G_{solv}^\circ = \Delta G_i^\circ(g) - \Delta G_i^\circ(soln) \quad (4\text{-}12a)$$

$$\delta_{Fc} = \Delta\Delta G_{solv}^\circ - \Delta\Delta G_{solv}^\circ(Cp_2Fe^{+/0}) \quad (4\text{-}12b)$$

to the parent neutral. Negative δ_{Fc} values indicate that the solvation energy of the ruthenocene couple is greater (more exoergic) than $Cp_2Fe^{+/0}$. For oxidation couples where the δ_{Fc} value is positive, a decrease in solvation stabilization is observed relative to $Cp_2Fe^{+/0}$. For example, the $\Delta\Delta G_{solv}^\circ$ value for $Cp^*_2Ru^{+/0}$ is -18 kcal/mol and δ_{Fc} = +16 kcal mol^{-1} in methylene chloride. In the gas phase, the methyl functions of the Cp* ligand can be thought of as a solvent layer around ruthenocene;

therefore, in a dielectric continuum which would be an additional solvent layer, Cp^*_2Ru and $Cp^*_2Ru^+$ are essentially equally solvated.

Application of the Born Model for Estimating Solvation Energetics for Ruthenocene Oxidation Couples

The Born model for predicting solvation free energies has been applied to metallocene $Cp_2M^{+/0}$ couples in Chapter 2. Values of $\Delta G_{el}°$ determined from the Born equation are equivalent to $\Delta\Delta G_{solv}°$ estimates from thermochemical cycles.[16,54,84] For all cases save the $Cp_2V^{+/0}$ couple, an experimental value for $\Delta\Delta G_{solv}° = -38 \pm 2$ kcal mol^{-1} was obtained for the first transition row metallocenes.[16] The Born model is successful in estimating the change in electrostatic free energies, $\Delta G_{el}°$, for the metallocene +/0 couples within 2 kcal mol^{-1} when acetonitrile (D = 36) is the solvent. The Born equation ($\Delta G_{el}° = (166z^2/r_{eff})(1\text{-}1/D)$) predicts $\Delta G_{el}°(L_2M^{+/0})$ values for ruthenocene and ferrocene couples of -34 kcal mol^{-1} when methylene chloride (D = 9) is the solvent; however, $\Delta G_{el}°$ values for several ruthenocene derivatives are inconsistent with experimental $\Delta\Delta G_{solv}°$ data. The $\Delta\Delta G_{solv}°$ value for Cp^*_2Ru = -20 kcal mol^{-1} but $\Delta G_{el}°(Cp^*_2Ru^{+/0})$ = -28 kcal mol^{-1} in methylene chloride. The overestimation of $\Delta G_{el}°(Cp^*_2Ru^{+/0})$ from equation 4-13 may indicate that a simple electrostatic model may not apply for nonspherical or asymmetrical complexes. The crystallographic radius for Cp^*_2Ru,[124] estimated from the Ru center to the van der Waals radii of the methyl protons, used to estimate $\Delta G_{el}°(Cp^*_2Ru^{+/0})$ is 5.2 Å. Because the Born model assumes that ions are charged spheres, a radius of 5.2 Å may inappropriate if decamethylruthenocene is not a spherical complex.

The $\Delta\Delta G_{solv}°$ value for the asymmetric complex Cp*IndRu is -26 kcal mol^{-1} and the $\Delta G_{el}°$ value is estimated to be -26 kcal mol^{-1} with methylene chloride as the solvent. The value r_{eff} = 5.6 Å was estimated based on the average distance from Ru to the protons of Cp* (5.2 Å) and indenyl (6.0 Å to the furthest benzoid proton) ligands.[91] However, the $\Delta G_{el}°$ value for Cp*FluRu based on the same crystallographic radius for Cp*IndRu is 6 kcal mol^{-1} more exoergic than the experimental $\Delta\Delta G_{solv}°$ value. The oxidation of **11** is irreversible and E_{pa} versus $E_{½}(Cp_2Fe^{+/0})$ was used to estimate a value for $\Delta\Delta G_{solv}°$ which may explain the disparity of the values. Using $E_{½}$(**11**) = 0.34 V measured by Gassman and Winter,[91] a value for $\Delta\Delta G_{solv}°$(**11**) in agreement with the $\Delta G_{el}°$ is obtained. For the halogenated complexes, the Born model gives approximate estimates for solvation energetics. The ligands C_5Cl_5 and C_5Br_5 are expected to be structurally similar to a pentamethylcyclopentadienyl in terms of steric bulk, r_{eff} = 5.1 Å for Cp*(C_5Cl_5)Ru (5.2 Å to the methyl proton and 5.0 Å to the chloride)[91] and $\Delta\Delta G_{solv}°$ of Cp*(C_5Cl_5)Ru is -24 ± 3 kcal mol^{-1} and $\Delta G_{el}°$ = -28 kcal mol^{-1}.

An alternative to using the maximum radius of a molecule to estimate $\Delta\Delta G_{el}°$ values, may be to use the molecular volume if the complex deviates significantly from a sphere. By comparing the volumes of two equally charged species an approximate ratio of relative $\Delta\Delta G_{el}°$ values may be assessed. For example, Cp^*_2Ru better qualifies as a cylindrical molecule rather than a sphere. The Ru-Cp* distance is 1.8 Å and the van der Waals radii of carbon is 1.85 Å resulting in a total molecular length of 7.3 Å, compared to a molecular radius of 5.2 Å. Rough schematic representations

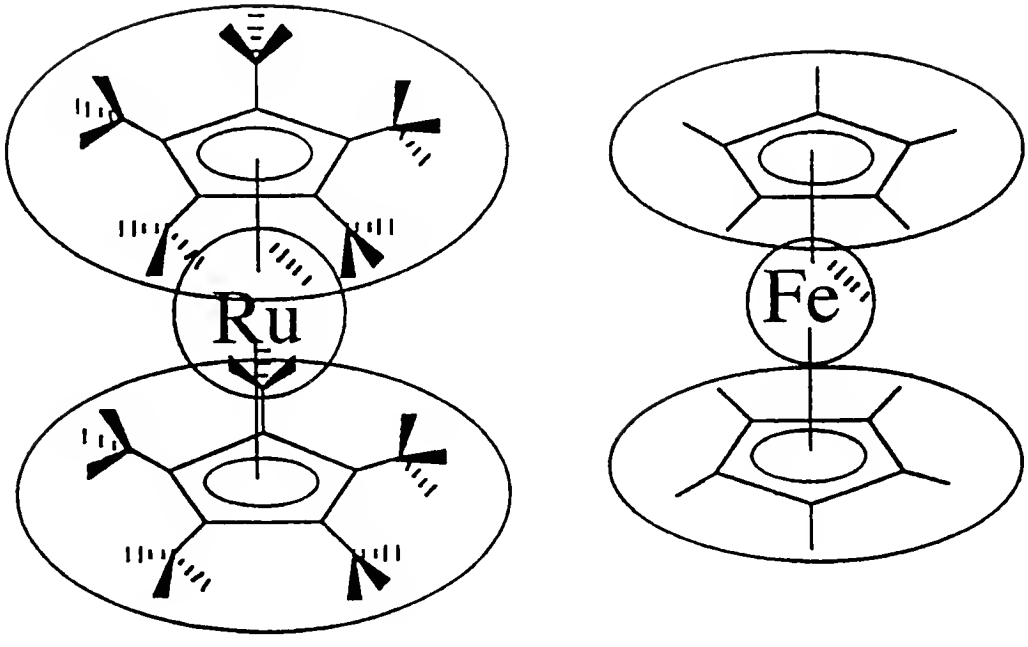

Figure 4-7 Structures of Cp^*_2Ru and ferrocene. The molecular representations help to illustrate the relation of size to solvation energy. The differential solvation energy of the $Cp^*_2Ru^{+/0}$ couple is 16 kcal mol^{-1} less than $\Delta\Delta G_{solv}(Cp_2Fe)^{+/0}$.

of the structures of Cp^*_2Ru and ferrocene are shown in Figure 4-7. The structures, although not exact scale representations, demonstrate distinct differences in the geometry of the two metal complexes and helps to illustrate the origin for the large positive δ_{Fc} value. Estimates of the molecular volumes for Cp^*_2Ru and ferrocene are approximately 530 $Å^3$ and 260 $Å^3$ respectively.[72,124] The ratio of the molecular volumes is consistent with the relative $\Delta\Delta G_{solv}°$ values for the two complexes. Although this is a crude approximation, it serves to demonstrate a possible source of the disparate values in estimated $\Delta G_{el}°$ values.

Conclusions

Gas-phase electron-transfer equilibria have been used to determine free energies of ionization of various ruthenocene derivatives at 350 K. The results provide an accurate measure of the intrinsic electronic effects of Cp substituent effects on ruthenocene oxidations. The trends in the ETE $\Delta G_i°$ values are consistent with electrochemical potentials and Ru 3d core binding energies[91] reported earlier; however, the correlation fails in some cases. Most notably is the reversal of the $\Delta G_i°$ values for Cp^*_2Ru and Cp*FluRu relative to the electrochemistry on the Ru 3d binding energies.[91] Therefore, the fluorenyl ligand does not stabilize the oxidation of ruthenocene to extant that Cp* does. The stabilizing ability of Flu is only ~60% of the Cp* electronic effect.

Perhalogenated Cp* ligands do not stabilize ruthenocene towards oxidation to the extent that is predicted by organic substituent parameters. The electronic effect of

the C_5Cl_5 is balanced by the electron-donating effects Cp* ligand, subsequently $\Delta G_i°(Cp^*(C_5Cl_5)) \sim \Delta G_i°(Cp_2Ru)$. The C_5F_5 ligand is only 1.5 more time electron-withdrawing than Cp* is electron-donating. The moderate electron-withdrawing nature of the C_5F_5 ligand is consistent with the findings of Paprott and Seppelt.[115] From equilibrium reactions, they determined that C_5F_5H was only slightly more acidic than CpH but less acidic than CF_3CH_2OH.[115] The small perfluorination effects can be attributed to π resonance effects of the F lone pair electrons.[5,115] For comparison, the $C(CF_3)_4H$ ligand is strongly electron-withdrawing which can be rationalized because CF_3 groups have electron-withdrawing qualities only.[5]

A Cp ancillary ligand parameter scale has been developed for the ligands investigated here. The parameters, termed γ and γ^* parameters depending on the derivation used, should provide the basis for correlating electronic effects of Cp ancillary ligands on the physical and chemical properties of other organometallic complexes. Such parameters may provide insight concerning the electronic effects of various Cp ligands on the activity and selectivity of homogeneous organometallic catalysts bearing these ligands. The initial gas-phase studies of the rates of the hydrogenolysis for several $L_2Zr\text{-}CH_3^+$ cations were aimed at achieving this goal. The application of the Cp ligand parameters towards predicting reactivity for such catalytic systems, in addition to alkene polymerization and C-H activation, is of great interest.

The Cp ligand parameters have been derived from gas-phase experiments absent of solvent effects. Application of these parameters in the condensed phase may not parallel the gas-phase trends. Modifications of the condensed phase trends due to

solvent effects associated with the metal complexes and structural differences (ring slippage, dimerization, or solvent coordination) must be considered.

Electrochemical studies for several of the ruthenocenes indicated that potentials reported to be irreversible[91] were found to be reversible or quasi-reversible under our conditions outlined here. The E_{pa} for Cp^*_2Ru was cathodically shifted relative to E_{pa}(Cp*FluRu) supporting the gas-phase trends in the $\Delta G_i°$values. Differential solvation energies for the complexes were consistent with $\Delta\Delta G_{solv}°$ values derived for other metallocenes. However, the $\Delta\Delta G_{solv}°$ values for several of the ruthenocene are not accurately predicted by the Born model. This demonstrates that structural deviations and charged localization may account for the disparity in the solvation energetics for non-spherical metal complexes.

Experimental Methods

Details of the electron-transfer equilibrium technique were provided earlier.[14-20,39-43] Ruthenocene derivatives were sublimed from a solids insertion probe to provide pressures in the 1×10^{-7} - 1×10^{-6} Torr range. For several of the ruthenocene derivatives additional heating of the solids probe was necessary to generate pressures of the neutrals in the 10^{-7} Torr range. Reference compounds were admitted into the high vacuum chamber through a precision leak valve. Molecular ions were generated through electron impact with beam voltages adjusted between 10 - 14 eV in order to generate ions in good yield and to minimize production of fragment

ions. Electron-transfer equilibrium was usually establish in ~1 s and was followed for an additional 5-10 s.

Pressures were measured directly by using a nude ion gauge with a Granville Phillips controller. Partial pressures were corrected for ion sensitivities and systematic error with an MKS baratron capacitance manometer in the 1 x 10^{-5} Torr range. Pressure calibrations varied only slightly within the series of ruthenocene derivatives.

Ruthenocene Derivatives and Reference Compounds

Organic reference compounds, ruthenocene, and ferrocene were purchased from Aldrich Chemicals. Ethylferrocene, manganocene, and nickelocene were purchased from Strem Chemicals. All ETE reference compounds were used without further purification.

Compounds **2, 5, 10, 11,** and **12** were prepared by using (η^5-pentamethylcyclopentadienyl)ruthenium(III) chloride oligomer, $(Cp^*RuCl_2)_x$, as described by Gassman and Winter.[91] All compounds were obtained in yields of 40% or greater and characterized by ^1H NMR (CD_3Cl solvent) and mass spectrometry. Resublimation of **11** was necessary prior to mass spectral studies to remove trace impurities of unreacted fluorenyl.

Many of the ruthenocene derivative studied by electrochemistry and mass spectrometry were donated by several researchers. Samples of $Cp^*(C_5(CF_3)_4H)Ru$, $Cp^*(C_5(CF_3)_4OSiEt_3)Ru$, and $Cp^*(NO_2Cp)Ru$ were donated by Dr. Mark Burk of E. I. du Pont de Nermours in Wilmington, Delaware.[20] Samples of Cp*(TMSCp)Ru,

$(TMSCp)_2Ru$, Ind_2Ru, were donated by Dr. Allen Siedle from 3M Corporate Research Laboratories in St. Paul, Minnesota.[20] Additionally, Dr. Siedle also provided purified samples of the zirconocene derivatives for the hydrogenolysis studies. Professor Russell Hughes of Dartmouth College donated a sample of $Cp^*(C_5F_5)Ru$.[113] Professor Charles Winter of Wayne State University donated a sample of $Cp^*(C_5Br_5)Ru$.[114]

Cyclic Voltammetry Studies

Cyclic voltammetry studies were performed with a PAR systems (Models 173/175). A platinum button working electrode and a Ag/AgCl reference electrode were used. Acetonitrile (Fisher HPLC grade) was purified by shaking the solvent with CaH_2 and filtering. The solvent was then distilled from P_2O_5 (5g/100 ml) onto CaH_2 and then redistilled from calcium hydride immediately prior to use. Pure CH_2Cl_2 (Fisher HPLC grade) was obtained by shaking the solvent with concentrated sulfuric acid, followed by an aqueous solution of Na_2CO_3, dried with anhydrous $CaCl_2$, filtered over neutral alumina, and stored over P_2O_5, finally CH_2Cl_2 was obtained from distillation with P_2O_5 immediately prior to use. The electrolyte Bu_4NPF_6 (Aldrich) was recrystallized from ethanol/acetone three times, washed with dry ethanol and dried in a vacuum oven at 100 °C for ca. 24 hr. Electrolytic solutions were freshly prepared prior to all voltammetry studies. Tetrabutylammonium tetrakis[3,5-bis(trifluoromethyl)phenyl]borate, TBA^+TFPB^-, was prepared and purified by the method of Nishida and Kobayashi.[125]

CHAPTER 5
GAS-PHASE IONIZATION ENERGETICS, THERMOCHEMISTRY, AND ELECTRON-TRANSFER KINETICS OF DECAMETHYLMETALLOCENES, CHROMOCENE, AND COBALTOCENE

Introduction

Many studies concerning the reactivity of metallocene complexes involve variations of the substituents on the η^5-cyclopentadienide ligand (Cp) and substitution of η^5-pentamethylcyclopentadienide (Cp*) for Cp is one common ligand variation.[107,125] The η^5-pentamethylcyclopentadienide ligand leads to changes in electronic effects and steric congestion with respect to η^5-cyclopentadienide. These changes in ancillary ligand character in many cases lead to desirable alterations of the structure, reactivity, and stability for transition metal complexes.[105] Furthermore, the development of a convenient synthesis[126] and commercial availability of pentamethylcyclopentadiene has lead to increased study of permethylated metallocene complexes.

Electronic effects due to permethylation of Cp ligands of metallocenes can be assessed by comparing the oxidation/reduction potentials of the Cp and Cp* metal complexes and solution electrochemical potentials,[34,107] and gas-phase vertical ionization energies[35,37] have been determined for a number of Cp* complexes. However, as discussed earlier, if electrochemical oxidation/reduction potentials for an

organometallic complex are irreversible, the measured $E_{1/2}$ value will not be a reliable indication of the thermodynamic potential. In addition, the intrinsic effect of permethylation on the oxidation energetics is modified by the differential solvation energies of the redox couple. Vertical ionization energies, measured by photoelectron spectroscopy are only accurate measure the adiabatic ionization potential, $\Delta H_{i,0}°$, if the equilibrium geometries of the ion and the neutral are similar.[27,36] Large structural differences between the neutral and the ion may lead to broad peaks, as observed for the decamethylmetallocenes,[35,37] and an adiabatic ionization potential significantly different from the measured vertical ionization potential.

Gas-phase electron-transfer equilibrium (ETE) techniques have been used extensively to determine thermal free energies of ionization, $\Delta G_i°$, for metal complexes[16-20] and organic compounds.[39-42] Application of ETE methods has been previously reported for a number of metallocenes and substituted ferrocenes with $\Delta G_i°$ values in the 6-7 eV range.[16,19] Fourier transform ion cyclotron resonance mass spectrometry,[44-47] FTMS, was used to determine thermal free energies of ionization for several decamethylmetallocenes, cobaltocene, and chromocene, which all have $\Delta G_i°$ values in the 5-6 eV range. The $\Delta G_i°$ values reported are for the oxidation process shown by equation 5-1, where L = Cp or Cp*. Free energies of ionization were determined from the measured equilibrium constant for the ETE reaction and are anchored to the estimated value of $\Delta G_i°$ for bis(benzene)chromium(0), Bz_2Cr,

$$L_2M\ (g) \rightarrow L_2M^+\ (g) + e^- \qquad (5\text{-}1)$$

which was estimated by a combination of photoelectron spectroscopy results and statistical mechanical analyses.

Through the application of thermochemical cycles,[16,18-20,84] the heterolytic and homolytic bond disruption enthalpies for M-Cp cleavage of $Cp_2Cr^{+/0}$ and $Cp_2Co^{+/0}$ have been derived. Additionally, by combining $\Delta G_i°$ values with reported $E_{½}$ data for cobaltocene and chromocene and measured $E_{½}$ values for the Cp^*_2M complexes,[89,105] differential solvation energies, $\Delta\Delta G_{solv}°$, have been estimated. The Born model for estimating $\Delta\Delta G_{solv}°$ values for $M^{+/0}$ couples has been previously applied to metallocene couples and other metal complexes.[54] The $\Delta\Delta G_{solv}°$ values for $Cp_2M^{+/0}$ and $Cp^*_2M^{+/0}$ couples are determined here through thermochemical cycles and the values are compared to values estimated by the Born model.

The rates of gas-phase electron-transfer reactions of several metallocenes couples have been reported previously,[14] and rate constants for the forward ET process have been determined for several of the reactions in this study. For most reactions, the approach to equilibrium was monitored and the forward and reverse rate constants were determined. The forward electron-transfer reaction is written, as shown in equation 5-2, so that the ETE reaction proceeds in an exoergic direction.

$$Cp^*_2M + R^+ \rightarrow R + Cp^*_2M^+ \qquad (5\text{-}2)$$

Overall, the forward rate constants, k_f, show some dependence upon the driving force of the electron-transfer reaction.

Gas-Phase Electron-Transfer Equilibrium Studies

Methods used for studying gas-phase electron-transfer equilibrium reactions have been described.[16-20,39-42] The general reaction studied is shown in equation 5-3, where L_2M denotes a metallocene and R is a reference compound with known a ΔG_i° value. From the measured K_{eq} for the ETE reaction, the reaction free energy, ΔG_{et}°,

$$L_2M + R^+ \rightleftharpoons R + L_2M^+ \qquad (5\text{-}3)$$

can be determined. Since ΔG_{et}° is equal to $\Delta\Delta G_i^\circ$ for the two compounds, $\Delta G_{i,T}^\circ$ of the metallocene can be derived provided $\Delta G_{i,T}^\circ$ of R is known (equation 5-4).

$$\Delta G_{et}^\circ = \Delta G_i^\circ(L_2M) - \Delta G_i^\circ(R) \qquad (5\text{-}4)$$

Because of the low values of the ionization potentials for the metallocenes studied in this chapter, suitable organic reference compounds for ETE were unavailable; organic reference compounds used in previous ETE studies have low ΔG_i° values approaching 140 kcal mol^{-1}. Accordingly, ΔG_i° values reported here are anchored to the ΔG_i° of Bz_2Cr = 125.6 ± 1.0 kcal mol^{-1} at 350 K. The ionization potential of Bz_2Cr was determined through high resolution photoelectron spectroscopy and assumptions necessary to obtain $\Delta G_{i,350}^\circ(Bz_2Cr)$ from the vIP are described later.

Figure 5-1 is an equilibrium ladder exhibiting all ETE reactions investigated in this chapter. All ΔG_i° values lie adjacent to the complex formula, and free energy

changes, $\Delta G°_{et,350}$, for specific reactions couples are adjacent to the arrows. Free energies of ionization energies along with accompanying spectroscopic vIP data[37,38] are presented in Table 5-1. Also in Table 5-1 are $\Delta\Delta G_i°$ values corresponding to the difference in $\Delta G_i°(Cp^*_2M)$ relative to $\Delta G_i°(Cp_2M)$. Error limits for the $\Delta G_{et}°$ values are estimated at 1.5 kcal mol^{-1}, due largely to errors in the measured pressures of the neutral reagent gases. Each reaction was repeated at least three times and examined from both endoergic and exoergic directions to insure that the equilibrium constants for the electron-transfer reactions were not dependent upon the direction of approach to equilibrium. Several checks were performed to test internal consistency and in all cases $\Delta G_{et}°$ values were consistent within the established limits of ± 1.5 kcal mol^{-1}.

Electrochemical Studies for Some Decamethylmetallocenes

The electrochemistry of several $Cp^*_2M^{+/0}$ couples (M = Mn, Fe, Ni, and Ru) were examined. Table 5-2 lists the electrode potentials, $E_{½}$, of the permethylmetallocenes as measured by cyclic voltammetry at a platinum button working electrode and a KCl saturated Ag/AgCl reference electrode in acetonitrile containing 0.1 M t-butylammonium hexafluorophosphate, Bu_4NPF_6. The $E_{½}$ of Cp^*_2Ru has been previously reported in methylene chloride containing 0.1 M t-butylammonium perchlorate,[91] TBAP, and is included in Table 5-2 along with our $E_{½}$ value measured in CH_2Cl_2 containing 0.1 M Bu_4NPF_6. All measured $E_{½}$ values are reported as reversible potentials and are consistent with literature values.

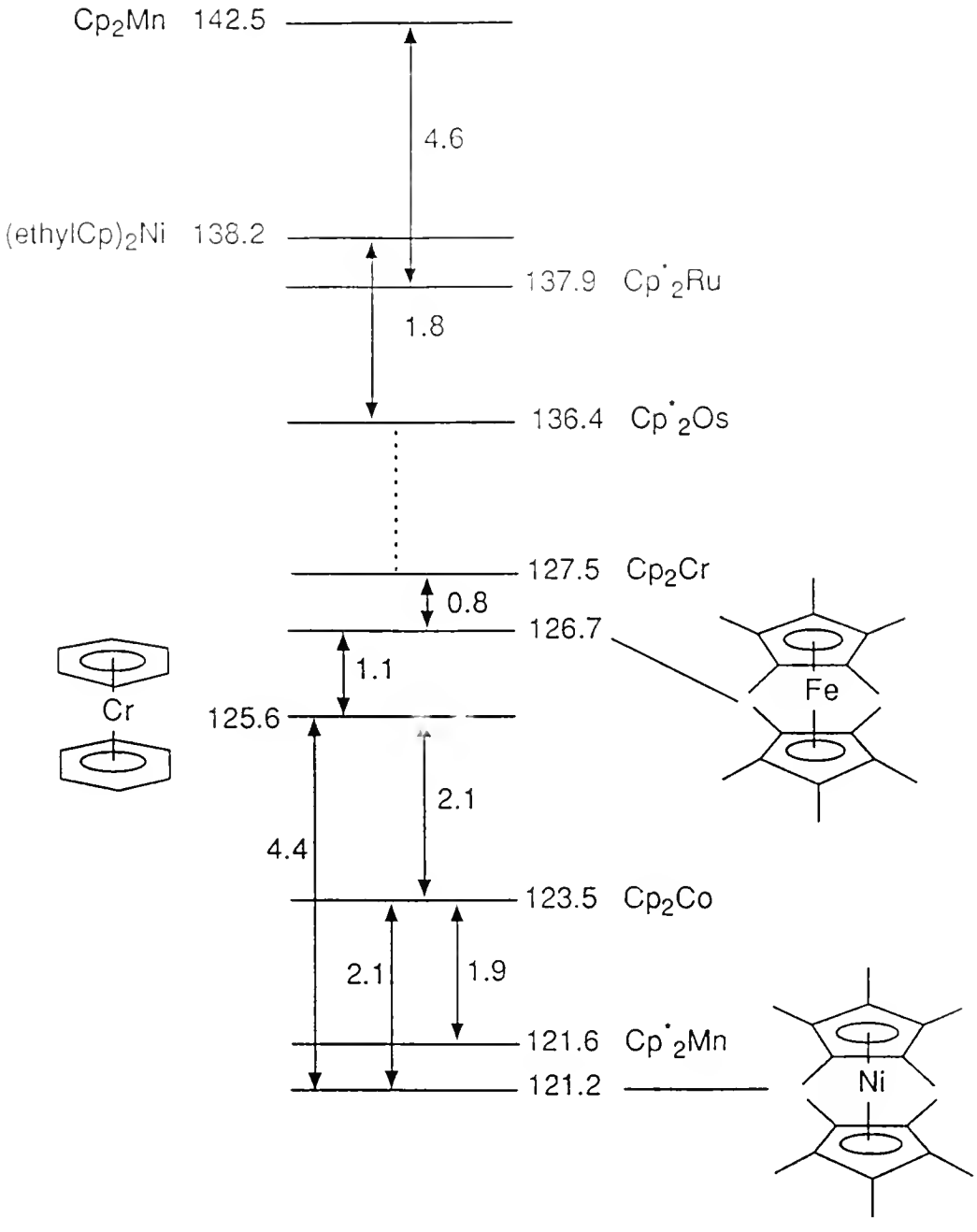

Figure 5-1 Electron-transfer equilibrium ladder for several decamethylmetallocenes. Values for individual ETE reactions are adjacent to arrows and free energies of ionization, $\Delta G_i°$ values, are adjacent to the complex formulas. Free energy values are reported at 350 K. All values anchored to the $\Delta G_i°$ value of Bz_2Cr except Cp^*_2Os and Cp^*_2Ru which are anchored to N,N-dimethylaniline.

Table 5-1. Ionization Energy Data for Some Metallocenes and Decamethylmetallocenes.

Cp_2M	$\Delta G_i°$[a]	vIP[a]	$-\Delta(\Delta G_i°)$[a,b]
Cp^*_2Mn	121.6	122.9[c]	21.0
Cp^*_2Fe	126.7	135.6[c]	26.4
Cp^*_2Ni	121.2	134.2[c]	22.7
Cp^*_2Ru	137.9[d]	-	26.7
Cp^*_2Os	136.4	-	24.2
Cp_2Cr	127.5	131.4[e]	
Cp_2Co	123.5	128.0[e]	

a. Units are kcal mol-1.
b. Difference in the ionization energy of Cp^*_2M and Cp_2M. Values of $\Delta G_i°(Cp_2M)$ taken from reference 16.
c. See reference 37.
d. See reference 20.
e. See reference 35.

Table 5-2 Electrochemical $E_{1/2}$ Data and Differential Solvation Free Energies of Some $Cp^*_2M^{+/0}$ and $Cp_2M^{+/0}$ Couples.

$Cp_2M^{+/0}$	$E_{1/2}$[a] (solv)	$E_{1/2}$[b]	$\Delta G_i°$(soln)[c]	$-\Delta\Delta G°_{solv}$[c]	δ_{Fc}
Cp_2Cr	-0.67[d] (CH_3CN)		92	36	2
Cp_2Co	-0.94[d] (CH_3CN)		86	38	0
Cp^*_2Cr	-1.14[e] (CH_3CN)		82	25[f]	13[f]
Cp^*_2Mn	-0.56[g] (CH_3CN)	-0.64	93	28	6
Cp^*_2Fe	-0.12[e] (CH_3CN)	-0.20	103	24	10
Cp^*_2Co	-1.47[e] (CH_3CN)		74	24[f]	10[f]
Cp^*_2Ni	-0.65[e] (CH_3CN)	-0.69	92	29	5
Cp^*_2Ru	(CH_3CN)	0.41	116	22	12
Cp^*_2Ru	0.58[h] (CH_2Cl_2)	0.55	120	18	16
Cp^*_2Os	(CH_2Cl_2)	0.35	115	21	13

a. Values reported in volts using 0.1 M Bu_4NBF_4 as supporting electrolyte against SCE, except chromocene and cobaltocene in 0.1 M Bu_4NPF_6 against SCE.
b. $E_{1/2}$ values determined in this work were measured in 0.1 M Bu_4NPF_6 in CH_2Cl_2 with ferrocene as an internal standard and then referenced against SCE.
c. Units are kcal mol^{-1}. Estimated error limits ± 2 kcal mol^{-1}.
d. See reference 89.
e. See reference 105.
f. Estimated from PES data and reported against SHE.
g. See reference 127.
h. See reference 91.

Potentials measured in methylene chloride were observed to be anodically shifted relative to potentials measured in acetonitrile since CH_2Cl_2 is a waeker dielectric medium. Values of $E_{½}$ were measured with ferrocene as an internal standard and referenced against SCE and $E_{½}(Fc^{+/0})$.[103]

Bis(benzene)Chromium as a Reference Compound for Electron-Transfer Equilibrium Investigations

Most $\Delta G_i°$ values in this work are anchored to an estimated value for $\Delta G_i°(Bz_2Cr)$, as shown in Figure 5-1. In this section, the assumptions used to estimate this anchor value are discussed. The photoelectron spectrum of Bz_2Cr (Figure 5-2) was measured for this study by Professor D. L. Lichtenberger and coworker.

Vertical ionization energies measured by photoelectron spectroscopy are approximately equal to adiabatic IP values if the difference between the ground state geometries of the ion and the neutral is negligible.[27] Figure 5-2 is a high resolution photoelectron spectrum of bis(benzene)chromium in the valence ionization region (5.0 - 7.5 eV). The very narrow first ionization band at 5.47 eV indicates that structural difference of the ion ground state with respect to the neutral is very small. Potential well diagrams for this process are represented by Figure 1-1B.

Ionization entropies for metal complexes have been estimated previously by using statistical mechanics.[16,74] The value of $\Delta S_i°$ for $Cp_2Fe^{+/0}$ calculated from spectroscopic data is ~5 cal $mol^{-1}K^{-1}$ at 350 K, and the positive value of $\Delta S_i°$ is primarily due to changes in the vibrational and electronic entropies for the ferrocene

couple.[16] Translational and rotational entropy changes were found to be only 0.1 cal $mol^{-1}K^{-1}$ at 350 K, and $\Delta S_{vib}°$ accounted for nearly half of the total $\Delta S_i°$. Sufficient spectroscopic data for bis(benzene)chromium and its cation do not exist to allow for detailed statistical mechanical analyses, however several important assumptions can be made in estimating a value of $\Delta S_i°(Bz_2Cr)$. First, differences in the translational and rotational entropies for $Bz_2Cr^{+/0}$ will be negligible since changes in the molecular mass and moments of inertia for the molecule and the ion will be small.[71] As inferred from the photoelectron spectrum, changes in the Cr-Bz metal-ligand bond length are minimal, therefore moments of inertia will not change significantly upon oxidation. The statistical mechanics study of $Cp_2Fe^{+/0}$ couple revealed that vibrational frequency shifts isolated at the Cp rings (i.e. ring skeletal vibrations) were minor components of $\Delta S_{vib}°$, but shifts in metal-ligand vibrational frequencies (i.e. asymmetric and symmetric Fe-Cp stretch and Fe-Cp bends) significantly contributed to $\Delta S_{vib}°$.[16] Since vibrational frequencies change little between Bz_2Cr and Bz_2Cr^+,[71] $\Delta S_{vib}°(Bz_2Cr^{+/0}) \approx$ 0 cal $mol^{-1}K^{-1}$ can be inferred.

The most significant estimated contribution to $\Delta S_i°$ for Bz_2Cr is $\Delta S_{elec}°$. The ground state configurations for Bz_2Cr and its cation are $^1A_{1g}$ and $^2A_{1g}$ respectively.[35] The electronic entropy change can then be determined from the change in electronic spin degeneracy given by $\Delta S_{elec}° = R(\ln g$,[35] where $g = 2$. Therefore, a value for $\Delta S_i°(Bz_2Cr^{+/0})$ is estimated to be 1.4 cal $mol^{-1}K^{-1}$ ($\Delta S_i° \approx \Delta S_{elec}°$) and at 350 K, $T\Delta S_i° = 0.5$ kcal mol^{-1}.

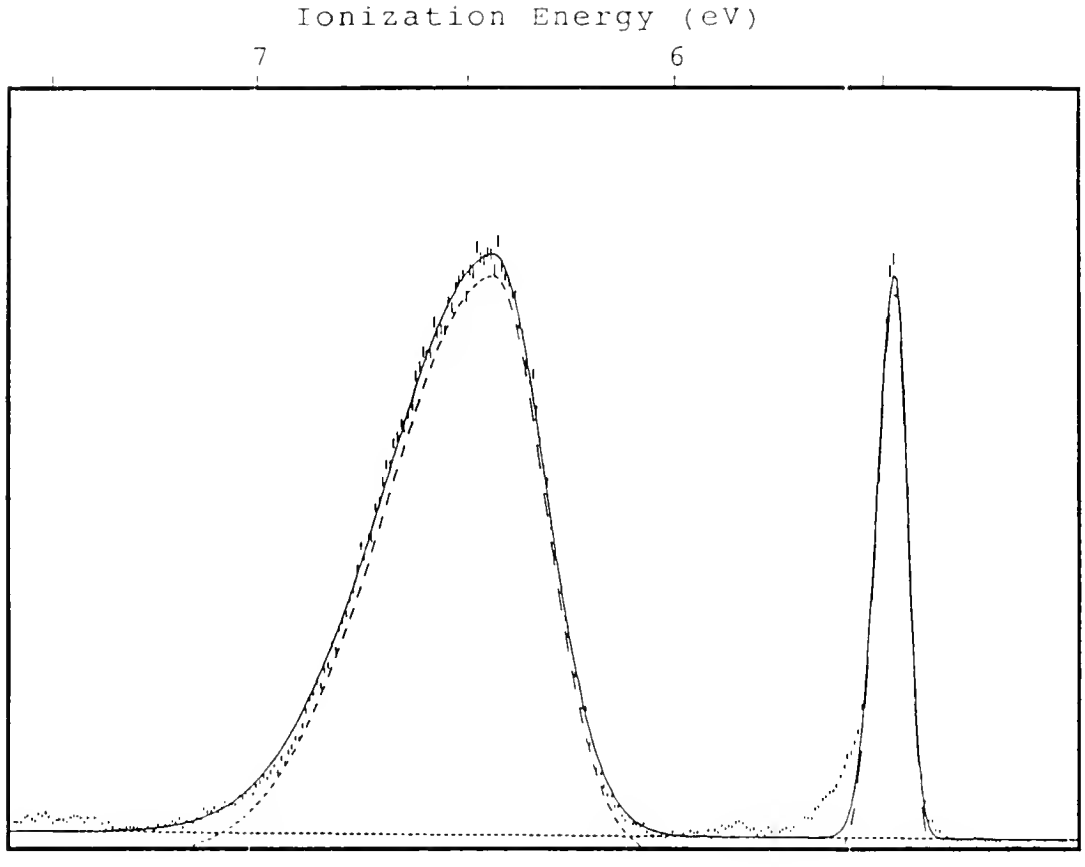

Figure 5-2 High resolution He (I) photoelectron spectrum of bis(benzene)chromium in the valence ionization region. Spectrum recorded for this study by Professor D. L. Lichtenberger and workers.

Changes in the integrated heat capacities for the $Bz_2Cr^{+/0}$couple are also expected to be small. A statistical mechanical analysis of the change in the integrated heat capacities for $Cp_2Fe^{+/0}$ couple indicates that $\Delta Cp°$ contributions are negligible and that $\Delta H_{i,T}°$ values from 300 - 600 K are expected to be equal to the $\Delta H_{i,0}°$ within ± 0.9 kcal mol^{-1}.[16] The difference in integrated heat capacities for benzene and the benzene cation determined from statistical mechanics are also estimated to be negligible (ca. 0.3 kcal mol^{-1} from 0 to 350 K), thus $\Delta H_{i,0}°$ closely approximates $\Delta H_{i,350}°$. Similarly, the difference in the integrated heat capacities for the $Bz_2Cr^{+/0}$ couple, from 0 K to 350 K, are not expected to be much larger than 1 kcal mol^{-1} and aIP = $\Delta H_{i,0}° \simeq \Delta H_{i,350}°$. Finally, $\Delta G_{i,350}°(Bz_2Cr)$ = 125.6 ± 1.0 kcal mol^{-1} can be derived from the estimated $\Delta H_i°$ and $\Delta S_i°$ values at 350 K.

Free Energies of Ionization for Some Decamethylmetallocenes and Comparison to Photoelectron Spectroscopy Results

As expected from previous studies, methylation of the cyclopentadienyl rings lowers the ionization potential with respect to the parent metallocenes.[35,37] In a classical model, the polarizability and inductive effects of the methyl groups stabilize the metallocene cation leading to a less endoergic ionization energy.[2,5] Structural evidence for the increased electron donating ability of pentamethylcyclopentadienyl ligand is clearly observed by a comparison of ruthenocene and Cp^*_2Ru.[91] Crystal structures of Cp_2Ru and Cp^*_2Ru indicate that the M-Cp distance is 0.08 Å larger for ruthenocene than decamethylruthenocene.[91] The smaller M-Cp* distance for Cp^*_2Ru increased Cp*-Cp* repulsions, can be rationalized by more electron rich Cp* rings

being better donors to the Ru(II) metal center (i.e Cp* is a stronger Lewis base the cyclopentadienyl).

Generally, $\Delta G_i°$ values for the Cp^*_2M compounds are approximately 24 ± 3 kcal mol^{-1} lower than their Cp analogues (Table 5-1). Similarly, the $E_{½}$ values for the oxidation potentials of the decamethyl derivatives (Table 5-2) are cathodically shifted by 0.65 ± 0.13 V (15 ± 3 kcal mol^{-1}).[105] The effect of alkyl substitution upon Cp_2M ionization energies is expected to be different for each metal due to several factors including the energy of the metal-based HOMO and different electronic degeneracies,[35] but the relative constant value of the shift in the $\Delta G_i°$ values upon substitution of Cp* for Cp indicates that the differences are not large as when metal center is varied.

Although the magnitudes of the effect of ten methyl groups on the $\Delta G_i°$ values for the metallocenes are somewhat different, seen in the $\Delta(\Delta G_i°)$ values in Table 5-1, present results are consistent with previous $\Delta G_i°$ values for alkylated metallocenes (e.g. $(C_5H_4R)CpFe$ and $(C_5H_4R)_2Ni$)). Comparison of $\Delta G_i°$ values for ferrocene[16] and nickelocene[19] (Figure 5-3) and their Cp* analogues indicates that ferrocene ionization energy is moderately more sensitive to alkylation than nickelocene. The derived ρ values for the two plots shown in Figure 5-3 are 57 ± 1 kcal mol^{-1} and 49 ± 1 kcal mol^{-1} for ferrocene[16] and nickelocene[19] respectively. Predicted $\Delta G_i°$ values for Cp^*_2Fe and Cp^*_2Ni based on previously published Taft analyses for ferrocene and nickelocene alkylated derivatives are within ± 1 kcal mol^{-1} of the experimentally determined values in this work. Plots of alkylnickelocene and alkylferrocene

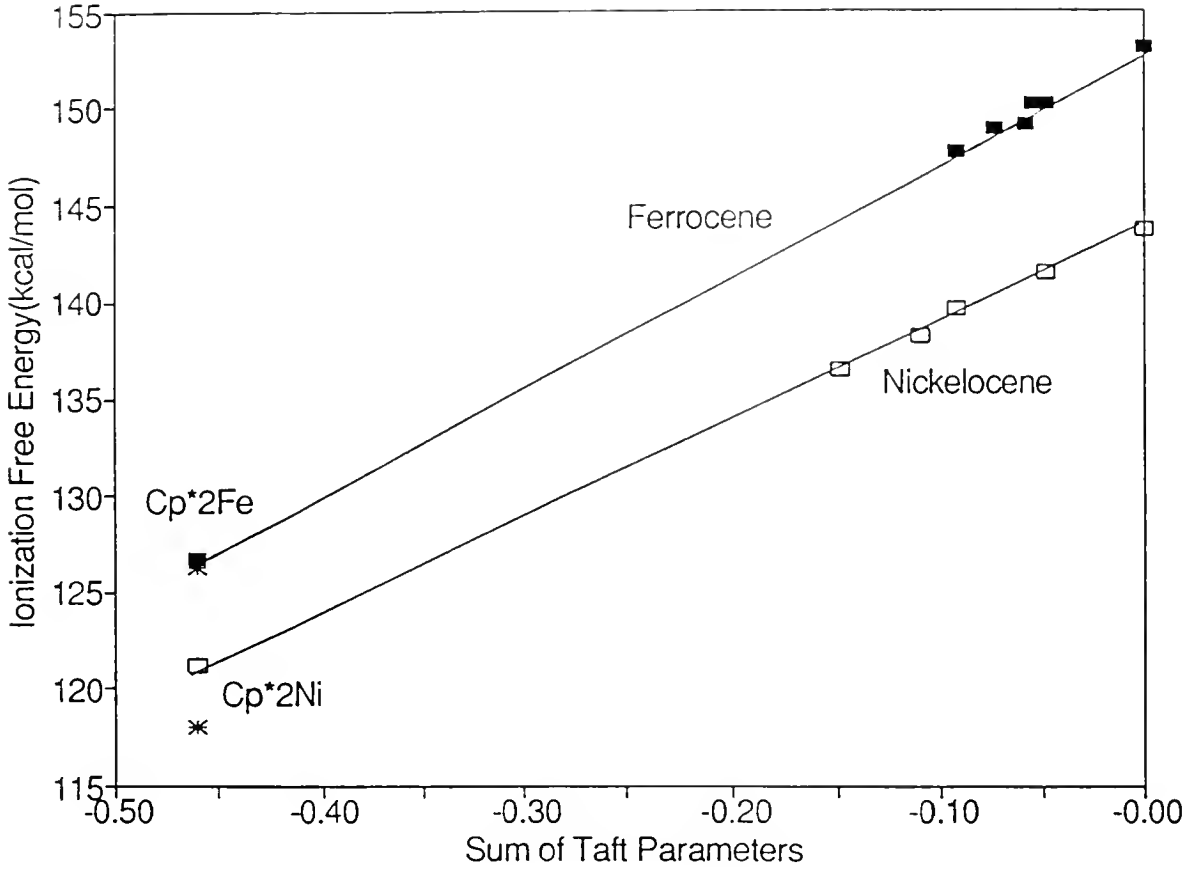

Figure 5-3 Plots of $\Delta G_i°$ values for alkylferrocene and nickelocene complexes versus Taft σ_I parameters. Best fit lines are drawn for ferrocene (r = 0.999) and nickelocene (r = 0.999). Predicted values are within ± 1 kcal mol^{-1} of experimental results. Asterisk represents $\Delta G_i°(Cp^*_2M)$ values predicted values based on Taft analyses of alkylmetallocene data excluding the Cp* derivatives (i.e. data from Chapters 2 and 3)

derivatives with Taft σ_I parameters,[5,52,53] (Figure 5-3) show strong correlation ($R = 0.999$ for both Ni and Fe). Therefore, although $\Delta\Delta G_i°(Cp^*_2M/Cp_2M)$ values for M = Fe and Ni are different, alkyl parameterization schemes demonstrate that $\Delta G_i°(Cp^*_2M)$ values are consistent with ionization free energy data for other alkyl substituents.

The vertical ionization energies from PES for Cp^*_2Mn, Cp^*_2Fe, and Cp^*_2Ni have been determined by Cauletti et al. The assigned electronic configurations for Cp^*_2Fe ($^1A_{1g}$), and Cp^*_2Ni ($^3E_{2g}$) are the same as the simple metallocene.[35,37] However, Cp^*_2Mn exists as a low spin $^2E_{2g}$ complex ($a_{1g}{}^2e_{2g}{}^3$)[37] rather than a high-spin $^6A_{1g}$ complex as observed for manganocene.[79] The PES of Cp_2Mn is extremely broad do to significant geometry changes for cation with respect to the neutral.[37] In comparison, the PES of Cp^*_2Mn is substantially different from manganocene and the first ionization band is quite narrow relative to manganocene.[37] The $\Delta G_i°$ value in this work is in agreement with the estimated adiabatic ionization potential (122 kcal mol^{-1}) determined from the onset of the first PES manifold.

The first ionization bands in the Cp^*_2Fe and Cp^*_2Ni photoelectron spectra have broader bands than are observed for the parent metallocenes and as a result, relaxation energies, determiend from equation 5-5, are ~12 kcal mol^{-1} for these complexes.[35,37]

$$E_r = vIP - \Delta G_i° \qquad (5\text{-}5)$$

However, the relaxation energy for Cp^*_2Mn is only 2 kcal mol^{-1} which is considerably lower than $E_r(Cp_2Mn)$ = 16.8 kcal mol^{-1}.

The $\Delta G_i°$ value for Cp^*_2Ru has been discussed in Chapter 4. The $\Delta G_i°$ for decamethylosmocene is 136.4 ± 2 kcal mol^{-1} which is 24.2 kcal mol^{-1} smaller than the $\Delta G_i°$ value for Cp_2Os. The trend in the $\Delta G_i°$ values for the Cp^*_2M complexes, where M = Fe, Ru, Os, is consistent with the ordering of the $\Delta G_i°$ values for the parent complexes.[16]

Free Energies of Ionization for Chromocene and Cobaltocene

Because of their low IP values, we have been unable to report $\Delta G_i°$ values of cobaltocene and chromocene until now. Estimates of thermochemical properties of the ions in previous publications were based on vertical ionization energies from PES.[16] The $\Delta G_i°$ values shown in Figure 5-1 are in agreement with vertical ionization data (E_r ≈ 5 kcal mol^{-1}).[37,38] Cauletti et al. measured the vertical ionization energies by photoelectron spectroscopy of both chromocene and cobaltocene and the values are 5.71 ± 0.1 and 5.56 ± 0.1 eV respectively.[37] The difference in the vertical ionization energies and the $\Delta G_i°$ values for the two compounds is consistent for the two studies. The ground state configuration for chromocene is $^3E_{1g}$ and the low value of $\Delta G_i°$ with respect to the ferrocene can attributed to the removal an essentially non-bonding unpaired electron from a 16 e^- open-shelled compound.[37,38] Since the molecular orbital scheme for cobaltocene ($a_{1g}^2e_{2g}^4e_{1g}^1$) has one unpaired electron residing in an

antibonding e_{1g} orbital, the low ionization potential relative to other metallocenes is easily rationalized.[35,37,38]

Bond Disruption Enthalpies for Chromocene and Cobaltocene

Thermochemical cycles that incorporate $\Delta G_i°$ data have been used in previous chapters to derive bond disruption enthalpies and differential solvation free energies. The assumptions required to combine free energy of ionization data referenced at 350 K with $\Delta H_{vap,298}°$ for metal sublimations[8] and $\Delta H_{i,0}°$ bare metal ionization energies[8] have been discussed earlier and will not be described here. The value for $\Delta H°$ in equations 5-6 and 5-7 represents twice the average homolytic, $\Delta H_{hom}°$, (equation 6) and heterolytic, $\Delta H_{het}°$, (equation 7) bond disruption enthalpies for metallocenes and metallocenium ions.

$$Cp_2M(g) \rightarrow 2Cp(g) + M^0(g) \qquad (5\text{-}6a)$$

$$Cp_2M^+(g) \rightarrow 2Cp(g) + M^+(g) \qquad (5\text{-}6b)$$

$$Cp_2M(g) \rightarrow 2Cp^-(g) + M^{2+}(g) \qquad (5\text{-}7a)$$

$$Cp_2M^+(g) \rightarrow 2Cp^-(g) + M^{3+}(g) \qquad (5\text{-}7b)$$

From the heats of formation for the respective ions and neutrals (estimated from vertical ionization energies) and $\Delta H_f°$ data for Cp_2Cr and Cp_2Co, average values for $\Delta H_{het}°$ and $\Delta H_{hom}°$ were derived and are given in Table 5-3. Error limits for heterolytic M-Cp bond disruptions enthalpies are larger than homolytic disruption

Table 5-3 Average Bond Disruption Enthalpies for Chromocene and Cobaltocene.

	$\Delta H_{het}°(Cp_2M^{3+})^a$	$\Delta H_{het}°(Cp_2M^{2+})^a$	$\Delta H_{hom}°(Cp_2M^{+})^a$	$\Delta H_{hom}°(Cp_2M^{0})^a$
Cp_2Cr	647 ± 5	354 ± 4	91 ± 3	77 ± 2
Cp_2Co	646 ± 5	394 ± 4	101 ± 3	72 ± 2

a. Units are kcal mol^{-1}. Auxiliary data used to determine bond disruption enthalpies were taken from references 8 and 27.

enthalpies due to the inclusion of extra thermochemical data necessary to estimate the $\Delta H_{het}°$ quantities.

Values for $\Delta H_{het}°$ and $\Delta H_{hom}°$ for chromocene and cobaltocene are consistent with other first transition row metallocenes. Although $\Delta G_i°$ values for chromocene and cobaltocene are much lower than other first transition row metallocenes, bond disruption enthalpies are not significantly different. In the thermochemical cycles used here, bond disruption enthalpies are dependent upon ionization energetics data for both the complexes and the corresponding bare metal ions. For example, $\Delta H_{het}°(Cp_2Co^+)$ is 53 kcal mol^{-1} larger than $\Delta H_{het}°(Cp_2Fe^+)$ primarily because $\Delta H_f°[Co(3+)(g)] > \Delta H_f°[Fe(3+)(g)]$ by 85 kcal mol^{-1}.[8] In terms of the thermochemical cycles, $\Delta H_i°$ values for the bare ions compensate for the low $\Delta G_i°$ values for Cp_2Cr and Cp_2Co relative to the other metallocenes.

Estimates of $\Delta H_{het}°$ and $\Delta H_{hom}°$ for the decamethylmetallocenes could not be made due to lack of thermochemical data for the heats of formation of the Cp^*_2M complexes and pentamethylcyclopentadienide (Cp*).

Evaluation of the Solvation Energetics for Decamethylmetallocenes Chromocene, and Cobaltocene

Differential solvation energies, $\Delta\Delta G_{solv}°$ for metallocene redox couples were determined from comparison of $\Delta G_i°(g)$ values with $\Delta G_i°(soln)$ values measured at 298 K. Assumptions necessary for combining free energies and $\Delta G_i°(soln)$ values have been discussed previously.[16,19,20,54,84] Values of $E_{½}$ for the metallocenes and decamethylmetallocenes are used to derive $\Delta G_i°(soln)$ values as described in previous

chapters. Corrections for liquid junction potentials have not been made for $E_{1/2}$ values. Entropy and heat capacity changes from 298 to 350 K are small for the metallocene redox couples and will only lead to minor errors.[54,84] The stationary electron convention is assumed for both gas-phase and solution redox couples, although near 298 K both the stationary and thermal electron convention yield essentially the same $\Delta G_i°$ values.[88]

Data used to calculate $\Delta G_i°$(soln) and $\Delta\Delta G_{solv}°$ values are shown in Table 5-2. The literature $E_{1/2}$ values for the decamethyl complexes were obtained from several sources[91,105,127] and different reaction conditions, therefore we redetermined the $E_{1/2}$ values for a more consistent comparison of $Cp_2*Mn^{+/0}$, $Cp*_2Fe^{+/0}$, $Cp*_2Ni^{+/0}$, and $Cp*_2Ru^{+/0}$, electrode potentials under uniform conditions (Table 5-2). Differential solvation free energies for the decamethyl complexes were then determined using our $E_{1/2}$ values. Data for the $E_{1/2}$ of $Cp*_2Ru$ measured in CH_2Cl_2 is included in Table 5-2 for comparison along with estimates of $\Delta\Delta G_{solv}°$ for chromium and cobalt decamethyl-metallocene derivatives derived from vIP data.[35]

Generally, the $\Delta\Delta G_{solv}°$ values for $Cp*_2M^{+/0}$ couples are 12 ± 2 kcal mol^{-1} smaller than the parent $Cp_2M^{+/0}$ couples. This difference is of course the origin of the differences in the shifts in electrode potentials and the gas-phase ionization energies for the decamethyl derivatives relative to their parent metallocenes (15 ± 3 kcal mol^{-1} versus 24 ± 3 kcal mol^{-1}, respectively). Figure 5-4 is a plot comparing gas-phase and solution $\Delta G_i°$ values. Estimates of $\Delta G_i°$(g) for $Cp*_2Cr$ and $Cp*_2Co$ were obtained from PES data[35] and $\Delta G_i°$(soln) values were determined from $E_{1/2}$ potentials measured

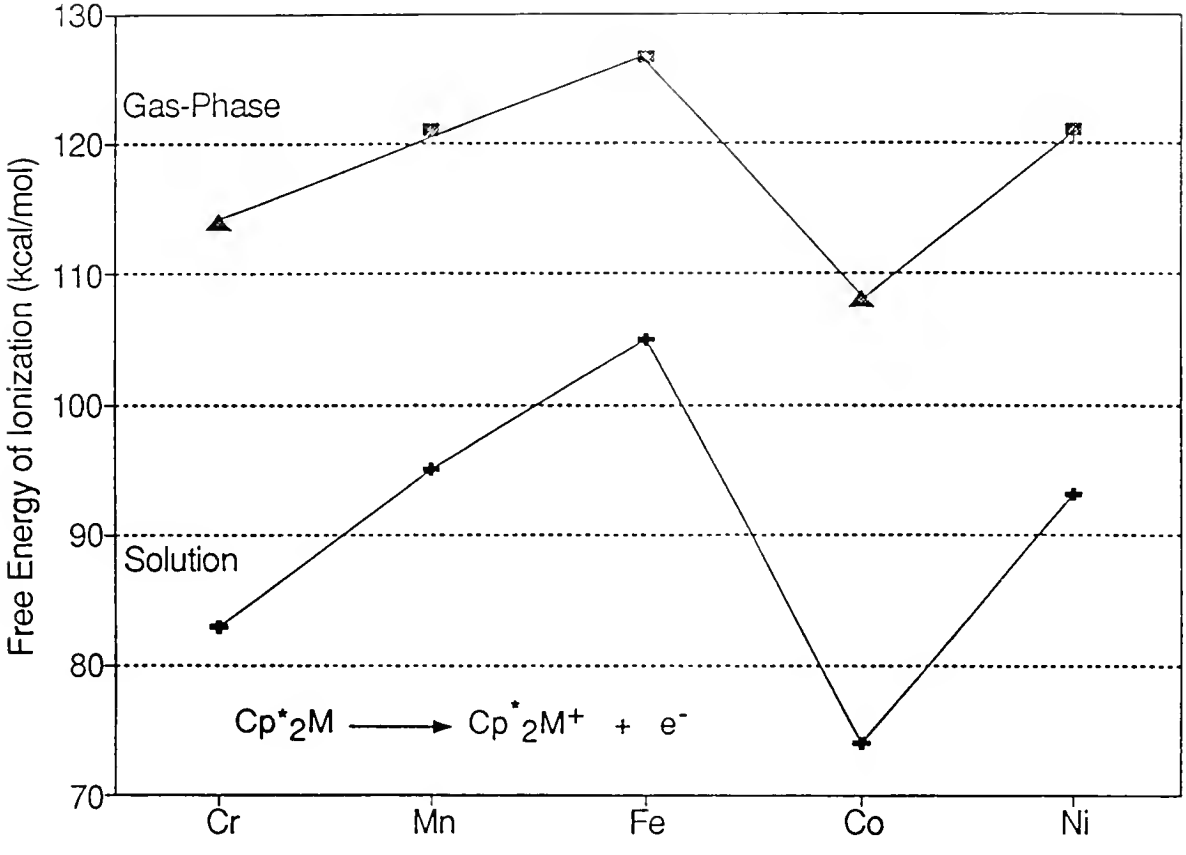

Figure 5-4 Plot demonstrating periodic trend of ionization energies for the first transition row decamethylmetallocenes. Gas-phase data include $\Delta G_i°$ values determined in this work (filled squares) and $\Delta G_i°$ values estimated from PES results (triangles). Solution $\Delta G_i°$ data were determined from $E_{1/2}$ values measured in CH_3CN/0.1 M Bu_4NPF_6 except for Cp^*_2Cr and Cp^*_2Co taken from reference 105.

by Robbins et al.[105] As was observed for the first transition row metallocenes, the trends in both the gas-phase data and solution are very similar.

Included in Table 5-2, are estimates of differential solvation energies relative to $\Delta\Delta G_{solv}°(Cp_2Fe^{+/0})$. The electrochemistry of ferrocene is reversible in a wide variety solvent systems and values for $E°$[34,103] and $\Delta G_i°$[16] for ferrocene have been well established resulting in a reliable estimate for $\Delta\Delta G_{solv}°(Cp_2Fe^{+/0})$ in CH_3CN. In light of this, relative $\Delta\Delta G_{solv}°$ values can be estimated for complexes that have reversible or quasi-reversible electrochemical responses in limited electrochemical conditions. Additionally, the formal potentials relative to $E_{½}(Cp_2Fe^{+/0})$ are constant in various conditions,[103] therefore relative $\Delta\Delta G_{solv}°$ values relative to ferrocene may be determined in several solvents. The term δ_{Fc} is used in place $\Delta(\Delta\Delta G_{solv}°)$ to denote solvation energetics relative to ferrocene (equation 5-8). Positive values of δ_{Fc} indicate that solvent stabilization of an $M^{+/0}$ couple is decreased relative to $Cp_2Fe^{+/0}$.

$$\delta_{Fc} \equiv \Delta\Delta G_{solv}°(M^{+/0}) - \Delta\Delta G_{solv}°(Cp_2Fe^{+/0}) \qquad (5\text{-}8)$$

A negative δ_{Fc} value indicates that solvation energetics for a reaction couple are increased (more exoergic) relative to the ferrocene/ferrocenium couple either due to poor solvation of the complex neutral or a strongly solvated complex ion.

For the decamethylmetallocenes, δ_{Fc} values are all positive. The size and lipophilicity of the methyl groups decreases the solvation of the $Cp^*_2M^{+/0}$ couple compared to the parent metallocenes. Further, as charge-to-solvent separation

increases, polarization of the surrounding solvent will decrease. The methyl groups function as a solvent sphere around the parent metallocene complex and the second solvent layer (the solvent itself) stabilizes the cation to a lesser extent than the methyl groups. For example, the $\Delta(\Delta G_i^\circ)$ for Cp_2Fe and Cp^*_2Fe is -26 kcal mol^{-1} and $\Delta\Delta G_{solv}^\circ(Cp^*_2Fe)$ is -24 kcal mol^{-1}. The effect is more apparent for ruthenocene where $\Delta(\Delta G_i^\circ)$ = -27 kcal mol^{-1} and $\Delta\Delta G_{solv}^\circ(Cp^*_2Ru^{+/0})$ in the lower dielectric methylene chloride is only -17 kcal mol^{-1} .

The Born equation (equation 5-9) has been used successfully for predicting ion solvation energies for $Cp_2M^{+/0}$ couples[16,19,54] but apparently does not predict ΔG_{el}° values accurately for Cp^*_2M complexes. The Born equation is used to estimate the

$$\Delta G_{el}^\circ = (-166z^2/r_{eff})(1-1/D) \text{ kcal mol}^{-1} \qquad (5\text{-}9)$$

change in electrostatic free energy ($\Delta G_{el}^\circ = \Delta\Delta G_{solv}^\circ$) when a charge z on a sphere of radius r_{eff} is transferred from a vacuum to a sphere of equivalent radius in medium of dielectric constant D.[54] The parent metallocenes have quasi-spherical, compact molecular structures and the decamethyl derivatives are less spherical than their Cp_2M analogues. For example, the maximum molecular radius for decamethylferrocene is estimated to be ~5 Å,[128] and the estimated ΔG_{el}° = -32 kcal mol^{-1} (equation 5-9) which can be compared to -24 kcal mol^{-1} estimated from experimental data. Alternatively, from the estimated $\Delta\Delta G_{solv}^\circ(Cp^*_2Fe^{+/0})$ = -24 kcal mol^{-1}, the Born model yields a thermochemical radius of 7.3 Å for Cp^*_2Fe.

The $\Delta\Delta G_{solv}°$ values for Cp_2Cr and Cp_2Co are in agreement with other first transition row metallocenes.[16] A comparison of $\Delta\Delta G_{solv}°$ indicates that a common value of -37 ± 2 kcal mol^{-1} is obtained for Cr, Fe, Co, Ni, and Ru metallocenes.

Electron-Transfer Kinetics

Forward electron-transfer reaction rate constants from ETE studies were determined from the approach to equilibrium. Electron-transfer reaction rate constants were measured in order to test the consistency of determined ETE reaction free energies, $\Delta G_{et}°$, and establish that random errors in our experiment do not exist. Several electron-transfer reactions were observed in which ETE data could not be obtained because the approach to equilibrium was hampered by inefficient reaction rates compared to ion loss from the ion trap. Electron-transfer reaction rate constants for selected reaction couples are presented in Table 5-4. A detailed discussion for determining second-order rate constants for gas-phase electron-transfer reactions has been given elsewhere,[14] and similar methods have been used here.

The barrier for electron-transfer process involving decamethylmetallocenes is expected to be similar to that for simple metallocenes. Nevertheless, reaction rates involving the decamethylmetallocenes were nearly an order of magnitude slower than for the metallocenes[14] and reaction efficiencies (k_f/k_L) were only 2-5% (an estimate of k_L, the Langevin collision rate constant, is 1.1 x 10^{-9} cm^3 $molec^{-1}s^{-1}$ for the Cp^*_2M complexes).

Table 5-4 Electron-Transfer Rate Constants for Some Metallocenes, $L_2M_a^+ + L_2M_b \rightarrow L_2M_a + L_2M_b^+$

	L_2M_a	L_2M_b	ΔG_{et}^{oa}	k_f^b	k_f/k_L^c
1	Cp^*_2Mn	Cp^*_2Ni	~0	2.5×10^{-12}	0.002
2	Cp_2Cr	Cp^*_2Fe	0.8	6.7×10^{-11}	0.06
3	Cp^*_2Fe	Bz_2Cr	1.1	5.1×10^{-11}	0.05
4	Cp_2Co	Cp^*_2Mn	2.0	3.6×10^{-11}	0.03
5	Bz_2Cr	Cp^*_2Mn	~4	6.7×10^{-11}	0.06
6	Bz_2Cr	Cp^*_2Ni	4.4	6.5×10^{-11}	0.06
7	Cp_2Cr	Cp^*_2Ni	~7	7.4×10^{-11}	0.07
8	Cp^*_2Fe	Cp^*_2Ni	~6	4.6×10^{-11}	0.04
9	Bz_2Cr	Cp_2Co	2.1	5.2×10^{-10}	0.52[d]
10	Cp^*_2Ni	Cp^*_2Ni	0	5.3×10^{-10}	0.48
11	Cp_2Ru	Cp^*_2Ni	43	3.8×10^{-10}	0.35

a. Units are kcal mol^{-1}.
b. Units are cm^3 $molec^{-1}s^{-1}$.
c. $k_L = 1.1 \times 10^{-9}$ cm^3 $molec^{-1}$ s^{-1} unless noted otherwise. See reference 14.
d. k_L estimated to be 1.0×10^{-9} cm^3 $molec^{-1}$ s^{-1}. See reference 14.

Electron transfer reaction involving Cp^*_2Ni were very slow and in most cases, equilibrium reactions needed to be followed for >10 s. For the Cp^*_2Ni/Cp^*_2Mn couple, electron-transfer equilibrium was never observed even with reaction times of 15-20 s. It was observed that the two ions were decaying at different reaction rates which is indicative of a slow electron-transfer process.[61,80] The estimated driving force for the reaction (~0 kcal mol^{-1}) may be too low to promote efficient electron-transfer. The electron-transfer reaction for $Cp^*_2Ni^{+/0}$ was studied and was anticipated to be slow in view of the cross reaction involving the $Cp^*_2Ni^{+/0}$ couple. The theoretical maximum rate constant for a metallocene self-exchange or thermoneutral reaction given is 5 x 10^{-10} cm^3 $molec^{-1}s^{-1}$ corresponding to $k_f/k_L = 0.5$.[80] However, the self-exchange rate constant for Cp^*_2Ni $k_f = 5.3 \pm 1.0 \times 10^{-10}$ cm^3 $molec^{-1}s^{-1}$. For comparison The reported self-exchange reaction for Cp^*_2Mn is 3.1 x 10^{-10} cm^3 $molec^{-1}s^{-1}$, eff = 0.28.[14] For the case of the Cp^*_2Ni/Cp^*_2Fe couple, the rate constant is an order of magnitude larger than the Ni/Mn couple. The driving force for the Ni/Fe couple, reaction **8** in Table 5-4, is ca. -6 kcal mol^{-1}, indicating that the some driving force dependence on ET reaction efficiency. The driving force for the electron-transfer reaction for Cp^*_2Ni with ruthenocene is -43 kcal mol^{-1}, well above the estimated activation barrier for the ET reaction, and the measured rate constant for the reaction ($k_f = 3.8 \pm 1.0 \times 10^{-10}$ cm^3 $molec^{-1}s^{-1}$) is in accord with other ET rate constants involving ruthenocene.[14] It is therefore possible that the anomalously fast self-exchange for $Cp^*_2Ni^{+/0}$ is in fact proceeding through an alternative reaction

pathway for exchange of the isotope label used to monitor the reaction (ligand exchange, for example).

Conclusions

Free energies of ionization for Cp^*_2Mn, Cp^*_2Fe, Cp^*_2Ni, Cp^*_2Ru and Cp^*_2Os determined from gas-phase electron-transfer equilibrium techniques were found to be consistent with previous ETE studies photoelectron spectroscopy results. Additionally, $\Delta G_i°$ values for Cp^*_2Fe and Cp^*_2Ni were found to be consistent with $\Delta G_i°$ data for other alkylated metallocene complexes.[16,18] The $\Delta G_i°$ value for manganocene is only 2 kcal mol^{-1} lower than the its reported vIP[35] indicating that the $Cp^*_2Mn^{+/0}$ couple is structurally more similar than the $Cp_2Mn^{+/0}$ couple. Larger relaxation energies were found for Cp^*_2Ni and Cp^*_2Fe.

Differential solvation free energies for chromocene and cobaltocene are in agreement with other first transition row metallocenes.[16] Thus, solvent interactions for the first transition row metallocenes are expected to be dependent upon complex size as inferred from the Born model. An average value for $\Delta\Delta G_{solv}° = 26 \pm 3$ kcal mol^{-1} was found for the decamethylmetallocenes, excluding ruthenocene. However, the Born model predicts values of $\Delta G_{el}°$ that are larger than found experimentally.

Electron-transfer reaction rate constants involving decamethyl complexes proceed at ~2-5% of the Langevin collision rate. Formation of a transition-state complex with inappropriate orbital overlap may inhibit electron transfer. Although the self-exchange reaction for Cp^*_2Ni was not inefficient, the electron-transfer reactions of

Cp^*_2Ni with other metallocenes was very slow unless the driving force of the reaction was substantial.

Experimental Methods

Electron-Transfer Equilibrium Investigations

Electron-transfer equilibrium studies were performed by using Fourier transform ion cyclotron resonance mass spectrometry. The spectrometer utilized in the present studies is equipped with a 3T superconducting magnet and controlled by an Ionspec data station. Details of the mass spectrometer and electron-transfer experimental procedures have been described previously.

Bis(benzene)chromium, cobaltocene, and chromocene were sublimed into the FTMS high vacuum chamber through a heated Varian precision leak valve. Decamethylmetallocenes were introduced into the vacuum chamber by using a heated solids probe positioned adjacent to the reaction cell.[80] When the ETE of two Cp^*_2M complexes was investigated, the metallocene with the lower $\Delta G_i°$ (therefore requiring a lower neutral vapor pressure for equilibrium studies) was introduced through a heated leak valve and the second compound was sublimed from a heated solids probe. Typical reaction pressures were between 10^{-7} and 10^{-6} Torr for all ETE studies.

The temperature of the reaction cell was 350 K as measured by an Omega RTD thin film detector. Ions were produced through electron impact at 9-12 eV with a 20-30 ms beam event. Ions were thermalized through ion-molecule collisions (~30 collisions s^{-1}) prior to detection. Through the use of ion ejections, fragment ions could

be removed from the cell before the ET reaction. Prior to the reaction period, one of the parent ions was ejected from the reaction cell and the population change of both parent ions with time was observed at set time intervals.

Partial pressures of the parent neutrals were measured directly with an ion gauge and then calibrated by using a Baratron capacitance manometer in the 10^{-5} Torr range. Pressure correction were extrapolated to experimental conditions in the 10^{-7}-10^{-6} Torr range. Details concerning partial pressure measurements and pressure calibrations for our 3T FTMS system have been discussed in detail elsewhere.[94]

For kinetic studies, pressure corrections and normalization for all molecular isotopes was performed prior to calculation of reaction rate constants. Corrections to account for diffusive loss of ions from the reaction cell were not performed. A home-made reaction cell with cell dimensions of 1.88" x 1.88" x 3.00" was used for the majority of ETE and kinetic experiments. Ions could be trapped for ~5 s without significant loss of ion signal. Additionally, since more ions can be stored in the larger cell, reactions could be followed for longer reaction times thus distinguishing from a slow electron-transfer reaction or an electron-transfer equilibrium.

Cyclic Voltammetry Studies

Cyclic voltammetry studies were performed with a PAR systems (Models 173/175). A platinum button working electrode and a Ag/AgCl reference electrode were used. Solvents used for electrochemistry were stored over molecular sieves for several days prior to purification. Pure dry acetonitrile and methylene chloride were prepared prior

to electrochemical studies. Electrolytes were crystallized several times from ethanol/acetone mixtures and dried in a vacuum oven. Electrolytic solutions were freshly prepared prior to all voltammetry studies.

Compounds

Decamethylnickelocene, decamethylmanganocene, decamethylosmocene, chromocene, cobaltocene and bis(benzene)chromium were purchased from Strem Chemicals and used without further purification except bis(benzene)chromium which was resublimed prior to use. Decamethylnickelocene is thermally unstable and after prolonged storage (months) in an inert atmosphere required recrystallization. Decamethylferrocene[129] and decamethylruthenocene[91] were prepared according to literature procedures and their purity was evaluated by mass spectrometry and ^1H NMR.

CHAPTER 6
OVERVIEW OF EXPERIMENTAL METHODS AND PROCEDURES

The procedures for studying electron-transfer equilibrium reactions by using FTMS have been described in the previous chapters. A general background to the principles and design of the Fourier transform mass spectrometer, in addition to further experimental considerations, is given in this chapter. Also, the utility of FTMS for investigating the thermodynamics and reactivity of inorganic complexes is discussed.

Fourier Transform Ion Cyclotron Resonance Mass Spectrometry

The fundamental principles of Fourier transform ion cyclotron resonance mass spectrometry, FTMS, are described by the elementary laws of electromagnetism.[45] In a homogeneous magnetic field, with magnetic field strength B, an ion of charge q and mass m will be subject to a force perpendicular to the direction of the ion motion. The magnetic force, called the Lorentz force, acting on the charged particle is described by equation 6-1, where v represents the ion velocity.

$$F = q(v \times B) \tag{6-1}$$

The Lorentz force confines the ion to a helical path, with a radius r proportional to the velocity of the ion.[45] The ion rotates at a characteristic frequency called the

cyclotron frequency, given by equation 6-2, such that each ion with a unique mass-to-charge ratio, *m/z*, will have a characteristic cyclotron frequency. Determination of the cyclotron frequency for an ion leads directly to its *m/z* value.

$$\omega = qB/2\pi m \tag{6-2}$$

Through the use of excitation and detection operations, different masses for an ensemble of ions may be determined.[44-47] The measurement of ω of an ion in order to determine *m/z* central to Fourier transform ion cyclotron mass spectrometry.[45]

Trapping Ions for Mass Analysis

To prevent ions from traveling along a helical path and being lost prior to detection, ions are produced between two trapping plates. A schematic representation of the sample region, the ion trap is shown in Figure 6-1. The trapping plates are located at the ends of the ion trap. An electrical potential is applied, perpendicular to the magnetic field, to the trapping plates which are in the XY-plane of the ions' helical motions. For positive ions, the trapping plates typically carry a +1 V potential and for negative ions, the trapping plates typically carry a -1 V potential. The trapping potential causes ions moving toward the end of the ion trap to be repelled back into the center of the ion trap. Thus, ions are constrained in the XY-plane by the magnetic field and along the z-axis by the trapping plates.

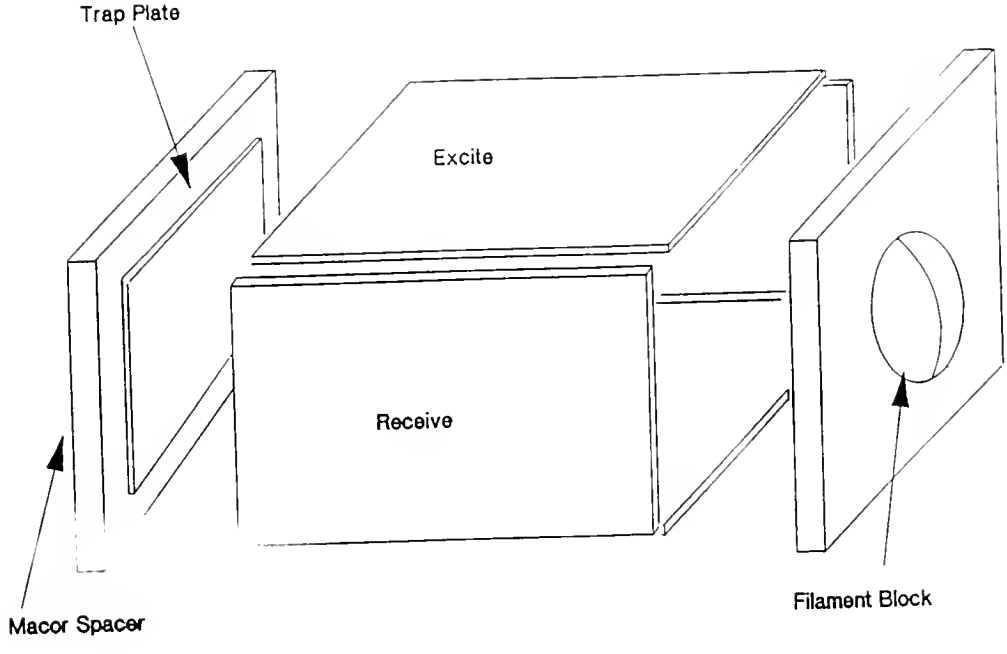

Figure 6-1 Orthorhombic ion trap used in a Fourier transform ion cyclotron resonance mass spectrometer

Ion Excitation and Detection

The ion trap is the region of the mass spectrometer in which all ion manipulations occur. As shown in Figure 6-1, the trap plates are perpendicular to the excitation and detection plates. Two excitation plate and two detection plates are required for ion detection. The two sets of excitation and detection plates (Figure 6-1) are positioned parallel to the magnetic field.

All ions are produced at random time intervals and have random velocities, even ions with the same *m/z* value.[44] Ions in a random phase can not produce a macroscopic signal for detection since their incoherent motion will average-out to zero net signal.[44] In order to detect the ions, an external energy pulse, in the radio-frequency range, is applied at the excitation plates. The radio-frequency, rf, pulse is swept throughout the range of all cyclotron frequencies of interest.[45] Ions absorb the energy from the oscillating electric field and spiral outward into larger orbits.[45] The absorbed kinetic energy of the ions transferred from a radio-frequency pulse is related to the cyclotron radius by equation 6-3. The process of transferring energy from an

$$\text{K.E.} = 2m\pi\omega^2r^2 \tag{6-3}$$

external source to ion in an orbiting path is called ion cyclotron resonance.[45]

As the ions absorb external energy from the applied rf-pulse, all ions of a given *m/z* will from a coherent ion packet with a unique cyclotron frequency[46] (equation 6-2). The orbit of the frequency is larger than the initial orbit. The ion packet will

induce an image current on the detect plates and the image current of each individual ion with a unique cyclotron frequency is measured by the detect plates. The image current is converted to a voltage, amplified and stored in a computer for Fourier transformations of the time-domain signal into a frequency signal. The sequence of exciting ions into ion packets and then detecting their image current can be repeated numerous times to generate an average signal.

Ion Formation and Mass Selection

Ions are formed by electron impact from an electron beam. Typical beam voltages for experiments in this work were from 9 to 15 V. Ion formation is also controlled by the duration and current of the electron beam. Beam currents are set by a potentiometer and are measured by a collector at the end of the ion trap opposed to the electron beam. The beam event varied for these studies, however a average beam time of ca. 20 ms is sufficient to ionize metallocene complexes in large ion concentrations.

During the beam event, ions are produced with a range of *m/z* values, i.e. unwanted molecular and fragment ions. It is therefore necessary to isolate the ions of interest in order to unambiguously follow ETE reactions or ion-molecule reactions. All unwanted ions are removed from the ion trap by ion ejections. A high energy rf-pulse is applied to the ion of interest causing the ion to spiral outward and crash into the cell plates.[46] By means of several ion ejection pulses, specific ions can be isolated. Ion ejection pulses require adjusting the energy of the ejection pulse, the

pulse duration and the mass window for ejection (the sweep width). Ejection energies ranged from 10 to 20 volts. Ion ejection times of ~10 ms were used for most ejections, however longer pulse widths were required for broad mass windows.

For electron-transfer equilibrium studies, the two molecular ions of interest are isolated by a series of ejections. Then an additional ion ejection is set for one of the ions of the ETE couple. In this way, the growth of a reactant ion to the other reactant ion can be monitored over time. For example, if the reaction of interest is $A + B^+ = B + A^+$ and ion A^+ is ejected, the growth of A^+ is monitored relative to the concentration of ion B^+ over time until equilibrium of the ion populations of A^+/B^+ is observed (see Figure 2-1).

Measurement of Equilibrium Constants

An advantage of monitoring electron-transfer equilibrium reactions by using FTMS, aside the obvious ability to trap ions for long periods of time, is that the coefficients needed to determine an equilibrium constant are all measured directly. For comparison, partial pressures in a high pressure mass spectrometer are determined from concentrations of the neutral reagents.[40-43] Direct pressure measurements for FTMS are made with an uncorrected ion gauge and are corrected for sensitivity and system factors after ETE investigations

Partial pressures are measured remote to the ion trap by an ion gauge as shown in Figure 6-2. During ETE studies, the HVC diffusion pump is throttled back to ca. 25% of full pumping capacity. This allows for a dynamic pressure equilibrium to be

established throughout the vacuum chamber. However, there may exist a pressure differential in the vacuum chamber resulting in a disparate pressure at the ion trap relative to the pressure at the ion gauge, i.e. systematic error. Also, the ion gauge may give biased pressure readings for different neutral gases (ion sensitivities). Ion sensitivities of the ion gauge are dependent on the ionization potential and the size of the neutral. System factors are dependent on the rate of diffusion of the neutrals through the FTMS high vacuum chamber (HVC). Pressure corrections therefore entail corrections of both factors. Pressures are calibrated by comparing ion gauge pressures to pressures measured at a Baratron capacitance manometer in the 10^{-5} Torr range and extrapolated back to experimental conditions. A Baratron capacitance manometer is used to correct ion gauge pressures because of the inherent biased of the ion gauge. The Baratron is insensitive to ionization cross sections and therefore is thought to give unbiased pressure readings. Details concerning the pressure corrections for metallocene complexes and aniline derivatives have been presented previously.[13,14,16,94]

For the metallocenes and metallocene derivatives, ion gauge sensitivities are essentially the same within ± 20%. System factors, the rate of flow (or resistance to flow) have been measured for several metallocenes. System factors are also consistent for the metallocenes.[13,16] For example, the system factors for both ferrocene and nickelocene are 1.6 ± 0.20 (dimensionless factor; corrected for ion gauge sensitivity), meaning the pressure at the ion trap is ~1.6 times higher than the pressure at the ion

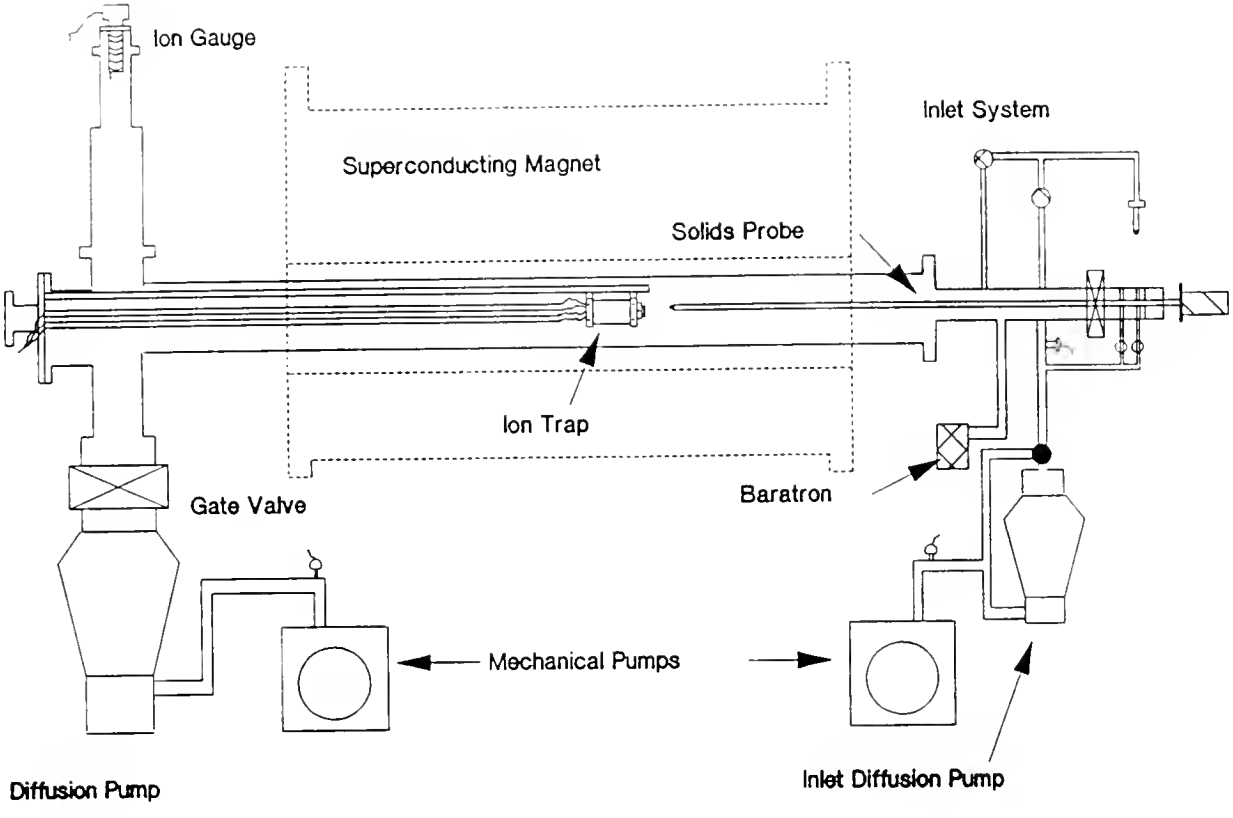

Figure 6-2 Schematic representation of a Fourier transform ion cyclotron resonance mass spectrometer.

gauge during experimental conditions. For comparison, the system factor for N,N'-diethlytoluidine is 1.4 ± 0.1.

Sensitivities for the organometallic complexes studied in this work do not vary significantly. The average sensitivity for the Cp^*_2M complexes, where M = Mn, Fe, Ni, and Ru, is 1.2 ± 0.2. Similarly, the average sensitivity for Cp_2Fe and several ferrocene derivatives is 1.3 ± 0.2. Generally, the ion sensitivities for the metallocene complexes have been found to be equivalent. Furthermore, the ion sensitivities of the organic reference compounds are also equivalent to the metallocenes. The sensitivity of azulene is 1.2 ± 0.1 and the sensitivity of DET is 1.1 ± 0.1. Generally, the overall pressure differential at the ion gauge and the ion trap for the metal complexes and the organic reference compounds are equivalent.

Corrections for ion sensitivities involve normalization for all isotopes of the ions involved in the ETE work. If only one isotope (the most abundant isotope, for example) is monitored during the course of an ETE study, the balance of the minor isotopes must be accounted. Isotopic corrections were performed by calculating the isotopic distribution of an ion and then adjusting the measured ion intensities of the ions followed during the ETE experiment to include 100% of the natural isotopic distribution. It is important to note that partial pressure and ion intensity ratios are used for the determination of equilibrium constants. Therefore, any systematic errors (assuming such errors are comparable for both species involved) will cancel in the determination of an equilibrium constant.

Temperature Dependence Studies

The vast majority of temperature dependence studies of electron-transfer equilibrium reactions have been performed by using PHPMS.[39-43] For FTMS, the technique has been scarcely been applied,[16,39] and most FTMS ETE data have been acquired at 350 K.[13,15,16,19,20,39,59] In order to assess the validity of investigating the temperature dependence of ETE reactions by using FTMS, and thus determine reaction enthalpies and entropies, a model reaction was initially investigated. The required model reaction must have well-defined thermodynamic parameters that can be critically compared to experimental results and must have an electron-transfer equilibrium constant that is accessible by FTMS (≤ 100).[60] The equilibrium reaction 6-4 was investigated as a function of temperature from 350 to 500 K.

$$CO^+ + Kr = Kr^+ + CO \qquad (6\text{-}4)$$

The temperature of the ion trap was heated by a custom built heater described in Chapter 2. In addition to heating the ion trap, the vacuum chamber was heated in order to minimize radiative cooling of the ion trap. The procedure described in Chapter 2 was developed from the methods that evolved from the study of the CO/Kr reaction couple.

For the model reaction, the heat capacities and entropies of all species were calculated by statistical mechanics[55] from known spectroscopic data for the $CO^{+/0}$ and $Kr^{+/0}$ couples in the gas-phase.[7] A van't Hoff plot for the electron-transfer

equilibrium CO/Kr couple is shown in Figure 6-3. The experimental derived parameters are ΔH_{et}° = +0.3 ± 0.8 kcal mol^{-1} and ΔS_{et}° = +3.1 ± 1.4 cal mol^{-1} K^{-1} reported at the 95% confidence limit. The thermodynamic parameters derived from the statistical mechanical analyses are ΔH_{et}° = -0.23 ± 0.01 kcal mol^{-1} and ΔS_{et}° = +1.42 ± 0.06 cal mol^{-1} K^{-1}. The enthalpy change is within the experimental limits for ETE studies which is usually ± 1.5 kcal mol^{-1}.[16-20,39-43] The error in the entropies is probably due to errors in the measured partial pressures of the neutral gases. Given the error limits for reported reaction entropies (ca. ± 50%)[42] determined from temperature dependent ETE studies, the overall error in the experimental and theoretical ΔS_{et}° values is acceptable. Thus, the application of FTMS to determine reaction entropies and enthalpies is validated through the relative success of the CO/Kr ETE couple.

Application of FTMS for the Study of Metal Complexes

There are several advantages of using FTMS for investigations of organometallic complexes. The advantage of low background pressures in the HVC region makes it possible to sample complexes with low volatilities, which includes most of the metallocene complexes studied in this work. Background pressures in the mass spectrometer used in these studies were typically less than 2 x 10^{-8} Torr. However, even at these low pressures, it is still possible to generate ion signals. Ion signals have been observed with background pressures in the 10^{-11} Torr regime.[47]

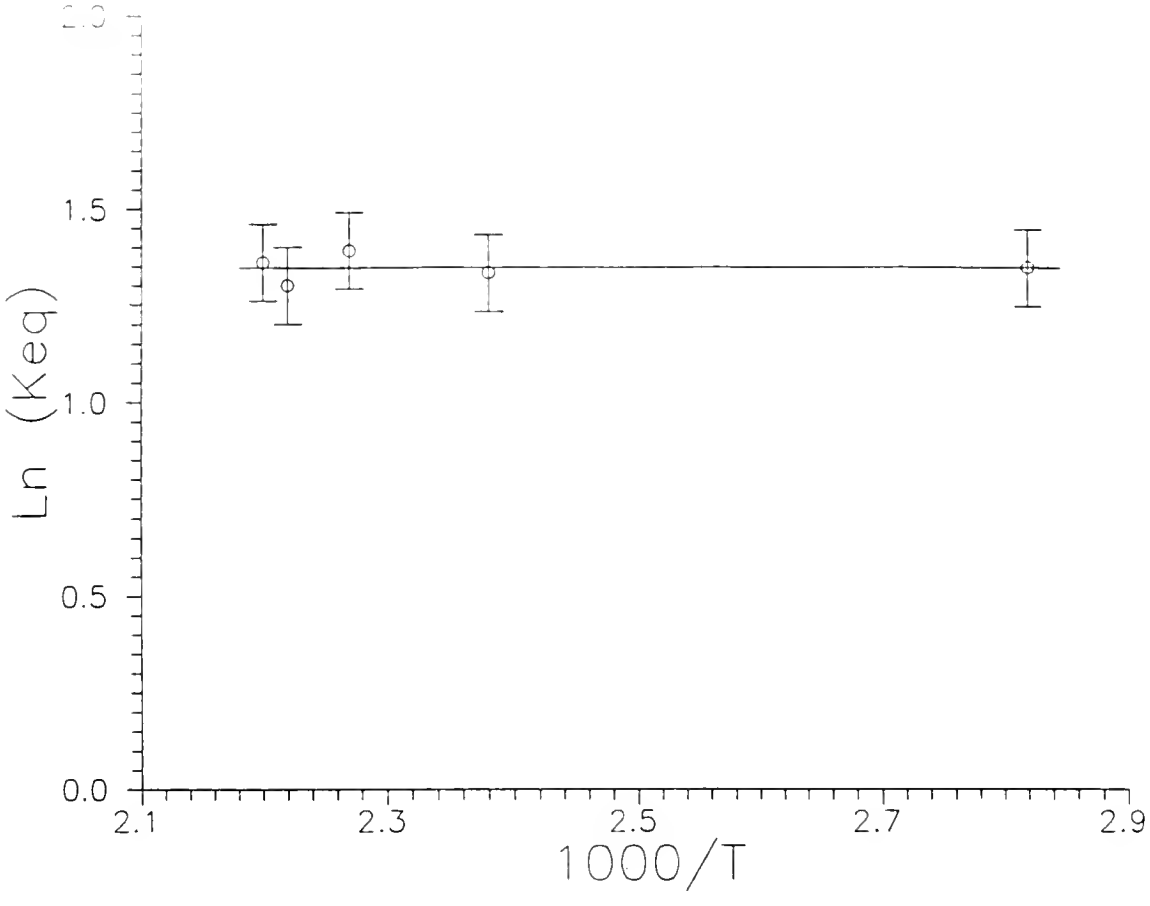

Figure 6-3 van't Hoff plot of the CO/Kr electron-transfer equilibrium reaction.

The melting point of Cp^*_2Ni is ca. 300 °C at STP,[105] however the sample was readily introduced into the mass spectrometer by a heated solids probe with T_{probe} ~ 80 °C. Thus, the need to heat samples to 200-300 °C (which often leads to decomposition of the complex) in order to achieve significant vapor pressures can be avoided. Therefore, the low working pressure in the FTMS vacuum region facilitates the study of inorganics and organometallics that have relatively small vapor pressures.

Further, only small amounts of sample are required for an experiment because of the low background pressures in the FTMS. A sample of less than 1 mg can realistically last for several hours on an unheated solids probe (vide infra). For organometallic complexes which are either costly to synthesize and/or difficult to isolate in high yields, this is a desirable quality. Additionally, oxygen and water sensitive samples can easily be sampled into the mass spectrometer and decomposition of these unstable complexes can be hindered by the low background pressure of the system.

CHAPTER 7
SUMMARY

Thermal free energies of ionization for some prototypical organometallic complexes have been measured by using Fourier transform ion cyclotron resonance mass spectrometry. Temperature dependence studies of electron-transfer equilibrium reactions were performed in order to measure reaction enthalpies and entropies. Comparison of the experimental $\Delta S_{et}°$ value for the Cp_2Fe/DET couple and the value predicted by statistical mechanical analyses indicates that the experimental reaction entropy for the couple may be too large. Through a combination of spectroscopic data and statistical mechanical analyses, the origins of the ionization entropy for the $Cp_2Fe^{+/0}$ couple have been determined. Vibrational entropy changes account for over 50% of the total $\Delta S_i°(Cp_2Fe)$. Although the $\Delta S_i°$ values for ferrocene in the 298 to 600 K range were found to be relatively large (~5 cal $mol^{-1}K^{-1}$), the experimentally derived value is about twice as large.

The $\Delta G_i°$ values have been used to derive estimates of the average heterolytic and homolytic M-Cp bond disruption enthalpies for the first transition-row metallocenes and metallocenium ion through the application of thermochemical cycles.

Thermochemical cycles which include $\Delta G_i°$ values in the gas phase and solution have been used to derive estimates of differential solvation energies, $\Delta\Delta G_{solv}°$, for numerous metallocene complexes. Although solvation energetics are

difficult to measure for individual ions, $\Delta\Delta G_{solv}°$ values can be used to understand relative solvation energetics for metal redox couples. Variations in the values of $\Delta\Delta G_{solv}°$ for the metallocenes have been shown to be primarily dependent on both size of the metal complex and not necessarily the net charge or the metal center. For example, the $\Delta\Delta G_{solv}°$ values for the $Cp_2Ni^{+/0}$ and the $Cp_2Ni^{0/-}$ couple are equivalent within experimental error.[19] Further the $\Delta\Delta G_{solv}°$ value for Cp^*_2Ru is nearly one-half $\Delta\Delta G_{solv}°(Cp_2Fe)$ which is consistent with the relative molecular volumes for the metal complexes (the volume of Cp_2Fe is ~50% the volume of Cp^*_2Ru). Overall, the $\Delta\Delta G_{solv}°$ values for the metallocenes studied in this work are consistent with $\Delta G_{el}°$ values estimated by the Born solvation model.[16,19]

Correlations of $\Delta G_i°$ values for alkylated ferrocene and nickelocene derivatives demonstrate that alkyl substituent parameters can be applied to predict thermodynamic values for organometallic complexes. The application of various models[5,53] allows for the separation of various electron effects. The contribution of inductive and polarization effects for the alkylnickelocenes is equally important in the stabilization of $(RCp)_2Ni^+$ complexes. For comparison, polarization effects (*P*) for aliphatic alcohols are more important in the stabilization of ROH_2^+ and RO^- species than inductive effects (*I*).[102]

The application of the alkyl Taft parameters failed to correlate with $\Delta G_i°$ values for several ruthenocene derivatives studied in this work. Therefore a parameterization scheme, γ parameters, based on the overall electronic nature of Cp ligands was developed. The utility of Cp γ parameters for correlating thermochemical

parameters has been applied to XPS data.[91,108] The application of these parameters for predicting reactivity of metal complexes bearing Cp derivative ligands is of great interest and studies have been designed and performed with this goal in mind. The ligand parameters are potentially useful in the areas of homogeneous catalysis and advanced material science.

The information presented in this work was determined with the idea of developing a foundation for organometallic thermochemistry. As stated earlier, thermochemical information is fundamentally important to chemistry. Thermochemistry allows chemists to better understand chemical transformations and subsequently attenuate, adjust, and further refine chemical reactivity of specific systems. More than a compilation of data, the values derived in this work have been critically analyzed and should be useful to other workers in the area of inorganic chemistry.

REFERENCES

1. Laidler, K. J. *Chemical Kinetics*; McGraw-Hill: New York, 1950.

2. March, J. *Advanced Organic Chemistry*, 3rd ed.; Wiley-Interscience: New York, 1985.

3. (a) Lowrey, T. H.; Richardson, K. S. *Mechanism and Theory in Organic Chemistry*; Harper and Row: New York, 1987. (b) Hine, J. *Structural Effects on Equilibria in Organic Chemistry*; Wiley-Interscience: New York, 1975.

4. Hammett, L. P. *Physical Organic Chemistry*; McGraw-Hill: New York, 1970.

5. (a) Taft, R. W.; Tompson, R. D. *Prog. Phys. Org. Chem.* **1986**, *18*, 1. (b) Taft, R. W. In *Steric Effects in Organic Chemistry*; Newman, M. S., Ed.; Wiley-Interscience: New York, 1956.

6. Dean, J. A. *Langes Handbook of Chemistry*; McGraw-Hill: New York, 1985.

7. Chase, M. W.; Davies, C. A.; Downey, J. R.; Fruip, R. A.; McDonald, R. A.; Syverud, A. N. *J. Chem. Phys. Ref. Data* **1985**, *14*, Sup. 1.

8. (a) Lide, D. R. *Handbook of Chemistry and Physics*; CRC Press: Boca Raton, FL, 1990. (b) Moore, C. E. *Analysis of Optical Spectra*; NSRDS-NBS 34, Office of Standard Reference Data, National Bureau of Standards, Washington, DC.

9. Beauchamp, J. L; Martinho Simões, J. A. *Chem. Rev.*, **1990**, *90*, 629.

10. Richardson, D. E. In *Energetics of Organometallic Species*, Martinho Simões, J. A., Ed.; NATO Advanced Study Institute Series C367; Kulwer: Dordrecht, Netherlands, 1992; p. 233

11. Marks, T. *Bond Energetics in Organometallic Chemistry*; ACS Symposium Series 428; American Chemical Society: Washington, DC, 1990.

12. (a) Skinner, H. A.; Conner, J. A. *Pure Appl. Chem.* **1985**, *57*, 79. (b) Chipperfield, J. R.; Sneyd, J. C. R.; Webster, D. E. *J. Organomet. Chem.* **1979**,

178, 177. (c) Nolen, S. P.; Lopez de la Vega, R.; Hoff, C. D. *J. Organomet. Chem.* **1986**, *315*, 187.

13. Ryan, M. F. *M. S. Thesis*; University of Florida: Gainesville, FL, 1990.

14. Richardson, D. E.; Christ, C. S.; Sharpe, P.; Eyler, J. R. *J. Am. Chem. Soc.* **1987**, *109*, 3894.

15. Sharpe, P.; Eyler, J. R.; Richardson, D. E. *Inorg. Chem.* **1990**, *29*, 2779.

16. Ryan, M. F.; Eyler, J. R.; Richardson, D. E. *J. Am. Chem. Soc.* **1992**, *114*, 8611.

17. Christ, C. S.; Eyler, J. R.; Richardson, D. E. *J. Am. Chem. Soc.* **1990**, *110*, 569.

18. Richardson, D. E.; Christ, C. S.; Sharpe, P.; Ryan, M. F.; Eyler, J. R. In *Bond Energetics in Organometallic Chemistry*; Marks, T., Ed.; ACS Symposium Series 428; American Chemical Society: Washington, DC, 1990; p. 70 - 83.

19. Richardson, D. E.; Ryan, M. F.; Khan, M. N. I.; Maxwell, K. A. *J. Am. Chem. Soc.* **1992**, *114*, 10482.

20. Ryan, M. F.; Siedle, A. R.; Burk, M. J.; Richardson, D. E. *Organometallics* **1992**, *11*, 4231.

21. (a) Buckner, S. W.; Freiser, B. S. *Polyhedron*, **1988**, *7*, 1583. (b) Buckner, S. W.; Freiser, B. S. In *Gas-Phase Inorganic Chemistry*; Russell, D. H., Ed.; Plenum: New York, 1989; p. 279. (c) Freiser, B. S. *Tantanla* **1985**, *32*, 697.

22. Armentrout, P. B. In *Bond Energetics in Organometallic Chemistry*; Marks, T., Ed.; ACS Symposium Series 428; American Chemical Society: Washington, DC, 1990; p. 18 - 32.

23. Eller, K.; Schwarz, H. *Chem. Rev.* **1991**, *91*, 1121.

24. Norwood, K.; Ali, A.; Flesch, G. D.; Ng, C. Y. *J. Am. Chem. Soc.* **1990**, *112*, 7502.

25. Schultz, R. H.; Crellin, K. C.; Armentrout, P. B. *J. Am. Chem. Soc.* **1991**, *113*, 8590.

26. Sunderlin, L. S.; Dingneng, W.; Squires, R. R. *J. Am. Chem. Soc* **1992**, *114*, 2788.

27. Lias, S. G.; Bartmass, J. E.; Liebman, J. F.; Holmes, J. L.; Levin, R. D.; Mallard, W. G. *Gas-Phase Ion and Neutral Thermochemistry;* American Institute of Physics: New York, 1988.

28. Reichardt, C. *Solvent Effects in Organic Chemisrty*; Verlag Chemie: New York, 1979.

29. (a) Hupp, J. T.; Weaver, M. J. *Inorg. Chem.* **1984**, *23*, 3639. (b) Blackborn, R. L.; Hupp, J. T. *Inorg. Chem.* **1989**, *28*, 3786. (c) Nielson, R. M.; McManis, G. E.; Golovin, M. N.; Weaver, M. J. *J. Chem. Phys.* **1988**, *92*, 3441.

30. (a) Taft, R. W. *Prog. Phys. Org. Chem.* **1983**, *14*, 247. (b) Kebarle, P. *Ann. Rev. Phys. Chem.* **1977**, *28*, 445. (c) Taft, R. W.; Bordwell, F. G. *Acc. Chem. Res.* **1988**, *21*, 463.

31. (a) Kochi, J. K. *Pure Appl. Chem.* **1980**, *52*, 571. (b) Newton, M. D.; Ohta, K.; Zhong, E. *J. Phys. Chem* **1991**, *95*, 2317.

32. Matsumura-Inoue, T.; Kuroda, K.; Umezawa, Y.; Achiba, Y.; *J. Chem. Soc. Faraday Trans 2*, **1989**, *85*, 857.

33. (a) Wada, M.; Kenji, S. *J. Chem. Soc. Dalton Trans.* **1981**, 240. (b) Wada, M.; Sameshima, K.; Nishiwaki, K.; Kawasaki, Y. *J. Chem. Soc. Dalton Trans.* **1982**, 783. (c) Tolman, C. A. *Chem. Rev.* **1977**, *77*, 313.

34. Kotz, J. C. In *Topics in Organic Electrochemistry*; Fry, A. J.; Britton, W. E., Eds.; Plenum Press: New York, **1986**; ch. 1.

35. Green, J. C. *Struct. Bonding* **1986**, *43*, 37.

36. Rabalais, J. W. *Principles of Ultraviolet Photoelectron Spectroscopy*; Wiley-Science: New York, 1977.

37. Cayletti, C.; Green, J. C.; Kelly, R; Powell, P.; Van Tilborg, J.; Robbins, J.; Smart, J. *J. Elec. Spec. Rel. Phen.* **1980**, *19*, 327.

38. (a) Evans, S; Green, M. L. H.; Jewitt, B.; Orchard, A. F.; Pygall, C. F. *J. Chem. Soc. Faraday II* **1972**, *68*, 1847. (b) Evans, S. Green, M. L. H.; Jewitt, B.; King, G. H.; Orchard, A. F. *J. Chem. Soc. Faraday II* **1973**, *70*, 356.

39. Lias, S. G.; Ausloos, P. J. *J. Am. Chem. Soc.* **1978**, *100*, 6027.

40. (a) Meot-Ner (Mautner), M.; Nelsen, S. F.; Willi, M. R.; Frigo, T. B. *J. Am. Chem. Soc.* **1984**, *106*, 7384. (b) Nelsen, S. F.; Rumack, D. T.; Meot-Ner (Mautner), M. *J. Am. Chem. Soc.* **1988**, *110*, 7945.

41. (a) Chowdhury, S.; Heinis, T.; Kerbarle, P. *J. Am. Chem. Soc.* **1986**, *108*, 4662. (b) Chowdhury, S.; Kerbarle, P. *J. Am. Chem. Soc.* **1986**, *108*, 5453. (c) Chowdhury, S.; Grimsrud, E. P.; Heinis, T.; Kerbarle, P. *J. Am. Chem. Soc.* **1986**, *108*, 3630. (d) Chowdhury, S.; Grimsrud, E. P.; Heinis, T.; Kerbarle, P. *J. Phys. Chem.* **1986**, *90*, 2747.

42. Kebarle, P.; Chowdhury, S. *Chem. Rev.* **1987**, *87*, 513.

43. Meot-Ner (Mautner), M. *J. Am. Chem. Soc.* **1989**, *111*, 2830.

44. Marshall, A. G. *Acc. Chem. Res.* **1985**, *18*, 316.

45. Eyler, J. R.; Baykut, G. *TrAc, Trends Anal. Chem.* **1986**, *5*, 44.

46 Comisarow, M. B. *Anal. Chimica Acta* **1985**, *178*, 1.

47. Gross, M. L.; Rempel, D. L. *Science* **1984**, *226*, 261.

48. Fagen, P. J.; Ward, M. D.; Calabrese, J. C. *J. Am. Chem. Soc.* **1989**, *111*, 1698.

49. Calabrese, J. C.; Cheng, L. T.; Green, J. C.; Marder, S. R.; Tam, W. *J. Am. Chem. Soc.* **1991**, *113*, 7227.

50. (a) Levitt, L. S.; Levitt, B. W *Tetrahedron*, **1975**, *31*, 2355. (b) Levitt, B. W.; Levitt, L. S. *J. Coord. Chem.* **1973**, *3*, 187. (c) Levitt, B. W.; Levitt, L. S. *Chem. Ind.* **1974**, 302.

51. Levitt, L. S.; Levitt, B. W. *J. Inorg. Nucl. Chem.* **1976**, *38*, 1907.

52. Herhe, W. J.; Pau, C. P.; Headly, A. D.; Taft, R. W.; Tompson, R. D. *J. Am. Chem. Soc.* **1986**, *108*, 1711.

53. Hansche, C.; Leo, A.; Taft, R. W. *Chem. Rev.* **1991**, *91*, 165

54. Richardson, D. E. *Inorg. Chem.* **1990**, *29*, 3213.

55. Pitzer, K. S.; Brewer, L. *Thermodynamics*; McGraw-Hill: New York, 1961

56. Celotta, R. J.; Bennett, R. A.; Hall, J. L. *J. Chem. Phys.* **1974**, *59*, 1740.

57. Grimsrud, E. P; Caldwell, G.; Chowdhury, S.; Kebarle, P. *J. Am. Chem. Soc.* **1985**, *107*, 4627.

58. Born, M. *Z. Phys.* **1920**, *1*, 45.

59. Lias, S. G.; Jackson, J. A.; Argenian, H.; Liebman, J. F. *J. Org. Chem.* **1985**, *50*, 333.

60. Davidson, W. R.; Bowers, M. T.; Su, T.; Aue, D. H. *Int. J. Mass. Spec. Ion. Phys.* **1977**, *24*, 83.

61. Grimsrud, E. P; Chowdury, S.; Kebarle, P. *J. Chem. Phys.* **1985**, *83*, 1059.

62. Rabalais, J. W.; Werme, L. O.; Karlson, L.; Hussain, M.; Siegbahn, K. *J. Chem. Phys.* **1972**, *57*, 1185.

63. Meot-Ner (Mautner), M.; Sieck, L. W. *J. Am. Chem. Soc.* **1991**, *113*, 4448.

64. Wang, M.; Marshall, A. G. *Anal. Chem.* **1990**, *62*, 515.

65. Huheey, J. E. *Inorganic Chemistry*; Harper and Row: Philadelphia, 1983; p. 618.

66. Ikonomou, M. G.; Sunner, J.; Kebarle, P. *J. Phys. Chem.* **1988**, *92*, 6308.

67. Foster, M. S.; Beauchamp, J. L. *J. Am. Chem. Soc.* **1975**, *97*, 4814.

68. Bodenheimer, J. S.; Low, W. *Spectrochemica Acta* **1973**, *29A*, 1733.

69. Pavlik I.; Klikorka J. *Coll. Czech. Chem. Comm.* **1991**, *30*, 664.

70. Duggan, M. D.; Hendrickson, D. N. *Inorg. Chem.* **1975**, *14*, 955.

71. Nakamoto K. *Infrared and Raman Spectra of Inorganic and Coordination Compounds*, 4th ed.; Wiley-Interscience: New York, 1986.

72. Haaland, A. *Acc. Chem. Res.* **1979**, *12*, 415.

73. Churchill, M. R.; Landers, A. G.; Rheingold, A. L. *Inorg. Chem.* **1981**, *20*, 849.

74. Richardson, D. E.; Sharpe, P. *Inorg. Chem.* **1991**, *30*, 1412.

75. Drago, R. S. *Physical Methods in Chemistry*; W. B. Saunders Co.: Philadelphia, 1977.

76. (a) Sackur, O. *Ann. Physik* **1911**, *36*, 598. (b) Tetrode, H. *Ann. Physik* **1912**, *38*, 434.

77. Prins, R. *Mol. Phys.* **1970**, *19*, 603.

78. Lichtenberger, D. L.; Copenhaven, A. S. *J. Chem. Phys.* **1989**, *91*, 663.

79. (a) Ammeter, J. H.; Bucher, R.; Oswald, N. *J. Am. Chem. Soc.* **1974**, *96*, 7833. (b) Switzer, M. E.; Wang, R.; Rettig, M. F.; Maki, A. H. *J. Am. Chem. Soc.* **1974**, *96*, 7669.

80. Richardson, D. E. *J. Chem. Phys.* **1986**, *90*, 3697.

81. Levitt, L. S.; Widing, H. F. *Prog. Phys. Org. Chem.* **1976**, *12*, 119.

82. Sharpe, P. *Ph.D. Dissertation*; University of Florida: Gainesville, FL, 1990.

83. Buckingham, D. A.; Sargenson, A. M. In *Chelating Agents and Metal Chelates*; Dwyer, F. P; Mellor, D. P., Eds.; Academic: New York, 1964; p. 237

84. Sharpe, P.; Richardson, D. E. *J. Am. Chem. Soc.* **1991**, *113*, 8339.

85. Lewis, K. E.; Smith, G. P. *J. Am. Chem. Soc.* **1984**, *106*, 4650.

86. Faulk, J. D.; Dunbar, R. C. *J. Am. Chem. Soc.* **1992**, *114*, 8596.

87. Conway, B. E. *J. Solution Chem.* **1978**, *7*, 721.

88. Sharpe, P.; Richardson, D. E. *Thermochimica Acta* **1992**, *202*, 173.

89. Holloway, J. D. L.; Geiger, W. E. *J. Am. Chem. Soc.* **1979**, *101*, 2038.

90. Hill, M. G.; Lamanna, W. M.; Mann, K. R. *Inorg. Chem.* **1991**, *30*, 4687.

91. Gassman, P. G.; Winter, C. H. *J. Am. Chem. Soc.* **1988**, *110*, 6130.

92. Gubin, S. P; Smirnova, S. A.; Denisovich, L. I.; Lubovich, A. A. *J. Organomet. Chem.* **1971**, *30*, 243.

93. Krishtalik, L. I.; Alpatova, N. M.; Ovsyannikova, E. V. *Electrochim. Acta* **1991**, *36*, 435.

94. Bruce, J. E.; Eyler, J. R. *J. Am. Soc. Mass Spectrom.* **1992**, *3*, 727.

95. Sohn, Y. S.; Hendrickson, D. C.; Gray, H. B. *J. Am. Chem. Soc.* **1971**, *93*, 3603.

96. (a) Cotton, F. A. *Chemical Applications of Group Theory*, 3rd ed.; Wiley-Interscience: New York, 1990. (b) Warren, K. D. *Struct. Bonding* **1976**, *27*, 45.

97. Fritz, H. P. *Adv. Organomet. Chem.* **1964**, *1*, 239.

98. Janousek, B. K.; Brauman, J. L. In *Gas-Phase Ion Chemistry*; Bowers, M. T., Ed.; Academic: New York, 1984: Vol. 2; p. 53.

99. Heinis, T.; Chowdhury, S.; Scott, S. L.; Kebarle, P. *J. Am. Soc. Chem.* **1988**, *110*, 400.

100. Brauman, J. L.; Blair, L. K. *J. Am. Soc. Chem.* **1970**, *92*, 5986.

101. (a) Brauman, J. L.; Blair, L. K. *J. Am. Soc. Chem.* **1971**, *93*, 4194. (b) Laurie, V. M.; Muenter, J. S. *J. Am. Soc. Chem.* **1966**, *88*, 2883.

102. Taft, R. W.; Taagepera, M.; Abboud, J. M.; Wolf, J. F.; Defrees, D. J.; Hehre, W. J.; Bartmess, J. E.; McIver, R. T. *J. Am. Soc. Chem.* **1978**, *100*, 7795.

103. Gagné, R. R.; Koval, C. A.; Lisensky, G. C. *Inorg. Chem.* **1980**, *19*, 2855.

104. Parker, V. D. *J. Am. Soc. Chem.* **1976**, *98*, 98.

105. Robbins, J. L.; Edelstein, N.; Spencer, B.; Smart, J. C. *J. Am. Soc. Chem.* **1982**, *104*, 1882.

106. (a) Barnett, K. W.; *J. Chem. Ed.* **1974**, *6*, 422. (b) Rettig, M. F.; Drago, R. S.; *J. Am. Soc. Chem.* **1969**, *91*, 1361. (c) Reynolds, R.T.; Wilkinson, G. *J. Inorg. Nucl. Chem.* **1959**, *9*, 86. (d) Leigh, T. *J. Chem. Soc.* **1964**, 3294. (e) Nesmeyanov, A. N.; Leonova, E. V.; Kochetkoav, N. S.; Butyugin, S. U.; Meisner, I. S.; *Acad. Sci. USSR Bull.* **1971**, *20*, 89.

107. (a) Collman, J. P; Hegedus, L. S.; Norton, J. R.; Finke, R. G. *Principles and Applications of Organotransition Metal Chemistry*, 2nd ed.; University Science Books: Mill Valley, CA, 1987. (b) *Comprehensive Organometallic Chemistry*; Wilkenson, G.; Stone, F. G. A.; Abel, E. W., Eds.; Pergamon Press: Oxford, UK, 1982.

108. Gassman, P. G.; Macomber, D. W.; Hershberger, J. W. *Organometallics* **1983**, *2*, 1470.

109. Burk, M. J.; Arduengo, A. J.; Calabrese, J. C.; Harlow, R. L. *J. Am. Soc. Chem.* **1989**, *111*, 8938.

110. Gassman, P. G.; Winter, C. H. *J. Am. Soc. Chem.* **1986**, *108*, 4228.

111. Gassman, P. G.; Mickelson, J. W.; Sowa, J. R. Jr. *J. Am. Soc. Chem.* **1992**, *114*, 6942.

112. Burk, M. J.; Calabrese, J. C.; Davidson, F.; Harlow, R. L.; Roe D. C. *J. Am. Soc. Chem.* **1991**, *113*, 2209.

113. Curnow, O. J.; Hughes, R. P. *J. Am. Soc. Chem.* **1992**, *114*, 5895.

114. Winter, C. H.; Han, Y. H.; Heeg, M. J.; *Organometallics*, **1992**, *11*, 3169.

115. Paprott, G.; Seppelt, K. *J. Am. Soc. Chem.* **1984**, *106*, 4060.

116. Gassman, P. G.; Deck, P. A. *Organometallics* **1992**, *11*, 959.

117. Jordon, R. F. *Adv. Organomet. Chem.* **1991**, *32*, 325.

118. Thompson, M. E.; Baxter, S. M.; Bulls, A. R.; Burger, B. J.; Nolan, M. C.; Santarsiero, B. D.; Schaefer, W. P; Bercaw, J. E. *J. Am. Soc. Chem.* **1987**, *109*, 203.

119. Spaleck, W.; Antberg, M.; Rorhmann, J.; Winter, A.; Bachmann, B.; Kiprof, P.; Behm, J.; Herrmann, W. A. *Angew. Chem. Int. Ed. Eng.* **1992**, *31*, 1347.

120. Crow, D. R. *Principles and Applications of Electrochemistry*; Chapman and Hall: London, 1974.

121. Bard, A. J.; Faulkner, L. R. *Electrochemical Methods*; John Wiley and Sons; New York, 1980.

122. Mann, C. K.; Barnes, K. K. *Electrochemical Reactions in Nonaqueous Solutions*; Marcel Dekker: New York, 1970.

123. Kuwana, T.; Bublitz, D. E.; Hoh, G. *J. Am. Soc. Chem.* **1960**, *82*, 5811.

124. (a) Liles, D. C.; Shaver, A.; Singelton, E.; Wiege, M. B.; *J. Organomet. Chem.* **1985**, *282*, C33. (b) Albers, M. O.; Liles, D. C.; Robinson, D. J.; Shaver, E.; Wiege, M. B.; Boeyens, J. C. A.; Levedis, D. C. *Organometallics* **1986**, *5*, 2321.

125. (a) Keske, G.; Lauke, H.; Mauermann, H.; Swepton, P. N.; Schumann, H.; Marks, T. J. *J. Am. Chem. Soc.* **1985**, *107*, 8091. (b) Jordan, R. F. *Adv. Organomet. Chem* **1991**, *32*, 325. (c) Evans, W. J. *Adv. Organomet. Chem* **1983**, *24*, 131.

126. (a) Threlkel, R. S.; Bercaw, J. E. *J. Organomet. Chem.* **1977**, *136*, 1. (b) Fendrick, C. M.; Mintz, E. A.; Schertz, L. D.; Marks, T. J.; Day, V. W. *Organometallics* **1984**, *3*, 819.

127. Smart, J. C.; Robbins, J. L *J. Am. Chem. Soc.* **1978**, *100*, 3936.

128. Freyberg, D. P; Robbins, J. L.; Raymond, K. N.; Smart, J. C. *J. Am. Chem. Soc.* **1979**, *101*, 892.

129. (a) King, R. B.; Bisnette, M. B. *J. Organomet. Chem.* **1967**, *8*, 287. (b) King, R. B.; Eisch, J. J., Eds. *Organometallic Syntheses*; Academic Press: New York, 1965.

BIOGRAPHICAL SKETCH

The author was born in Brooklyn, New York, in 1965 and was raised in the Long Island town of Kings Park. He graduated from Kings Park High School in June of 1983 and left the small north shore community in August of 1983 in order to attend college at the State University of New York in Oneonta, New York. Because of his strong interest in science, he chose to study chemistry at the state college and graduated in 1987 with a B.S. degree in chemistry. In addition to fostering and developing academic interests at school, he learned a great deal of life and formed several lifelong friendships.

After Oneonta, he enrolled in the University of Florida to pursue an advanced degree in inorganic chemistry. He received his master's in the summer of 1990. He later completed his requirements for a Doctor of Philosophy in Inorganic Chemistry in the Spring of 1993 under the guidance of Professor David E. Richardson. The author has accepted a postdoctoral appointment with Professor Helmut Schwarz of the Technische Universität Berlin in Germany and will begin work in the summer of 1993.

I certify that I have read this study and that in my opinion it conforms to acceptable standards of scholarly presentation and is fully adequate, in scope and quality, as a dissertation for the degree of Doctor of Philosophy.

David E. Richardson, Chair
Associate Professor of Chemistry

I certify that I have read this study and that in my opinion it conforms to acceptable standards of scholarly presentation and is fully adequate, in scope and quality, as a dissertation for the degree of Doctor of Philosophy.

John R. Eyler
Professor of Chemistry

I certify that I have read this study and that in my opinion it conforms to acceptable standards of scholarly presentation and is fully adequate, in scope and quality, as a dissertation for the degree of Doctor of Philosophy.

Russell S. Drago
Graduate Research Professor of Chemistry

I certify that I have read this study and that in my opinion it conforms to acceptable standards of scholarly presentation and is fully adequate, in scope and quality, as a dissertation for the degree of Doctor of Philosophy.

Gus J. Palenik
Professor of Chemistry

I certify that I have read this study and that in my opinion it conforms to acceptable standards of scholarly presentation and is fully adequate, in scope and quality, as a dissertation for the degree of Doctor of Philosophy.

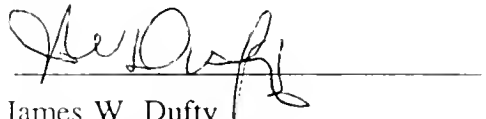

James W. Dufty
Professor of Physics

This dissertation was submitted to the Graduate Faculty of the Department of Chemistry in the College of Liberal Arts and Sciences and to the Graduate School and was accepted as partial fulfillment of the requirements for the degree of Doctor of Philosophy.

May 1993

Dean, Graduate School